

University of Windsor

Scholarship at UWindsor

Electronic Theses and Dissertations

Theses, Dissertations, and Major Papers

2004

Piles embedded in p-y sand below water table subjected to static loading-sensitivity investigations.

Zain Al Abedin
University of Windsor

Follow this and additional works at: <https://scholar.uwindsor.ca/etd>

Recommended Citation

Abedin, Zain Al, "Piles embedded in p-y sand below water table subjected to static loading-sensitivity investigations." (2004). *Electronic Theses and Dissertations*. 3097.
<https://scholar.uwindsor.ca/etd/3097>

This online database contains the full-text of PhD dissertations and Masters' theses of University of Windsor students from 1954 forward. These documents are made available for personal study and research purposes only, in accordance with the Canadian Copyright Act and the Creative Commons license—CC BY-NC-ND (Attribution, Non-Commercial, No Derivative Works). Under this license, works must always be attributed to the copyright holder (original author), cannot be used for any commercial purposes, and may not be altered. Any other use would require the permission of the copyright holder. Students may inquire about withdrawing their dissertation and/or thesis from this database. For additional inquiries, please contact the repository administrator via email (scholarship@uwindsor.ca) or by telephone at 519-253-3000ext. 3208.

PILES EMBEDDED IN *p-y* SAND BELOW WATER TABLE
SUBJECTED TO STATIC LOADING – SENSITIVITY
INVESTIGATIONS

By
Zain Al Abedin

A Thesis
Submitted to Faculty of Graduate Studies and Research
through the Department of Civil and Environmental Engineering
in Partial Fulfillment of the Requirement for
the Degree of Mater of Applied Science at the
University of Windsor.

Windsor, Ontario, Canada

2004

© 2004 Zain Al Abedin



Library and
Archives Canada

Bibliothèque et
Archives Canada

Published Heritage
Branch

Direction du
Patrimoine de l'édition

395 Wellington Street
Ottawa ON K1A 0N4
Canada

395, rue Wellington
Ottawa ON K1A 0N4
Canada

Your file *Votre référence*
ISBN: 0-612-96115-X
Our file *Notre référence*
ISBN: 0-612-96115-X

The author has granted a non-exclusive license allowing the Library and Archives Canada to reproduce, loan, distribute or sell copies of this thesis in microform, paper or electronic formats.

L'auteur a accordé une licence non exclusive permettant à la Bibliothèque et Archives Canada de reproduire, prêter, distribuer ou vendre des copies de cette thèse sous la forme de microfiche/film, de reproduction sur papier ou sur format électronique.

The author retains ownership of the copyright in this thesis. Neither the thesis nor substantial extracts from it may be printed or otherwise reproduced without the author's permission.

L'auteur conserve la propriété du droit d'auteur qui protège cette thèse. Ni la thèse ni des extraits substantiels de celle-ci ne doivent être imprimés ou autrement reproduits sans son autorisation.

In compliance with the Canadian Privacy Act some supporting forms may have been removed from this thesis.

Conformément à la loi canadienne sur la protection de la vie privée, quelques formulaires secondaires ont été enlevés de cette thèse.

While these forms may be included in the document page count, their removal does not represent any loss of content from the thesis.

Bien que ces formulaires aient inclus dans la pagination, il n'y aura aucun contenu manquant.

Canada

ABSTRACT

Laterally loaded pile is a complex system involving pile-soil interaction which is dependent on a number of parameters. They are coefficient of subgrade reaction k , flexural stiffness of pile EI , submerged unit weight of sand γ' , angle of internal friction ϕ of sand, coefficient of active lateral earth pressure of Rankine type K_a , the width of the pile b . The performance of the pile is connected to these parameters, termed as design variables, of pile as well as of soil. Under lateral load, deflection of the pile is dependent on the soil response and the soil response is a nonlinear function of pile deflection and depth of soil below surface. The above stated reasons make the design process of laterally loaded pile lengthy and at times obscure. This study aims at visualizing this process and relating performance of the pile to the design variables through sensitivity analysis.

Short as well as long single piles, both hinged and fixed, embedded in sand, under different range of lateral static loads have been studied. Pile groups have also been studied. The behaviour of the pile is modeled by means of one dimensional beam element. The adjacent soil is simulated by means of p - y model developed by Cox, Reese and Grubbs (1974).

The maximum kinematic quantities of the pile-soil system being of crucial importance according to the serviceability limit state design criteria are subjected to sensitivity analysis assessment. They are investigated in the scope of variational calculus with aid of the adjoint system notion that demonstrates the path independent features.

The performance functional that involves the maximum generalized deformations is formulated based of the virtual work principle. The first variation of the performance functional caused by the changes of the design variables defines the sensitivity of the maximum generalized displacement due to the changes of the physical parameters of pile soil system. They are expressed by means of sensitivity operators that are integrands of the spatial variable x . The graphical representations of sensitivity integrands visualize in practical fashion the effect of changes of the design variables on the variations of maximum generalized deformations.

ACKNOWLEDGEMENT

I would like to give great thanks and appreciations to my supervisor, Dr. B. B. Budkowska for her guidance and advice for the completion of this thesis. I am also grateful to her for her financial support.

I am grateful to Dr. W. J. Altenhof and Dr. F. Ghrib for their constructive suggestions and encouragements.

I would like to express my sincere appreciation and gratitude to Dr. R. Balachandar and Dr. M. K. S. Madugula for their moral support, advice and help.

I feel fortunate that I had the opportunity to earn advanced level knowledge from Dr. F. Ghrib and Dr. M. K. S. Madugula through the courses they have taught.

I would like to thank NSERC for providing fund for the research and OGSST for financial support as scholarship.

I would like to express my sincere appreciation and gratitude to Ms. JoAnn Grondin for her cooperation and help.

TABLE OF CONTENT

ABSTRACT	iii
ACKNOWLEDGEMENT	iv
LIST OF FIGURES	viii
LIST OF TABLES	xviii
NOMEMCLATURE	xix
CHAPTER I. INTRODUCTION	
1.1 Laterally loaded pile	1
1.2 Objective	2
1.3 Scope	4
CHAPTER II. REVIEW OF THE LITERATURE	
2.1 Pile-soil behaviour	8
2.2 Nature of loading	12
2.3 Group of bored piles versus driven piles	13
2.4 Literature review on sensitivity in general	15
2.5 Review of literature on sensitivity of laterally loaded piles	17
2.6 p - y relationships used by contemporary researchers	20
2.7 Soil model employed in the current research	31
CHAPTER III. BEHAVIOR OF LATERALLY LOADED SINGL PILE EMBEDDED IN SAND	
3.1 Behaviour of laterally loaded pile embedded in sand	33
3.2 The p - y relationship used to model the sand around a pile	36
3.3 Computer program COM624P used in the investigation of single piles	47
CHAPTER IV. GROUP OF PILES	
4.1 Introduction	49
4.2 p -multiplier, f_m employed to model pile group	51
4.3 Efficiency of pile group	53
4.4 Computer program FB Pier used in the investigation of group of piles	54

CHAPTER V. THEORITICAL FORMULATION OF SENSITIVITY	
5.1 Introduction	57
5.2 Sensitivity analysis of laterally loaded single piles embedded in sand	58
5.3 Sensitivity analysis of laterally loaded pile group	67
5.4 Primary and adjoint structure	68
CHAPTER VI. ASSESSMENT OF SENSITIVITY	
6.1 Assessment of sensitivity factors affecting the first variation of maximum generalized deformation due to changes of the design variables	71
6.2 Regression analysis of sensitivity of $\delta y_{(.)}^{P_i}$ due to the change of the design variables when the pile structure is subjected to variable lateral force P_i	78
CHAPTER VII CHARACTERISTIC LENGTH OF PILE	
7.1 Introduction	81
7.2 Relative stiffness factor	81
7.3 Definition of short and long pile	84
CHAPTER VIII NUMERICAL INVESTIGATION	
8.1 Properties of pile-soil system	86
8.2 Determination of relative stiffness factor of pile	88
8.3 Development of p - y curve	89
8.4 Sensitivity analysis of single piles	93
8.5 Sensitivity analysis of group of piles	120
CHAPTER IX OBSERVATION AND DISCUSSION	
9.1 Discussion on graphical representation of sensitivity operators	134
9.2 Discussion on sensitivity factors	137
9.3 Discussion on relative sensitivity factors	138
9.4 Discussion on soil phases	140
9.5 Verification of results	141

CHAPTER X CONCLUSION AND FUTURE RESEARCH WORK	
10.1 Closing notes	152
10.2 Conclusion	153
10.3 Engineering applications	155
10.4 Recommendation for future research	156
REFERENCES	158
APPENDIX A Explicit form of sensitivity operators	162
APPENDIX B Results of sensitivity analysis of single isolated piles and group of piles - Enclosed CD	
VITA AUCTORIS	179

LIST OF FIGURES

Figure 2-1	Design reaction curves (Baguelin et al., 1978).	11
Figure 2-2	Ultimate soil resistance of stiff clay below water table (Reese et al. 1975).	21
Figure 2-3	p - y curve for stiff clay (Reese et al., 1975).	23
Figure 2-4	Ultimate soil resistance of soft clay below water table (Matlock, 1970).	25
Figure 2-5	p - y curve for soft clay (Matlock, 1970).	27
Figure 2-6	Ultimate soil resistance of stiff clay above water table (Welch et al. 1972)	29
Figure 2-7	p - y curve for stiff clay (Welch et al., 1972).	30
Figure 3-1	Laterally loaded pile embedded in sand.	33
Figure 3-2	Qualitative diagram pile of deflection and associated soil reaction.	34
Figure 3-3	Typical p - y curve for arbitrary depth $x > 0$.	38
Figure 3-4	Value of coefficient A_s (Reese et al., 1974).	39
Figure 3-5	Value of coefficient B_s (Reese et al., 1974).	40
Figure 3-6	Variability of ultimate soil resistance p_s (p_{st} and p_{sd}) of qualitative type around laterally loaded piles embedded in sand.	44
Figure 3-7	Family of p - y curves for different value of x .	45
Figure 3-8a	Components of p - y curve above x_r .	46
Figure 3-8b	Components of p - y curve below x_r .	47
Figure 4-1	3x3 pile group and pile cap in a group of piles.	50
Figure 4-2	Orientation of rows in a plan of group of piles.	52
Figure 4-3	Geometrical characteristics of the pile group.	53
Figure 4-4	Proposed p -multiplier design curves (Mokwa and Duncan, 2001).	55
Figure 5-1	The geometry of pile-soil system before and after deflection.	59
Figure 5-2	The geometry of pile-soil system (primary system), type of load, boundary conditions and the adjoint system.	62
Figure 5-3	The primary and adjoint system for determination of sensitivity of top lateral deflection δy_t when the primary structure is subjected to lateral force P .	69

Figure 5-4	The primary and adjoint system for determination of sensitivity of top flexural rotation $\delta\theta_t$ when the primary structure is subjected to lateral force P .	69
Figure 5-5	The primary and adjoint system for determination of sensitivity of top lateral deflection δy_t when the primary structure is subjected to bending moment M .	69
Figure 5-6	The primary and adjoint system for determination of sensitivity of top flexural rotation $\delta\theta_t$ when the primary structure is subjected to bending moment M .	70
Figure 6-1	Qualitative length of pile involved in different soil phases.	74
Figure 6-2	Graphical representation of sensitivity δy_t expressed in m .	79
Figure 8-1	Geometry of pile, soil properties and type of load.	86
Figure 8-1a	Cross section of pile.	87
Figure 8-2	Ultimat soil resistance.	91
Figure 8-3	p-y curves at different depth, x .	91
Figure 8-4	Distribution of sensitivity operators S_{EI}^{Py} affecting the change of δy_t due to the variation of design variable δEI for the pile of length, $2.0T_m = 3.5$ m subjected to variable horizontal forces.	93
Figure 8-5	Distribution of sensitivity operators S_k^{Py} affecting the change of δy_t due to the variation of design variable δk for the pile of length, $2.0T_m = 3.5$ m subjected to variable horizontal forces.	94
Figure 8-6	Distribution of sensitivity operators $S_{\gamma'}^{Py}$ affecting the change of δy_t due to the variation of design variable $\delta \gamma'$ for the pile of length, $2.0T_m = 3.5$ m subjected to variable horizontal forces.	94
Figure 8-7	Distribution of sensitivity operators S_{ϕ}^{Py} affecting the change of δy_t due to the variation of design variable $\delta \phi$ for the pile of length, $2.0T_m = 3.5$ m subjected to variable horizontal forces.	95

Figure 8-8	Distribution of sensitivity operators $S_{K_a}^{Py}$ affecting the change of δy_t due to the variation of design variable δK_a for the pile of length, $2.0T_m = 3.5$ m subjected to variable horizontal forces.	95
Figure 8-9	Distribution of sensitivity operators S_b^{Py} affecting the change of δy_t due to the variation of design variable δb for the pile of length, $2.0T_m = 3.5$ m subjected to variable horizontal forces.	96
Figure 8-10	Quantitative assessment of location and size of soil phases developed with depth determined based on the distributions of sensitivity operators of δy_t for pile (free head) of length, $2.0T_m = 3.5$ m, subjected to variable horizontal forces, P .	96
Figure 8-11	Quantitative assessment (in %) of sensitivity of top lateral displacement δy_t due to design variables for pile (free head) length of, $2.0T_m = 3.5$ m subjected to variable horizontal forces, P .	97
Figure 8-12	The quantitative assessment of sensitivity factors $A_{EI}^{Py}, A_k^{Py}, A_{\gamma'}^{Py}, A_{\phi}^{Py}, A_{K_a}^{Py}$ and A_b^{Py} affecting the top lateral deformation y_t of free head pile of length $2T_p = 3.5$ m due to the changes of design variables $EI, k, \gamma', \phi, K_a$ and b .	98
Figure 8-13	Distribution of sensitivity operators $S_{EI}^{M\theta}$ affecting the change of $\delta\theta_t$ due to the variation of design variable δEI for the free head pile of length, $4.5T_m = 7.5$ m subjected to variable bending moment M_i .	102
Figure 8-14	Distribution of sensitivity operators $S_k^{M\theta}$ affecting the change of $\delta\theta_t$ due to the variation of design variable δk for the free head pile of length, $4.5T_m = 7.5$ m subjected to variable bending moment M_i .	102

Figure 8-15 Distribution of sensitivity operators $S_{\gamma'}^{M\theta}$ affecting the change of $\delta\theta_t$ due to the variation of design variable $\delta\gamma'$ for the free head pile of length, $4.5T_m = 7.5$ m subjected to variable bending moment M_i .	103
Figure 8-16 Distribution of sensitivity operators $S_{\phi}^{M\theta}$ affecting the change of $\delta\theta_t$ due to the variation of design variable $\delta\phi$ for the free head pile of length, $4.5T_m = 7.5$ m subjected to variable bending moment M .	103
Figure 8-17 Distribution of sensitivity operators $S_{K_a}^{M\theta}$ affecting the change of $\delta\theta_t$ due to the variation of design variable δK_a for the free head pile of length, $4.5T_m = 7.5$ m subjected to variable bending moment M_i .	104
Figure 8-18 Distribution of sensitivity operators $S_b^{M\theta}$ affecting the change of $\delta\theta_t$ due to the variation of design variable δK_b for the free head pile of length, $4.5T_m = 7.5$ m subjected to variable bending moment M_i .	104
Figure 8-19 Quantitative assessment of location and size of soil phases developed with depth determined based on the distributions of sensitivity operators of $\delta\theta_t$ for free head pile of length, $4.5T_m = 7.5$ m, subjected to variable bending moment, M_i .	105
Figure 8-20 Quantitative assessment (in %) of sensitivity of top lateral displacement due to design variables for free head pile of length $4.5T_m = 7.5$ m subjected to variable bending moments, M_i .	105
Figure 8-21 The quantitative assessment of sensitivity factors $A_{EI}^{M\theta}$, $A_k^{M\theta}$, $A_{\gamma'}^{M\theta}$, $A_{\phi}^{M\theta}$, $A_{K_a}^{M\theta}$ and $A_b^{M\theta}$ affecting the top angle of flexural rotation θ_t of free head pile of length $4.5T_m = 7.5$ m due to the changes of design variables EI , k , γ' , ϕ , K_a and b .	106

Figure 8-22 Distribution of sensitivity operators S_{EI}^{Py} affecting the change of δy_t due to the variation of design variable δEI for the pile of length, $7.0T_p = 12.5$ m subjected to variable horizontal forces.	108
Figure 8-23 Distribution of sensitivity operators S_k^{Py} affecting the change of δy_t due to the variation of design variable δk for the pile of length, $7.0T_p = 12.5$ m subjected to variable horizontal forces.	108
Figure 8-24 Distribution of sensitivity operators $S_{\gamma'}^{Py}$ affecting the change of δy_t due to the variation of design variable $\delta \gamma'$ for the pile of length, $7.0T_p = 12.5$ m subjected to variable horizontal forces.	109
Figure 8-25 Distribution of sensitivity operators S_{ϕ}^{Py} affecting the change of δy_t due to the variation of design variable $\delta \phi$ for the pile of length, $7.0T_p = 12.5$ m subjected to variable horizontal forces.	109
Figure 8-26 Distribution of sensitivity operators $S_{K_a}^{Py}$ affecting the change of δy_t due to the variation of design variable δK_a for the pile of length, $7.0T_p = 12.5$ m subjected to variable horizontal forces.	110
Figure 8-27 Distribution of sensitivity operators S_b^{Py} affecting the change of δy_t due to the variation of design variable δb for the pile of length, $7.0T_p = 12.5$ m subjected to variable horizontal forces.	110
Figure 2-28 Quantitative assessment of location and size of soil phases developed with depth determined based on the distributions of sensitivity operators of δy_t for pile (free head) of length, $7.0T_p = 12.5$ m, subjected to variable horizontal forces, P .	111
Figure 8-29 Quantitative assessment (in %) of sensitivity of top lateral displacement δy_t due to design variables for pile (free head) length of, $7.0T_p = 12.5$ m subjected to variable horizontal forces, P .	111

Figure 8-30 The quantitative assessment of sensitivity factors

$A_{EI}^{Py}, A_k^{Py}, A_{\gamma'}^{Py}, A_{\phi}^{Py}, A_{K_a}^{Py}$ and A_b^{Py} affecting the top

lateral deformation y_i of free head pile of length $7T_m = 12.5$ m

due to the changes of design variables $EI, k, \gamma', \phi, K_a$ and b .

112

Figure 8-31 Distribution of sensitivity operators $S_{EI}^{M\theta}$ affecting the change

of $\delta\theta_i$ due to the variation of design variable δEI for the free

head pile of length, $10T_m = 17.0$ m subjected to variable

bending moment M_i .

114

Figure 8-32 Distribution of sensitivity operators $S_k^{M\theta}$ affecting the change

of $\delta\theta_i$ due to the variation of design variable δk for the free

head pile of length, $10T_m = 17.0$ m subjected to variable

bending moment M_i .

114

Figure 8-33 Distribution of sensitivity operators $S_{\gamma'}^{M\theta}$ affecting the change

of $\delta\theta_i$ due to the variation of design variable $\delta\gamma'$ for the free

head pile of length, $10T_m = 17.0$ m subjected to variable

bending moment M_i .

115

Figure 8-34 Distribution of sensitivity operators $S_{\phi}^{M\theta}$ affecting the change

of $\delta\theta_i$ due to the variation of design variable $\delta\phi$ for the free

head pile of length, $10T_m = 17.0$ m subjected to variable

bending moment M_i .

115

Figure 8-35 Distribution of sensitivity operators $S_{K_a}^{M\theta}$ affecting the change

of $\delta\theta_i$ due to the variation of design variable δK_a for the free

head pile of length, $10T_m = 17.0$ m subjected to variable

bending moment M_i .

116

Figure 8-36 Distribution of sensitivity operators $S_b^{M\theta}$ affecting the change of $\delta\theta_t$ due to the variation of design variable δK_b for the free head pile of length, $10T_m = 17.0$ m subjected to variable bending moment M_i .	116
Figure 8-37 Quantitative assessment of location and size of soil phases developed with depth determined based on the distributions of sensitivity operators of $\delta\theta_t$ for free head pile of length, $10T_m = 17.0$ m, subjected to variable bending moment, M_i .	117
Figure 8-38 Quantitative assessment (in %) of sensitivity of top lateral displacement due to design variables for free head pile of length, $10T_m = 17.0$ m subjected to variable bending moments, M_i .	117
Figure 8-39 The quantitative assessment of sensitivity factors $A_{EI}^{M\theta}$, $A_k^{M\theta}$, $A_{\gamma'}^{M\theta}$, $A_{\phi}^{M\theta}$, $A_{K_a}^{M\theta}$ and $A_b^{M\theta}$ affecting the top angle of flexural rotation θ_t of free head pile of length $7T_m = 12.5$ m due to the changes of design variables EI , k , γ' , ϕ , K_a and b .	118
Figure 8-40 Geometry and initial numerical data employed in numerical Investigations.	121
Figure 8-41 The comparison between horizontal forces P_g of piles of different row and single isolated pile for same value of pile cap deflection y_t .	122
Figure 8-42 Distribution of sensitivity operators G_{EI}^{Py} affecting the change of δy_t due to the variation of design variable δEI for the pile of length, $10T=18$ m, located at centre of leading row subjected to variable horizontal forces P_G applied to the group.	123
Figure 8-43 Distribution of sensitivity operators G_{EI}^{Py} affecting the change of δy_t due to the variation of design variable δEI for the pile of length, $10T=18$ m, located at centre of 1 st trailing row subjected to variable horizontal forces P_G applied to the group.	123

-
- Figure 8-44 Distribution of sensitivity operators G_{EI}^{Py} affecting the change of δy_i due to the variation of design variable δEI for the pile of length, $10T=18m$, located at centre of 2st trailing row subjected to variable horizontal forces P_G applied to the group. 124
- Figure 8-45 Distribution of sensitivity operators G_k^{Py} affecting the change of δy_i due to the variation of design variable δk for the pile of length, $10T=18m$, located at centre of leading row subjected to variable horizontal forces P_G applied to the group. 124
- Figure 8-46 Distribution of sensitivity operators G_k^{Py} affecting the change of δy_i due to the variation of design variable δk for the pile of length, $10T=18m$, located at centre of 1st trailing row subjected to variable horizontal forces P_G applied to the group. 125
- Figure 8-47 Distribution of sensitivity operators G_k^{Py} affecting the change of δy_i due to the variation of design variable δk for the pile of length, $10T=18m$, located at centre of 2nd trailing row subjected to variable horizontal forces P_G applied to the group. 125
- Figure 8-48 Distribution of sensitivity operators $G_{\gamma'}^{Py}$ affecting the change of δy_i due to the variation of design variable $\delta \gamma'$ for the pile of length, $10T=18m$, located at centre of leading row subjected to variable horizontal forces P_G applied to the group. 126
- Figure 8-49 Distribution of sensitivity operators $G_{\gamma'}^{Py}$ affecting the change of δy_i due to the variation of design variable $\delta \gamma'$ for the pile of length, $10T=18m$, located at centre of 1st trailing subjected to variable horizontal forces P_G applied to the group. 126

-
- Figure 8-50 Distribution of sensitivity operators $G_{\gamma'}^{Py}$ affecting the change of δy_i due to the variation of design variable $\delta \gamma'$ for the pile of length, $10T=18m$, located at centre of 2nd trailing subjected to variable horizontal forces P_G applied to the group. 127
- Figure 8-51 Distribution of sensitivity operators G_{ϕ}^{Py} affecting the change of δy_i due to the variation of design variable $\delta \phi$ for the pile of length, $10T=18m$, located at centre of leading row subjected to variable horizontal forces P_G applied to the group. 127
- Figure 8-52 Distribution of sensitivity operators G_{ϕ}^{Py} affecting the change of δy_i due to the variation of design variable $\delta \phi$ for the pile of length, $10T=18m$, located at centre of 1st trailing row subjected to variable horizontal forces P_G applied to the group. 128
- Figure 8-53 Distribution of sensitivity operators G_{ϕ}^{Py} affecting the change of δy_i due to the variation of design variable $\delta \phi$ for the pile of length, $10T=18m$, located at centre of 2nd trailing row subjected to variable horizontal forces P_G applied to the group. 128
- Figure 8-54 Distribution of sensitivity operators $G_{K_a}^{Py}$ affecting the change of δy_i due to the variation of design variable δK_a for the pile of length, $10T=18m$, located at centre of leading row subjected to variable horizontal forces P_G applied to the group. 129
- Figure 8-55 Distribution of sensitivity operators $G_{K_a}^{Py}$ affecting the change of δy_i due to the variation of design variable δK_a for the pile of length, $10T=18m$, located at centre of 1st trailing row subjected to variable horizontal forces P_G applied to the group. 129

Figure 8-56 Distribution of sensitivity operators $G_{K_a}^{Py}$ affecting the change of δy_t due to the variation of design variable δK_a for the pile of length, 10T=18m, located at centre of 2 nd trailing subjected to variable horizontal forces P_G applied to the group.	130
Figure 8-57 Distribution of sensitivity operators G_b^{Py} affecting the change of δy_t due to the variation of design variable δb for the pile of length, 10T=18m, located at centre of leading row subjected to variable horizontal forces P_G applied to the group.	130
Figure 8-58 Distribution of sensitivity operators G_b^{Py} affecting the change of δy_t due to the variation of design variable δb for the pile of length, 10T=18m, located at centre of 1 st trailing row subjected to variable horizontal forces P_G applied to the group.	131
Figure 8-59 Distribution of sensitivity operators G_b^{Py} affecting the change of δy_t due to the variation of design variable δb for the pile of length, 10T=18m, located at centre of 2 nd trailing row subjected to variable horizontal forces P_G applied to the group.	131
Figure 9-1 Free head pile with design variables.	142
Figure 9-2 Comparison between deflections COM624P and FB Pier.	144
Figure 9-3 Soil and pile properties.	145

LIST OF TABLES

Table 1-1 Single piles investigated.	5
Table 1-2 Groups of pile investigated.	6
Table 2-1 Conversion factor for converting E_{sh} (Menard, 1962).	9
Table 7-1 Values of exponents m and n for Equation 7- 3 and 7-4.	84
Table 8-1 Length, boundary condition and type of sensitivity investigated for single isolated pile category.	92
Table 8-2 Loading, boundary conditions and types of sensitivity investigated for group of piles pile investigated.	120
Table 9-1a Average value in percentage of relative sensitivity factors.	140
Table 9-1b Out put data from COM624P.	146
Table 9-2 Soil resistance calculated applying equations of p - y model.	147
Table 9-3 Comparison values of Table 1 and Table 2.	148
Table 9-4 Out-put from FB Pier for free head pile of length 9.0 m.	149
Table 9-5 Out-put from COM 624P for free head pile of length 9.0 m.	150
Table 9-6 An example of percent of error of sensitivity factor $A_{(.)}^{Py}$ for the sensitivity analysis of a free head long pile of length $L = 5T_p = 9.0$ m subjected to variable lateral force P .	151

NONEMCLATURE

- A_b = Sensitivity factors of maximum general deformation connected to changes of design variable, b
- A_{EI} = Sensitivity factors of maximum general deformation connected to changes of design variable EI
- A_k = Sensitivity factors of maximum general deformation connected to changes of design variable k
- $A_{\gamma'}$ = Sensitivity factors of maximum general deformation connected to changes of design variable γ'
- A_{ϕ} = Sensitivity factors of maximum general deformation connected to changes of design variable ϕ
- A_{K_a} = Sensitivity factors of maximum general deformation connected to changes of design variable K_a
- A_s = Dimensionless coefficient
- B_s = Dimensionless coefficient
- b = Width of the pile
- D = Diameter of member piles in a group
- EI = Flexural stiffness of the beam,
- F_{EI} = Relative sensitivity factors connected with the design variable, K_a
- $F_{\gamma'}$ = Relative sensitivity factors connected with the design variable, γ'
- F_{ϕ} = Relative sensitivity factors connected with the design variable, ϕ
- F_{K_a} = Relative sensitivity factors connected with the design variable, K_a
- F_k = Relative sensitivity factors connected with the c design variable, k
- F_b = Relative sensitivity factors connected with the design variable
- f_m = p -multiplier
- ϕ = Angle of internal friction

-
- ϕ_t = Top flexural rotation of the pile
 G_e = Pile group efficiency
 γ' = Unit weight of the soil
 k = Coefficient of subgrade reaction
 K_a = Coefficient of active lateral earth pressure of Rankine type
 M = Bending moment applied to pile head
 M_a = Bending moment of the adjoint system generated by application of unit generalized load
 P = Horizontal force applied to pile head
 p = Soil response
 P_G = Force applied to the cap of primary pile group
 p_a = Soil reaction of the adjoint system generated by application of unit generalized load
 P_k = Sensitivity operators affecting generalized maximum deflections due to the changes of the design variables, k
 p_{gp} = Lateral load resistance of a pile in a group that is p -value for the pile in the group
 p_{sp} = Lateral load resistance of a single pile that is p -value for a single pile
 S_{EI} = Sensitivity operators affecting generalized maximum deflections due to the changes of the design variables EI
 $S_{\gamma'}$ = Sensitivity operators affecting generalized maximum deflections due to the changes of the design variables, γ'
 S_{ϕ} = Sensitivity operators affecting generalized maximum deflections due to the changes of the design variables, ϕ
 S_{K_a} = Sensitivity operators affecting generalized maximum deflections due to the changes of the design variables, K_a
 S_b = Sensitivity operators affecting generalized maximum deflections due to the changes of the design variables, b

-
- T_m = Relative stiffness of pile under bending moment
 T_p = Relative stiffness of pile under horizontal force
 y = Deflection of the pile at a arbitrary depth
 y_t = Top lateral deflection

CHAPTER I

INTRODUCTION

1.1 Laterally loaded pile

Piles are mainly used to transmit axial forces, from various structures, to the subsoil. Since the main structure forces are gravity loads, the majority of piles are then constructed vertically to carry these loads. However, many structures which must be constructed on piles are not only subjected to vertical gravity forces, but also to horizontal forces. In order to transmit these horizontal forces through pile as axial forces, some of the piles should be constructed as inclined piles. Construction of inclined piles in most of the cases is either not possible or if possible not feasible from an economical point of view. For such structures, piles, constructed vertically, must be designed not only to transmit vertical forces, but also to transmit horizontal forces to the subsoil. Horizontal loading that is exerted to the piles may result from the following:

- Wind forces on buildings, bridges, large signs or other structures ,
- Centripetal forces from vehicular traffic on curved bridges,
- Loads on bridges resulting from accelerating, braking or turning of vehicles,
- Lateral seismic forces from earthquakes,
- Forces on offshore or near shore structures resisting ocean wave or water currents,
- Lateral load on earth retaining structures and dams.

1.2 Objective

In order to accomplish efficient and optimum design it is important to study and visualize the behaviour of laterally loaded pile embedded in soil. A well designed pile should have its top lateral deflection or rotation at the top within certain limits. This means that lateral deflection and rotation of pile at the top are the measures of engineering performance of the pile. Calculation of deformation of laterally loaded pile is lengthy and complicated. Unlike axial deformation under vertical loads, lateral deformation is substantial which must be taken into account. The analysis of pile under lateral loading is a problem in soil-structure interaction; that is the deflection of the pile is dependent on the soil response and the soil response is a function of pile deflection. Iteration must be employed because the soil response p is a nonlinear function of pile deflection y and position along the length of the pile. Performance of the laterally loaded pile depends on number of parameters, called design parameters such as:

- Stiffness of the pile EI ,
- Coefficient of subgrade reaction k ,
- Unit weight of the soil γ' ,
- Angle of internal friction ϕ ,
- Coefficient of active lateral earth pressure K_a of Rankine type,
- Width of the pile b .

Traditionally, the design of infrastructure involves consideration of only initial conditions, loads, geometry, and material properties as the primary input variables for

structural design without taking into account the result of material degradation due to environmental effects with time. Such an approach does not adequately assess the actual service life of the structure. With the concept of serviceability state design, structures to be designed to maintain desired serviceability through out the span of time for which the structure is designed for. The structure will have a good performance if it provides an acceptable level of serviceability when constructed as well as through out its designed lifetime. As part of infrastructure that supports the superstructure, laterally loaded piles require maintenance services, future rehabilitations, renovations and replacements. The deterioration of the pile-soil system results in increase of deformations especially top lateral deflection y_t and top flexural rotation ϕ_t of the pile. The key factors that cause such deterioration of pile-soil system are material degradation due to aging and construction quality. It is therefore essential to develop a method that provides a theoretical basis for assessment of change of maximum deformations expressed in terms of possible changes of material properties.

This study involves sensitivity analysis of laterally loaded pile, embedded in sand below water table. The purpose of sensitivity analysis is to determine how sensitive the structural response is to the changes of the design variables. Sensitivity analysis also displays the relative influence of change of each design variables on change of deformation at the top of the pile, subjected to different range of horizontal force and moment applied to the pile top, for different length of the pile with different boundary conditions.

The performance functional of kinematic quantities is formulated in the framework of variational calculus. It allows incorporating the design variables of spatial dependence. The sensitivity operators of maximum kinematic quantities due to changes of the design variables are determined for increasing lateral forces considered in a discrete fashion to account for the nonlinearity of pile deformation with increase in load. The distribution of sensitivity operators with respect to depth of the pile provides information of substantial importance on the spatial location of the design variables affecting maximum generalized deflection. The graphical representation of sensitivity integrands visualizes in practical fashion the effect of changes of the design variables on the variations of maximum generalized deformation. The outcomes of sensitivity analysis are used at various stages of pile-soil life cycle-cost analysis. They include a design, rehabilitation, a renovation, a replacement or an improvement of a system.

1.3 Scope

The sensitivities of top lateral deformation studied in this research are of the changes of the lateral displacements and the change of the angle of flexural rotation at the top of the pile due to the changes of pile-soil strength parameters. Single isolated piles of different length in terms of T , the relative stiffness of the pile, have been investigated. The piles are modeled both as free (hinged) and fixed to the pile cap. To represent complete range of working and ultimate load, horizontal force and moment applied at top of the pile have been varied from a low value to ultimate moment capacity of the pile in a discrete fashion. Different boundary conditions have also been studied. Table 1.1 shows the

single piles investigated with various lengths, boundary conditions and applied load. The physical $p - y$ model of the soil employed in those investigations provides reliable basis for assessment of the pile-soil interaction behaviour. The $p - y$ model of soil connects the soil resistance p to the pile's deflection y at arbitrary depth x below the surface. The modeling of sand below water table in this investigation has been accomplished through

Table 1-1 Single piles investigated.

SINGLE PILES			
<i>Boundary conditions</i>	<i>Pile length L</i>	<i>Deformation type under study</i>	<i>Load steps</i>
Free head pile under lateral load	2.0T _p , 2.5T _p , 3T _p , 3.5T _p , 4.5T _p , 5.0T _p , 6.0T _p , 7.0T _p , 8.0T _p , 9.0T _p , 10T _p	Deflection & flexural rotation	Varied
Fixed head pile under lateral load	2.0T _p , 2.5T _p , 3T _p , 3.5T _p , 4.5T _p , 5.0T _p , 6.0T _p , 7.0T _p , 8.0T _p , 9.0T _p , 10T _p	Deflection	Varied
Free head pile under bending moment	2.0T _m , 2.5T _m , 3T _m , 3.5T _m , 4.5T _m , 5.0T _m , 6.0T _m , 7.0T _m , 8.0T _m , 9.0T _m , 10T _m	Deflection & flexural rotation	Varied
T _p = relative stiffness of pile under horizontal force T _m = relative stiffness of pile under bending moment			

the use of computer program COM624P (1993) developed by The University of Texas at Austin. The program solves the differential equations of pile modeled as beam giving pile deflection, rotation, bending moment, shear and soil reaction by using iterative procedures because of the nonlinear response of the soil. COM624P (1993) employs finite difference method and uses the p - y model to calculate the soil response.

Pile groups consisting of nine piles arranged in 3x3 matrix form and connected to concrete rigid pile cap have been investigated. Groups of piles with different spacing between the piles and boundary condition are investigated and shown in Table 1-2. The analysis of laterally loaded pile group is performed by means of FB-pier (2001) computer program. P-multipliers used in the analysis of group of piles are proposed by Mokwa and Duncan (2001).

Table 1-2 Groups of piles investigated.

GROUP OF PILES			
<i>Boundary conditions</i>	<i>Pile spacing</i>	<i>Deformation type under study</i>	<i>Load steps</i>
Free head pile under lateral load	2D, 3D, 3D, 4D and 5D	Deflection & flexural rotation	Varied
Fixed head pile under lateral load	2D, 3D, 3D, 4D and 5D	Deflection	Varied
D = diameter of pile			

All material strength parameters of the pile-soil system are taken as the design variables. The investigation has been conducted with the aid of adjoint method. The requirement that the nonlinear adjoint system when subjected to dummy load must correspond to the current state of deformation of the primary system is developed in the investigation. The performance functional that involves the maximum generalized deformations is formulated based on the virtual work principle. The first variation of the performance functional caused by the changes of the design variables defines the sensitivity of the maximum generalized displacement due to the changes of the physical parameters of pile-soil system.

CHAPTER II

REVIEW OF THE LITERATURE

2.1 Pile-soil behaviour

Winkler (1867) used the concept of modulus of subgrade reaction to evaluate soil reaction. In Winkler's model it is assumed that reaction developed in the soil p is proportional to the displacement, y . Thus:

$$p = k y \qquad \qquad \qquad 2-1$$

where: k is the modulus of reaction.

Poulos (1971), through the analysis of three dimensional elastic model showed that a single value of modulus of subgrade reaction cannot be valid through entire range of possible horizontal force or moment applied to pile top. The research also showed that it is not possible to find an equivalent reaction modulus that will be valid for different length of the pile.

Baquelin et al. (1977) developed the idea that assigning a single value of k is an approximation and could be improved to some extent considering actual conditions of fixity, rigidity and length of the pile. Later Baquelin found the actual situation to be much more complicated. Baguelin et al. (1978) modeled laterally loaded pile. They used the Winkler concept of proportionality of soil reaction to the displacement. Soil reaction,

$$p = ky.$$

They proposed a more generalized equation which still contains the assumption that p depends only on the displacement y , such as:

$$p = f(y) \quad 2-2$$

where f is a function of y .

They have used modulus of subgrade reaction which was proposed by Menard (1962) as given below.

$$\frac{1}{k} = \left(\frac{2}{9 E_M} \right) B_o \left(\frac{B}{B_o} \times 2.65 \right)^\alpha + \frac{\alpha}{6 E_M} B \quad (B < 0.6 \text{ m}) \quad 2-3$$

$$\frac{1}{k} = \left(\frac{B}{E_M} \right) \left(\frac{4 (2.65)^\alpha + 3\alpha}{18} \right) \quad (B > 0.6 \text{ m}) \quad 2-4$$

Table 2-1 Conversion factor for converting E_{sh} (Menard,1962)

		Ratio E_{sh} / E_M	
		$B < 0.6 \text{ m}$	$B = 1.20 \text{ m}$
Peat	$\alpha = 1$	1.33	1.33
Clay	$\alpha = 2/3$	1.90	2.25
Silt	$\alpha = 1/2$	2.30	3.00
Sand	$\alpha = 1/3$	2.80	4.00
Sand & gravel			

The reference diameter B_o is 0.6 m. The coefficient α depends on the types of soil and values are shown in Table 2-1. The modulus, E_{sh} , is related to the pressuremeter modulus, E_M .

The modulus of subgrade reaction k can be obtained by equating the product kb to E_{sh} . As proposed in this model, value of k is valid for static and cyclic loads. According to this model soil reaction near the surface is less than that at a depth. The reason, as the researchers explained, was due to soil heave. There is a depth, termed the critical depth, z_c below which soil reaction,

$$p = -\frac{1}{B} \cdot \frac{dT}{dz} \quad 2-5$$

where, T is the shear across pile section. For a shallower depth a reduction coefficient λ_z should be used.

$$\lambda_z = \frac{1 + (z/z_c)}{2} \quad 2-6$$

So, above critical depth z_c modulus of subgrade reaction becomes $\lambda_z k$.

Baquelin and his team proposed (1978) the value of z_c to be of the order of $2B$ for cohesive soil and $4B$ for granular soil. A graphical representation of the model is given in Figure 2-1.

They also suggest a simpler and approximate method of ascertaining soil reaction. In this method, to compensate for soil heave, soil reaction can be neglected up to a depth of $0.5B$ to $.075B$, and then full reaction according Equations 2-1 and 2-2 has to be considered.

In this model, for large lateral movement soil pressure p has been held limited to creep pressure p_f and near the ground surface the value should be $\lambda_z p_f$. For a system where soil pressure reaches value higher than p_f , Equation 2-1 does not remain valid instead the reaction locus OABC has to be followed. However for design purposes a more conservative curve OAB' may be adopted as suggested by researchers of this model.

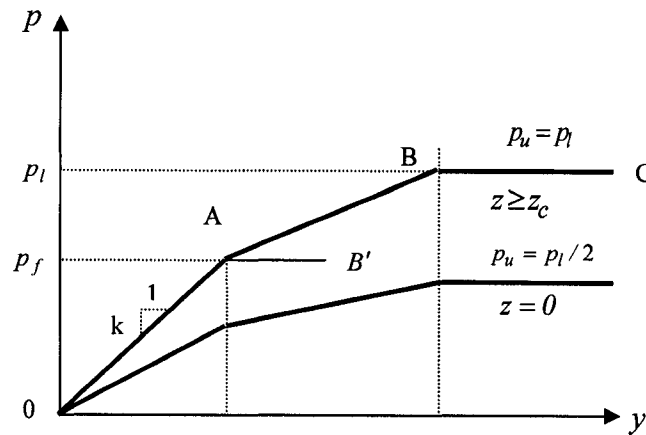


Figure 2-1 Design reaction curves (Baguelin et al., 1978).

This model, when compared to the most refined p - y models (some of them have been discussed in Section 2.6, shows that almost all the critical consideration have been taken into accounts although not in very accurate manner. Physically the pressure curves also

resemble p - y curves. In this model dependence of soil pressure has been linked to depth of point in question below surface, pile deflection, type of soil and the size of pile which is the case in p - y model.

2.2 Nature of loading

In practice four kinds of loads may be encountered. They are static, cyclic, sustained and dynamic loadings. The type of loading conditions needs careful consideration in evaluation of soil response due to the application of the loading. For a particular design situation appropriate loading condition has to be prudently selected and the corresponding soil-response curve to be used. As appears in COM624P (1993) manual a short description is given here.

Static loading: A load which does not undergo a change in magnitude or direction during a measurement procedure. Static load is the short term load. In the field test static load is employed to obtain response of a soil and response due to this type of load can be correlated with the properties of the soil. In fact p - y curves for static lateral loading to a pile embedded in a soil serves as basis for estimating soil response under other type of loading.

Cyclic loading: Cyclic or repeated loads are not uncommon to the structures subjected to lateral forces. Wind gusts, traffic loads on curved bridges, force from braking vehicle over bridges, current and sea wave loads and ice loads are examples of cyclic loading. Although the p - y curves that are being used for design purposes, for cyclic loading are

proposed based on field tests, only a limited number of tests have been performed. Careful study of design parameter and loading conditions are essential the appropriate p - y curve for design purposes. Judgment of an experienced engineer is recommended for assigning proper load factor.

Sustained loading: Retaining walls, dams, bulkheads, and bridge abutments are subjected to sustained loading. For design, proposed p - y curves for short term load are being used for sustained loading. Theoretically, an analysis could be employed to increase the deflection values y to accommodate the time related displacement and revised set of p - y curves could be proposed. But no adjustment has so far been worked on and considerations must be employed into this matter.

Dynamic loading: Most known case of dynamic load is seismic load or the force that generates due to earthquake. There may instances where lateral load comes from vibration as from oscillating machinery.

2.3 Group of bored piles versus driven piles

In a laterally loaded pile group, where the piles are closely spaced, deformation and stress field generated around and vicinity of one pile influences the response of the adjacent pile and vice versa. This phenomenon occurs due to pile-soil-pile interaction, called shadowing. Piles in the group are tied together by the cap. Top deflection y_t is the same for all the piles in the group. Piles in different rows shares different fraction of load P_G applied to the group. Pile in the group behaves differently from the single isolated pile

because of pile-soil-pile interaction. Deflections of piles in group are greater than deflections of single pile at the same load per pile. Piles in a group carry unequal lateral loads, depending on their location within the group and the spacing between them. To incorporate group effect the soil resistance values, p in a family series of p - y curves for a given pile or a pile in a row is reduced by a constant factor, called p -multiplier. Most software which can be used to analyze group of piles allow the user to specify the values of p -multiplier. Determination of these p -multipliers is based on the full scale loading test on driven piles. O'Neil, M. W. and Gazioglu, S. M. in their 1984 paper delineate the experimental finding of installation effect on performance of group of piles. They have tested group of pile consisting of bored piles and group of driven piles. The test site was on a flat coastal plain of Chaiyi, Taiwan. The classification and properties of soil were experimentally found through drilling bores. They have identified experimentally that p -multiplier differ in value in driven piles from that of bored piles. "The differences in p -multipliers apparently reflects the differing effect of boring and of driving displacement pile on the density and stress state in the soil within the pile group". No numerical value for correction has been suggested by the researchers in the paper. Parameters that could perhaps effected the experimental result could not been controlled and the tests were not performed in identical setup. Since p -multipliers suggested by Mokwa et al. (2001) are based on research of many geotechnical engineers and are treated as state-of-art values will be employed in this research.

2.4 Literature review on sensitivity in general

The aim of devising better design solution, satisfying safety and performance constraints, that involves minimum time and cost is not new. A design engineer investigates several alternatives and chooses the best one of these. Unfortunately, time and cost usually limits very severely the number of alternatives that can be investigated. In the competitive market like today's not only the construction time and cost are intended to be minimized but also the designers' work-hour is valuable. So, it is desirable to develop a more effective and rapid technique for the search of the absolute best or optimum solution out of many, especially where independent parameters are considerable in number. This is especially of greater importance where the performance of the system bears nonlinear and complex connection to the design parameters. Sensitivity analysis laterally loaded pile is one of those kinds. Haftka et al. (1990) worked on structural optimization in solid mechanics and its applications. In their book, "Elements of Structural Optimization", they have elaborately discussed the methods of structural optimization and cited numerous practical examples. Haftka et al. writes, "Optimization is concerned with achieving the best outcome of a given objective while satisfying certain restrictions." The purpose of such endeavor is to utilize the existing parameters connected to a given system in a manner that maximize the output or ensures best desired service or performance. Before the advent of high speed computers most of the solutions of structural analysis problems were based on formulations employing differential equations. Today high speed computers have a profound effect on structural analysis solution procedures. Techniques that were well suited to computer implementation, in particular the finite element method have become dominant. In the finite element method the structural system is discretized

into finite elements and as a result the unknowns are the discrete values of displacements, reactions and stresses at the nodes of the finite element model, rather than the functions. As a clear advantage over earlier methods is that the differential equations solved by the earlier analyst are replaced by system of algebraic equations for the variables that describe the discretized system. In the present environment a designer is expected to provide interface between a commercially available analysis program, and a commercially available optimization software package. The three most important ingredients of the interface are: sensitivity derivative calculations, construction of an approximate problem and evaluation of results for the purpose of fine-tuning the approximate problems or the optimization method for maximum efficiency and reliability.

Conte, J. P. et al. (2003) published the research work on response sensitivities of dynamic models of structural systems to both material and (discrete) loading parameters. They have employed plasticity-based finite-element models of structural systems subjected to base excitation such as earthquake loading in their investigation. The two methods for computing the response sensitivities, namely, (1) discretizing in time the time continuous-spatially discrete response equations and differentiating the resulting time discrete-spatially discrete response equations with respect to sensitivity parameters, and (2) differentiating the time continuous-spatially discrete response equations with respect to sensitivity parameters and discretizing in time the resulting time continuous-spatially discrete response sensitivity equations, are clearly distinguished. In the paper the procedure to obtain the exact sensitivities of the numerical nonlinear finite-element

response is described and their discontinuities are identified. Application examples illustrating the concepts are presented at the end.

Sanders, B. F. and Katopodes, N. D. (2003) employed adjoint method of sensitivity to water wave control in river and estuarine systems. This adjoint sensitivity method based on the shallow-water equations is developed for water wave control in river and estuarine systems. Suitable equations have been derived for the adjoint problem and a new formulation is proposed for the sensitivity of shallow-water flow to boundary changes in depth and discharge. New adjoint boundary conditions are developed for river and estuarine forecasting models with open-water inflow and outflow sections.

2.5 Review of literature on sensitivity of laterally loaded piles

Sensitivity analysis of pile is relatively a new field; not too many researchers worked on sensitivity of laterally loaded pile. It is not recorded if any researcher has yet worked on sensitivity of laterally loaded pile embedded in sand. The purpose of sensitivity analysis is to determine how sensitive is the performance or structural response of a system to the change of the design variables.

Budkowska, B.B. (1997) in her paper showed generalized theoretical approach to the formulation of sensitivity of laterally loaded pile embedded in homogeneous linear elastic soil. The approach in the paper is based on variational calculus. The determination of variation of functional, which depends on generalized state variables and the design variable vector, was devised through solving differential equation. The methods of

sensitivity analysis have been proposed. Method of adjoint or dummy load has been highlighted, and requirements and conditions of this method have been stated. In the application of general formulation to the sensitivity analysis of laterally loaded piles, the main focus is concentrated on the functional of kinematic and static field components. This paper provides the theoretical expertise and tools required for sensitivity analysis of laterally loaded pile. The pile is modeled as one-dimensional beam element. Each vector and the identified operation defined in the general formulation of sensitivity problem, is presented explicitly for investigation of laterally loaded pile in the framework of sensitivity theory.

Budkowska, B. B. and Szymczak. C. (1995) published a paper on sensitivity of laterally loaded piles. In the paper on sensitivity analysis of internal forces generated in the pile and arbitrary displacement of the pile due to change in cross sectional dimension, material constant of pile and parameters of soil has been performed. This has been done with the aid of adjoint structure. Through this research formulation of variation of extremum value of displacement and internal forces was developed for engineering problems dealing with system optimization, identification and reliability of pile structure. The pile has been modeled as one dimensional beam and soil around the pile is represented as Winkler type elastic foundation. Because of the nature of the modeling of the pile-soil system the researchers suggested that the procedure could be applied to both linear and nonlinear systems. Then constant variations of design variables, EI and k have been injected to the system. Change in the flexural moment has been determined and graphically represented. The maximum change and the location of the occurrence the maximum change have been identified. Accuracy of the procedure has been discussed in

the paper. The results obtained in the numerical example using the formulation have been compared with the actual values calculated through finite element method. For the finite element method the pile has been discretized into twenty elements. The calculated value of change of maximum flexural moment, determined with the proposed formulation, was approximate and close to the actual value obtained by finite element method. Through the study of the values of the numerical example the researchers found the procedure works good for changes of design variables up to 40% of initial values.

Budkowska, B. B. and Priyanto, D. G. (2002)^b compared the sensitivity integrands for short piles and long piles embedded in soft clay located below water table. They considered cyclic loading that was applied at the soil surface. The p - y model was employed to simulate the soil effect on the behaviour of the pile-soil system. The pile-soil strength parameters were chosen as the design variables and identified a five parameter system. The equation of first variation of deformation determined depend on the sensitivity operators connected to each of the design variables. The sensitivity operators presented are strongly dependent on the magnitude of the applied load.

In 2002, Budkowska, B. B. and Suwarno, D. presented the sensitivity analysis of maximum displacement of a pile group, embedded in stiff clay below water table, under lateral loading and performed the assessment of sensitivity parameters. The p -multipliers were applied to account for the group effect. The sensitivity formulation was developed by the aid of the adjoint method. A procedure was developed to make the adjoint structure be in the state of deformation as the primary structure. The sensitivity of

maximum deflections due to the changes of the variables are presented in terms of the space dependent sensitivity intergrands.

2.6 p - y relationships used by contemporary researchers

Suwarno, D. (2003) in his thesis worked on sensitivity analysis of laterally loaded pile embedded in stiff clay under the thesis title – “Nonlinear deformation of laterally loaded piles embedded in stiff clay located below the water table – sensitivity analysis.” In his research work of sensitivity analysis of laterally loaded single piles and group of piles by means of adjoint method, the soil around the pile is modeled by p - y relationship and the pile is modeled as one dimensional beam element. The parameters, which define the mechanical behaviour of soil, are a cohesion of the soil (c), the modulus of subgrade reaction (k), effective unit weight (γ') and the strain at which 50% soil strength is mobilized (ε_{50}). Suwarno, D. in his research used the p - y model proposed by Reese, Cox and Koop in 1975. According to this model the ultimate soil resistance p_s is given by the equation as follows:

p_{st} = ultimate soil pressure p_s at a depth $x < x_r$ and

p_{sd} = ultimate soil pressure p_s at a depth $x > x_r$

$$p_{st} = 2c_a b + \gamma' b x + 2.83c_a x \quad 2-7$$

$$p_{sd} = 11c_a b \quad 2-8$$

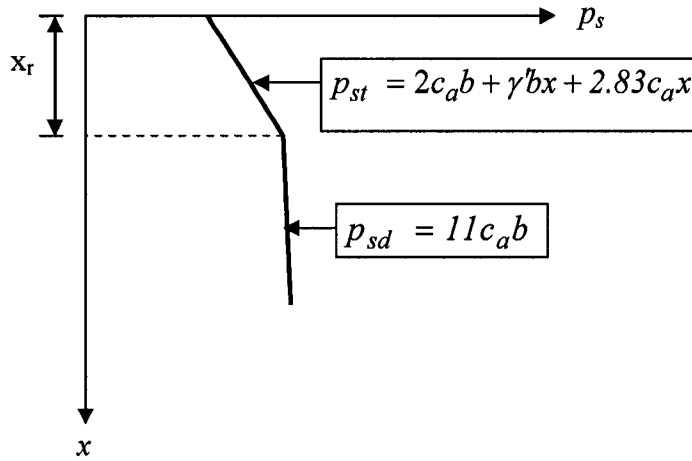


Figure 2-2 Ultimate soil resistance of stiff clay below water table (Reese et al. 1975).

where:

c_a = average undrained soil shear strength,

b = width of diameter of pile,

γ' = submerged weight of the soil,

The depth above and below which the function for ultimate soil response p_s differs is give by the equation:

$$x_r = \frac{9c_a b}{\gamma' b + 2.83c_a} \quad 2-9$$

Ultimate soil resistance of stiff clay located below water table according to this model is graphically shown in Figure 2-2.

The p - y curve for stiff clay below water table consists of five segments corresponding to five phases of soil behaviour. These phases are: the linear elastic, the non-linear elastic, the non-linear softening, the linear softening and the plastic flow. The soil reaction equations for soil resistance p according to the investigated soil model are as follows.

For linear elastic zone, $0 \leq y \leq y_l$ and soil pressure,

$$p = kxy \quad 2-10$$

where:

y = the deflection of pile.

For nonlinear elastic zone, $y_l \leq y \leq A_s y_{50}$ and soil pressure,

$$p = 0.5p_u \left(\frac{y}{y_{50}} \right)^{0.5} \quad 2-11$$

$$y_{50} = 2.5(\varepsilon_{50})b \quad 2-12$$

The y_l can be obtained by equating value of p of linear elastic zone (Equation 2-10) and nonlinear elastic zone (Equation 2-11).

For nonlinear softening zone, $A_s y_{50} \leq y \leq 6A_s y_{50}$ the soil pressure,

$$p = 0.5p_u \left(\frac{y}{y_{50}} \right)^{0.5} - 0.055p_u \left(\frac{y - A_s y_{50}}{A_s y_{50}} \right)^{1.25} \quad 2-13$$

where A_s is a coefficient that depends on depth, x (COM 624 Manual).

A graphical representation of soil resistance versus deflection y is shown in Figure 2-3.

For linear softening zone, $6A_s y_{50} \leq y \leq 18A_s y_{50}$ the soil pressure,

$$p = 0.5p_s (6A_s)^{0.5} - 0.411p_u - \frac{0.0625}{y_{50}} p_u (y - 6A_s y_{50}) \quad 2-14$$

For plastic flow zone, $18A_s y_{50} \leq y$ the soil pressure,

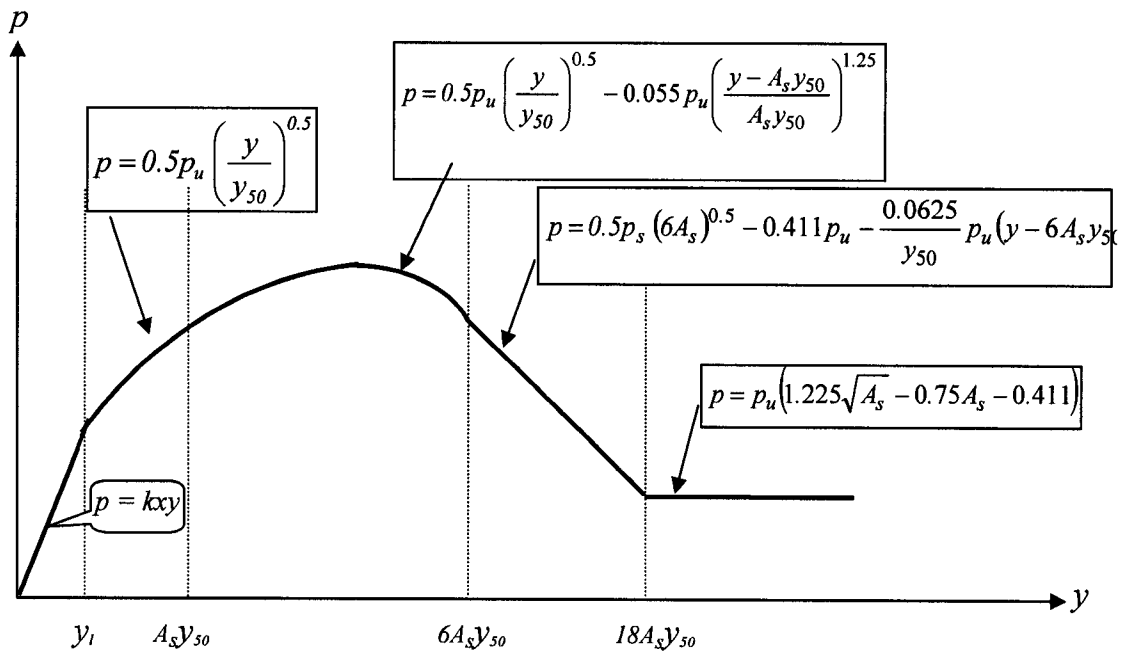


Figure 2-3 p - y curve for stiff clay (Reese et al., 1975).

$$p = p_u (1.225\sqrt{A_s} - 0.75A_s - 0.411) \quad 2-15$$

Priyanto, D. G. (2002) worked on sensitivity analysis of laterally loaded pile embedded in soft clay under the thesis title – “Piles embedded in soft clay located below the water table subjected to lateral cyclic loadings – sensitivity analysis.” Although soft clay and the stiff clay both have same type of physical parameters to represent their mechanical behaviour, their behaviour under lateral load is substantially different. They cannot be represented by same soil model. Priyanto, D. G. modeled the soft clay soil by p - y curve proposed by Matlock (1970). In his research work of sensitivity analysis of laterally loaded single piles and group of piles by means of adjoint method, the soil around the pile is represented by p - y model and the pile is modeled as one dimensional beam element. The parameters, which define the mechanical behaviour of soil, are the cohesion of the soil (c), the modulus of subgrade reaction (k), submerged unit weight (γ') and the strain at which 50% soil strength is mobilized (ϵ_{50}). The p - y model that has been used in research was proposed by Matlock, H (1970). Matlock had performed full scale experiment on pile embedded in soft clay located below water table. According to Matlock-model ultimate soil resistance p_s is given as follows.

p_{st} = ultimate soil pressure at depths $x < x_r$

p_{sd} = ultimate soil pressure at depths $x > x_r$

$$p_{st} = \left(3 + \frac{\gamma'}{c} x + \frac{0.5}{b} x \right) cb \quad 2-16$$

$$p_{sd} = 9cb \quad 2-17$$

where: c – undrained cohesion of soil,

b – width of diameter of pile,

γ' - submerged weight of the soil

and

$$x_r = \frac{6c_d b}{\gamma' b + 0.5c} \quad 2-18$$

Equations 2-16 to 2-18 are represented graphically in Figure 2-4.

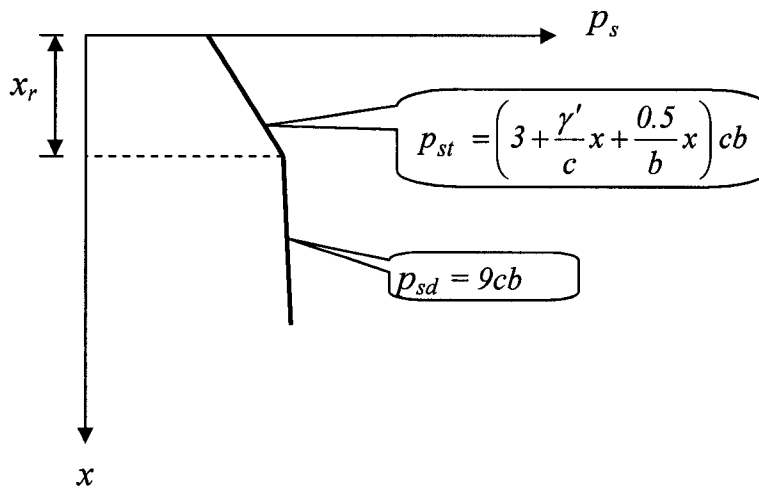


Figure 2-4 Ultimate soil resistance of soft clay below water table (Matlock, 1970).

The horizontal displacement of the soil y is defined in terms of y/y_{50} , the value of y_{50} for soft clay is given by the following expression.

$$y_{50} = 2.5 (\epsilon_{50}) b \quad 2-19$$

Under lateral load, soft clay and stiff clay display different mode of deformation. Stiff clay, as shown in Suwarno's research, is able to create five different phases with different values of deflection, y , whereas, soft clay displays maximum of three phases, which are nonlinear elastic, linear softening and plastic flow. According to Matlock (1970) model of soft clay below water table has the soil reaction pressure p given by the following equations.

For $0 \leq y \leq 3y_{50}$ and $x \leq x_r$ soil pressure,

$$p = 0.5 p_{st} \left(\frac{y}{y_{50}} \right)^{1/3} \quad 2-20$$

For $3y_{50} \leq y \leq 15y_{50}$ and $x \leq x_r$ soil pressure,

$$p = p_{st} \left[\left(0.9 - 0.18 \frac{x}{x_r} \right) - 0.06 \left(\frac{y}{y_{50}} \right) \left(1 - \frac{x}{x_r} \right) \right] \quad 2-21$$

For $y \geq 15y_{50}$ and $x \leq x_r$ soil pressure,

$$p = 0.72 p_{st} \frac{x}{x_r} \quad 2-22$$

For $0 \leq y \leq 3y_{50}$ and $x \geq x_r$ soil pressure p ,

$$p = 0.5 p_{sd} \left(\frac{y}{y_{50}} \right)^{1/3} \quad 2-23$$

And for $y \geq 3y_{50}$ and $x \geq x_r$ soil pressure,

$$p = 0.72 p_{sd}$$

2-24

A graphical representation of soil resistance versus deflection y according to Matlock's model is shown in Figure 2-5.

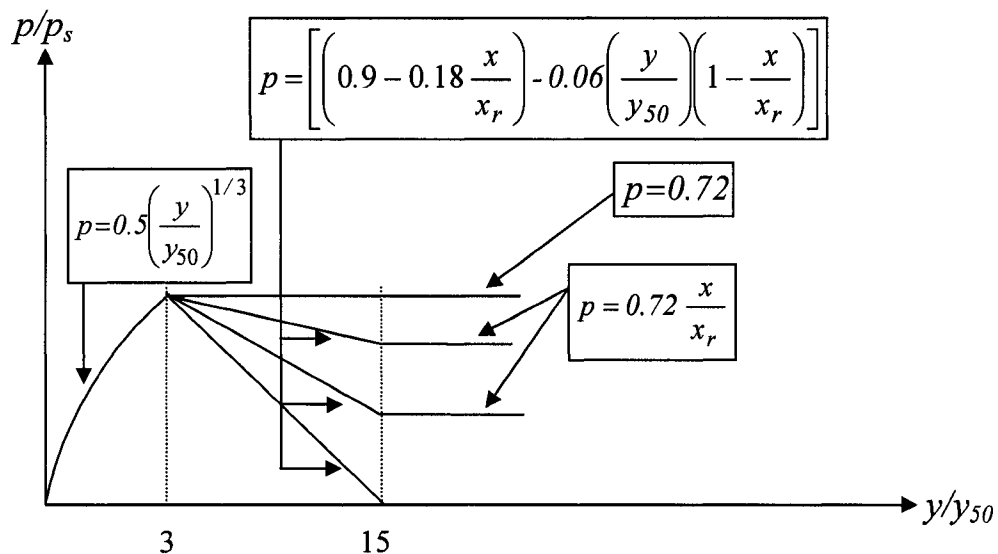


Figure 2-5 p - y curve for soft clay (Matlock, 1975).

Liu, L. (2004) worked on sensitivity analysis of laterally loaded pile embedded in stiff clay above the water table under the thesis title – “Piles embedded in stiff clay located above the water table subjected to lateral cyclic loadings – sensitivity analysis.”

Stiff clay above water table and stiff clay below water table displays different mode of deformation under lateral load. Although both have same physical parameters to represent their mechanical behaviour, their behaviour under lateral load is substantially different. They cannot be represented by same soil model. Liu, L. modeled the soil by p - y curve proposed by Welch, R. C. and Reese, L. C. (1972). In his research work of sensitivity analysis of laterally loaded single piles and group of piles by means of adjoint method, the soil around the pile is represented by p - y model and the pile is modeled as one dimensional beam element. The parameters, which define the mechanical behaviour of soil, are cohesion of the soil (c), the modulus of subgrade reaction (k), unit weight of soil (γ) and the strain at which 50% soil strength is mobilized (ϵ_{50}). According to this model ultimate soil resistance p_s is given as follows.

p_{st} = ultimate soil pressure at a depth $x < x_r$

p_{sd} = ultimate soil pressure at a depth $x > x_r$

$$p_{st} = \left(3 + \frac{\gamma}{b} x + \frac{0.25}{b} x \right) cb \quad 2-25$$

$$p_{sd} = 9cb \quad 2-26$$

where:

c – undrained cohesion of soil,

b – width of diameter of pile,

γ - weight of the soil,

$$x_r = \frac{6c_a b}{\gamma b + 0.25 c} \quad 2-27$$

Equations 2-35 to 2-37 are represented graphically in Figure 2-6.

The horizontal displacement of the soil y is defined in terms of y/y_{50} , the value of y_{50} for soft clay is given by the following expression.

$$y_{50} = 2.5 (\epsilon_{50}) b \quad 2-28$$

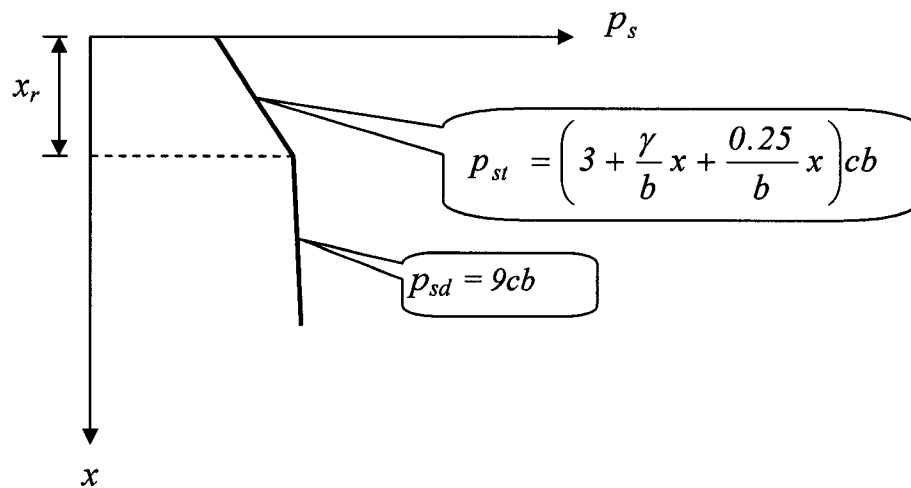


Figure 2-6 Ultimate soil resistance of stiff clay above water table (Welch et al., 1972).

According to Welch's et al. (1972) model the soil pressure is given by the following equations.

For $y \leq 16 y_{50} + 9.6 y_{50} \log N$, soil response,

$$p = .05 p_u \left(\frac{y}{y_{50} \left(1 + \frac{9.6}{16} \log N \right)} \right)^{\frac{1}{4}} \quad 2-29$$

where:

N = number of load cycles.

For $y \geq 16 y_{50} + 9.6 y_{50} \log N$, soil response,

$$p = p_u \quad 2-30$$

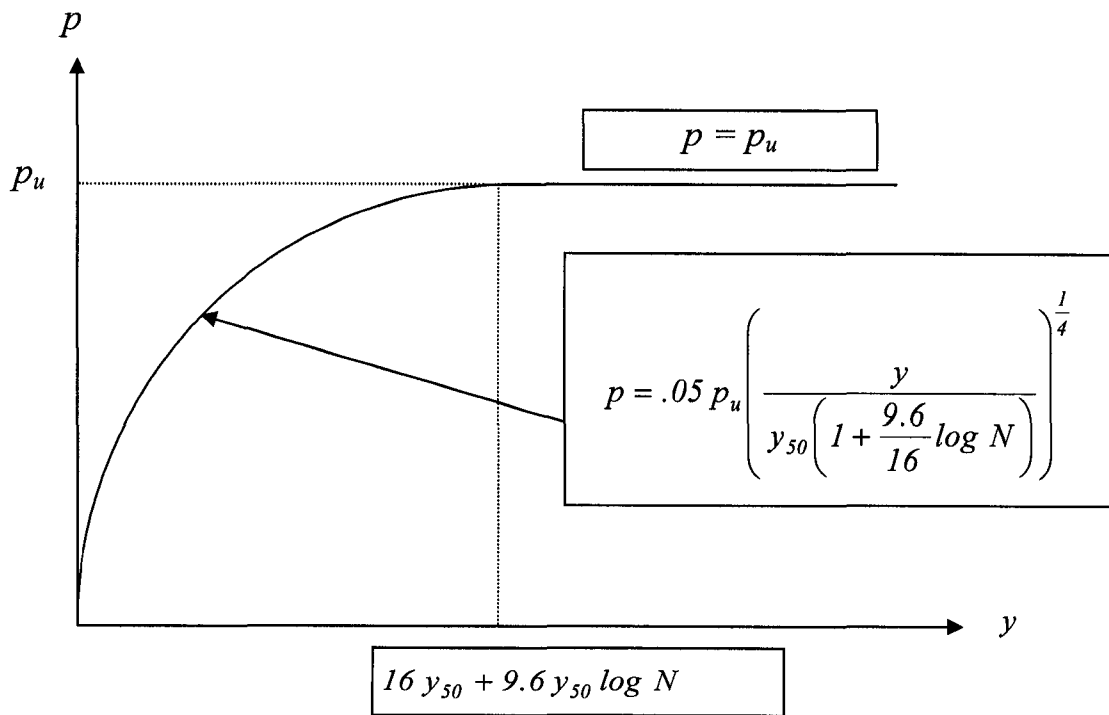


Figure 2-7 p - y curve for stiff clay (Welch et al., 1972).

A graphical representation of soil resistance versus deflection y according to Welch et al. (1972) model is shown in Figure 2-7.

2.7 Soil model employed in the current research

The current research is the analysis of laterally loaded piles, single piles and group of piles, embedded in sand subjected to lateral loadings- sensitivity investigation. The soil around the pile has been represented by p - y model of sand. The p - y model of sand that is employed in this investigation provides reliable basis for assessment of the pile-soil interaction behaviour. This soil model developed by Cox, Reese and Grubbs (1974) is based on extensive field studies of natural size piles subjected to bending. It is developed for sand adjacent to the pile. This model enjoys high popularity among engineers and designers all over the world. Its formulation employs the ultimate soil resistance p_s , which is the continuous function of spatial variable x . This investigation has a resemblance to work of Priyanto (2002), Suwarno (2003) and Liu (2004). The soil models used by three of the researchers are different from each other. Although soil in all of the three models has the same soil parameters, their mode of deformation under lateral load are different. The p - y model of sand that is employed in this investigation is also different from the two soil models mentioned above. The p - y model employed in this research had been proposed for frictional soil by Cox, et al. in 1974. The mechanical parameters of the pile-soil system include the coefficient of subgrade reaction k , the submerged unit weight γ' , the angle of internal friction ϕ , the coefficient of active lateral

earth pressure K_a of Rankine type and the width b of the pile at which the soil reaction p is developed. They are termed as design variables and expressed in vector form as:

$$\bar{s} = [EI, k, \gamma', \phi, K_a, b]^T \quad 2-31$$

Detailed model of p-y and sensitivity investigation on sand are included in the following chapters.

CHAPTER III

BEHAVIOR OF LATERALLY LOADED SINGLE PILE EMBEDDED IN SAND

3.1 Behaviour of laterally loaded pile embedded in sand

When a pile is loaded by lateral force the pile deflects creating soil resistance to pile movement due applied force. A schematic representation of laterally loaded pile is given in Figure 3-1.

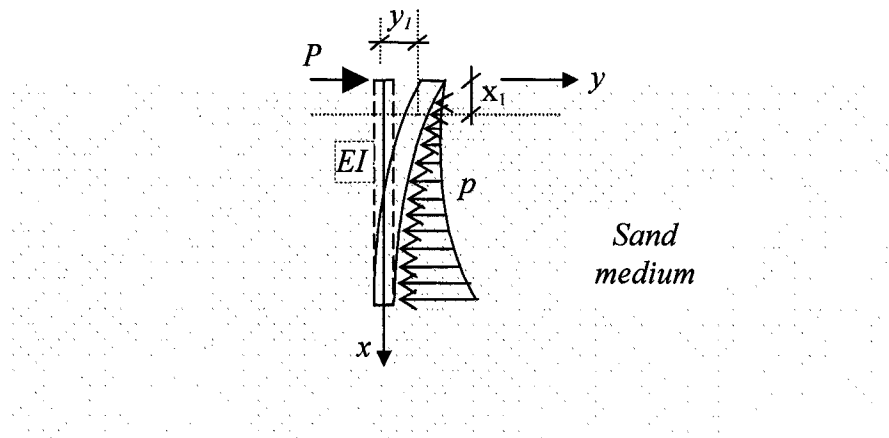


Figure 3-1 Laterally loaded pile embedded in sand.

Without application of lateral load the pile embedded in soil is subjected to static soil pressure; under applied lateral force P , the pile deflects and active, passive, frictional forces etc. come into being making the analysis a bit complicated. Assuming pile deflection y_1 at a depth x_1 due to the application of force P as shown in Figure-3-1 a qualitative diagram at depth y_1 can be drawn showing soil reaction on the pile. If a

horizontal force P is applied to the pile head in the y direction as shown in Figure 3-1 resultant of soil response p will be in negative y direction as shown qualitatively in the Figure 3-2.

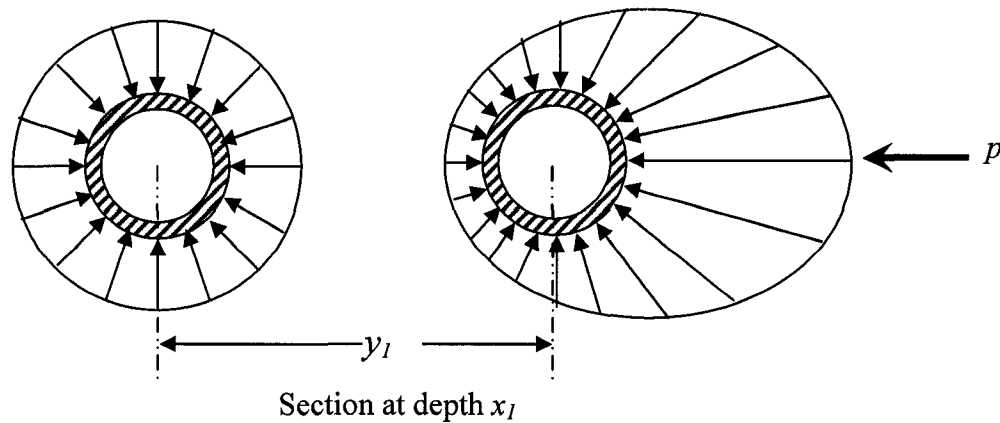


Figure 3-2 Qualitative diagram of pile deflection and associated soil reaction .

The analysis of pile under lateral loading is a problem in soil-structure interaction; that is the deflection of the pile is dependent on the soil response and the soil response is a function of pile deflection. Thus, the problem cannot be solved by the equations of static equilibrium, but a differential equation must be solved to obtain the deflection of the pile. Iteration must be employed because the soil response is a non-linear function of pile deflection and position along the length of the pile.

The pile can be considered as a beam supported by soil reaction p developed due to deflection of the pile as a result of horizontal force P or bending moment M applied at the top of the pile. The differential equation that governs the relationship of force and deformation along the length of the pile when modeled as beam can be written as follows.

$$EIy^{IV} + p = 0$$

3-1

where:

EI = is the flexural stiffness of the beam,

y = is the deflection of the pile at a depth x ,

p = is the resultant reaction of soil on the pile per unit length of the pile due to the deflection of the pile caused by application of load P at pile head.

Equation 3-1 holds well when the soil mass is unaffected by the installation process of the pile and to have no slippage or separation of the interface with the pile and the surrounding soil. In practice variety of sets of boundary conditions at the top of the pile is possible. The condition of equilibrium and compatibility has to be satisfied. If a pile extends upwards to support a road sign, the two boundary conditions consists of a shear and a moment. If a pile extends upward to form a part of the superstructure, the two boundary conditions consist of a shear and a rotational restraint. In order to select the proper magnitude of the rotational restraint, iteration between pile foundation and the superstructure is usually necessary. If a pile extends upward and is embedded in a concrete mat such as the base of a retaining wall, an acceptable solution in some cases is to assume that the pile head is fully fixed against rotation. The shear force may be selected by dividing the total lateral load of the wall by the number of piles. There may be occasions when the deflection at the pile head is one of the known boundary conditions. For example, a bridge may be constructed in such a way that the lateral

deflection of the pile head is limited to a known amount. The model pile may be either in free or fixed head condition. In order to solve Equation 3-1 the pile-soil system has to be represented by appropriate model. There are three well-known approaches of analyzing pile-soil system under lateral load. They are: modulus of subgrade approach, the elastic continuum theory and p - y relationship approach. The p - y method is employed in this research.

3.2 The p - y relationship used to model the sand around a pile

In this approach the pile-soil system is modeled as one dimensional beam, with the pile resting on adjacent soil. The $p - y$ relationship, developed by Cox, Reese and Gubbs (1974), connects the soil resistance p to the pile's deflection y at arbitrary depth x below the surface through p - y curves. For a particular depth there is a p - y curve, unique for a sample of sand but to represent the entire medium of sand adjacent to the pile in question families of infinite number of p - y curves have to be drawn. This model uses common soil strength parameters to simulate the soil resistance-deflection behaviour. It is developed for sand adjacent to the pile. It is based on extensive field studies of piles embedded in soil. An extensive series of tests were performed at a site on Mustang Island, near Corpus Christi (Cox, Reese, and Grubbs, 1974). Two steel pipe piles, 0.61m (24 inch) in diameter, were driven into sand in a manner to simulate the driving of an open-ended pipe, and were subjected to lateral loading. The embedded length of the piles was 21.0 m (69 feet). One of the piles was subjected to short-term loading and the other to repeated loading. The soil at the site was uniformly graded, fine sand with an angle of

internal friction $\phi = 39^\circ$. The submerged unit weight was 10.37 kN/m^3 (66 lb/ft^3). The water surface was maintained a few inches above the mudline throughout the test program. This model is applicable to sand above and below ground water table.

The correlation that has been developed for predicting soil responses have been based on the best estimate of the properties of the in-situ soil with no adjustment for the effects on soil properties of the method of installation. The logic supporting the approach is that the effect of pile installation on soil properties are principally confined to a zone of soil close to the pile surface, while a mass of soil of several diameters from the pile is stressed as lateral deflection occurs. There are instances, for example, if a pile is jettied into place, a considerable volume of soil could be removed with a significant effect on the soil response.

The formulation of p - y sand model employs the ultimate soil resistance p_s , which is the continuous function of spatial variable x that starts from the soil surface and is directed downwards along the pile axis in the top part of the soil. For arbitrary depth, x , the graphical representation of the p - y relationship is shown in Figure 3-3. Three values of lateral deflection y denoted as y_k , y_m and y_u established the characteristic points of p - y curve. They are shown in Figure 3-3 and marked as points 0, 1, 2 and 3. They are assessed based on the pile's width b as:

$$y_m = \frac{b}{60} \quad 3-2$$

$$y_u = \frac{3b}{80} \quad 3-3$$

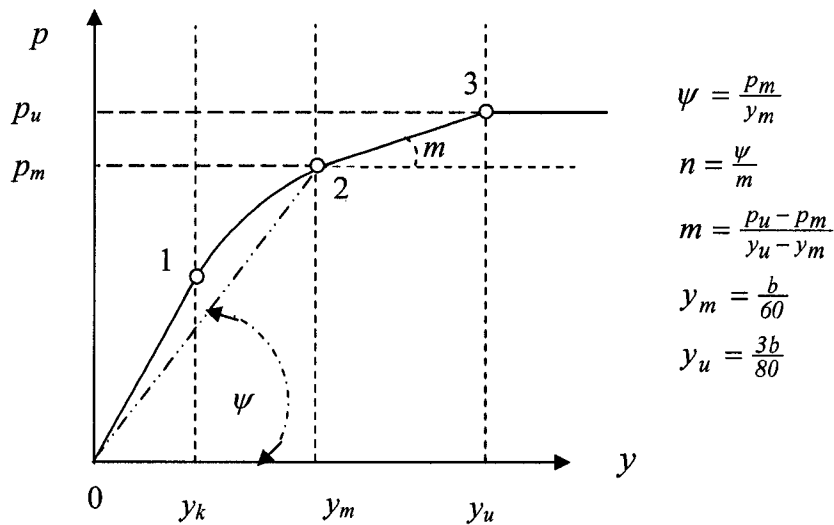


Figure 3-3 Typical p - y curve for arbitrary depth $x > 0$.

As found in the experiment, the value of y_k depends on type of sand whereas those of y_m and y_u are independent of type of sand. Expression for derivation of y_k will be shown later. The ordinates of points 2 and 3 are defined as p_m and p_u , respectively, and are described as:

$$p_m = p_s * B_s \tag{3-4}$$

$$p_u = p_s * A_s \tag{3-5}$$

where:

p_s = the ultimate soil resistance,

A_s and B_s = dimensionless coefficients which depend on depth x and are shown in Figures 3-4 and 3-5, respectively, as a function of normalized quantity x/b as proposed by Reese et al. (1974).

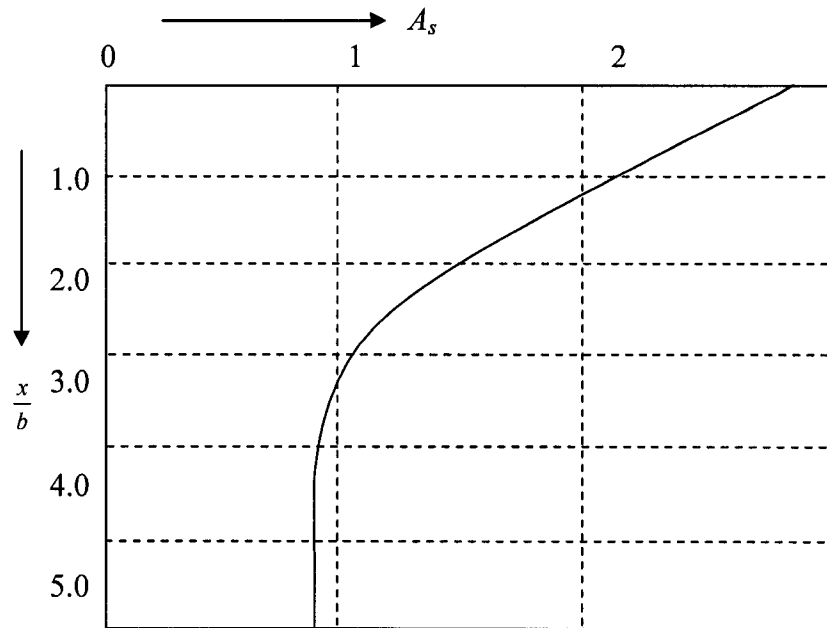


Figure 3-4 Values of coefficient A_s (Reese et al., 1974).

The key constitutive relationship of nonlinear type for arbitrary depth x that passes through points 1 and 2 of Figure 3-3 is given as:

$$p = C y^{\frac{1}{n}} \tag{3-6}$$

The exponent n can be expressed by means of p_m and y_m as follows:

$$n = p_m / (y_m \cdot m) \tag{3-7}$$

The constant, m can be expressed as:

$$m = [p_s(A_s - B_s)]/(y_u - y_m) \quad 3-8$$

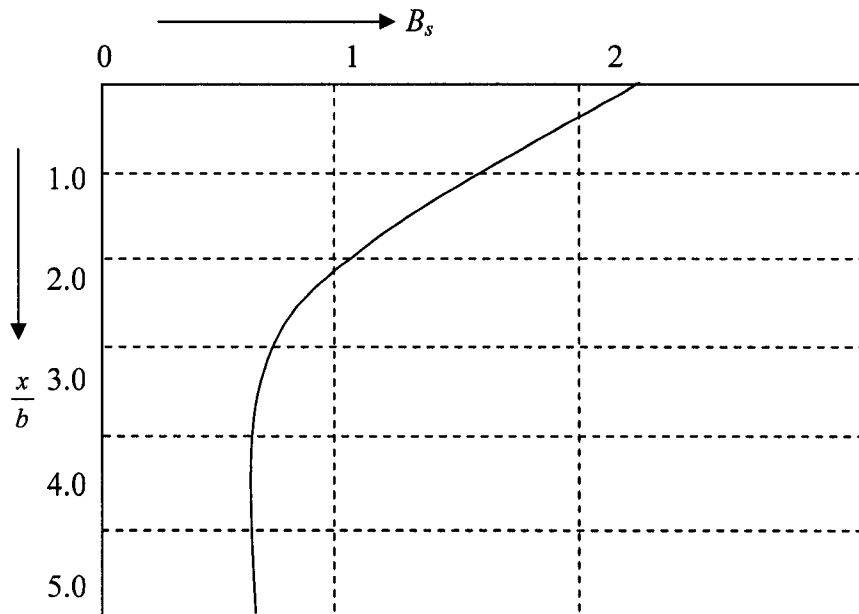


Figure 3-5 Value of coefficient B_s (Reese et al., 1974).

The Equations 3-4 and 3-5 can be interpreted by means of Figure 3-3. The parameter m represents the gradient of point 2 with respect to point 3 whereas the ratio p_m/y_m of Equation 3-4 is the gradient ψ of point 0 with respect to point 2. Taking into account Relationships 3-2 and 3-3, the parameter m can be also expressed as:

$$m = p_s(A_s - B_s)/(3b/80 - b/60) \quad 3-9$$

Equation 3-9 shows that in fact m is dependent on the ultimate soil resistance p_s and dimensionless coefficient A_s as well as B_s . The Equation 3-9 leads to the conclusion that

m is cognate to p_s . Substitution of Equation 3-9 together with Equation 3-4 into Equation 3-5 enables one to express n as:

$$n = 1.25 / (A_s / B_s - 1) \quad 3-10$$

This means that exponent $1/n$ of Equation 3-10 can be written in the following form:

$$1/n = 0.8(A_s / B_s - 1) \quad 3-11$$

The C value of Equation 3-6 can be established from the fact that physical relationship given by Equation 3-6 must be satisfied at point 2 of Figure 3-3. Thus,

$$p_m = C (y_m)^{\frac{1}{n}} \quad 3-12$$

Substituting Equation 3-4 for p_m and Equation 3-11 for the exponent $\frac{1}{n}$ in Equation 3-12 we arrive at:

$$C = B_s p_s (60/b)^{0.8(A_s/B_s - 1)} \quad 3-13$$

Finally combining Equations 3-13 and 3-11 with Equation 3-6, the p - y relationship that passes through points 0, 1, and 2 is given as:

$$p = B_s p_s (60y/b)^{0.8(A_s/B_s - 1)} \quad 3-14$$

The p - y model of sand discussed in the initial stage of deformation described between points 0, 1 that is for $y \leq y_k$ is defined by the following relationship:

$$p = kxy \quad 3-15$$

where:

k - the coefficient of subgrade reaction.

The sand at this stage of deformation is called to be in linear phase and equation 3-15 represents the portion of the curve between point 0 and 1.

The physical behaviour of sand when subjected to lateral deformations $y_m \leq y \leq y_u$ is described by the following relationship:

$$p = p_s \left[B_s + \left(y - \frac{b}{60} \right) \frac{A_s - B_s}{0.02086 b} \right] \quad 3-16$$

It is worth noting that for constant depth x , Equation 3-16 defines bi-linear behavior. When the lateral deformations approach $y = y_u$ the soil reaction p_u is given by Equation 3-5. The graphical representation of Equation 3-5 which describes plastic flow is shown in Figure 3-3. For any value of deflection greater than y_u , that is for $y > y_u$, Equation 3-5 remains valid.

At value of $y = y_k$, the soil (sand) pressure obtained from Equations 3-14 and 3-15 should be the same. So, equating value of p from Equations 3-14 and 3-15 after inserting, $y = y_k$, the following is obtained:

$$y_k = \left[\frac{B_s p_s}{kx} \left(\frac{60}{b} \right)^{0.8} \left(\frac{A_s}{B_s} - 1 \right) \right] \left(\frac{1.25}{2.25 - \frac{A_s}{B_s}} \right) \quad 3-17$$

The ultimate soil resistance in sand, p_s per unit length of pile is a function of depth x and there is a characteristic depth x_r above which the soil resistance p_{st} is given by Equation 3-18 (Cox, Reese, and Grubbs, 1974).

$$p_{st} = \gamma' x \left[\frac{K_0 x \tan \phi \tan \beta}{\tan(\beta - \phi) \tan \alpha} + \frac{\tan \beta}{\tan(\beta - \phi)} (b + x \tan \beta \tan \alpha) + K_0 x \tan \beta (\tan \phi \sin \beta - \tan \alpha) - K_a b \right] \quad 3-18$$

and the ultimate soil resistance in sand, p_{sd} below x_r is given by Equation 3-19 as:

$$p_{sd} = K_a b \gamma' (\tan^2 \beta - 1) + K_0 \beta \gamma' x \tan \phi \tan \beta \quad 3-19$$

where:

γ' = submerged unit weight of sand,

ϕ = angle of internal friction,

$\alpha = \phi/2$,

$\beta = 45 + \frac{\phi}{2}$,

K_a = the coefficient of active lateral earth pressure of Rankine's type equal to

$$= \tan^2 (45 - \phi/2)$$

K_o = coefficient earth pressure at rest = 0.4,

b = width of pile at depth x .

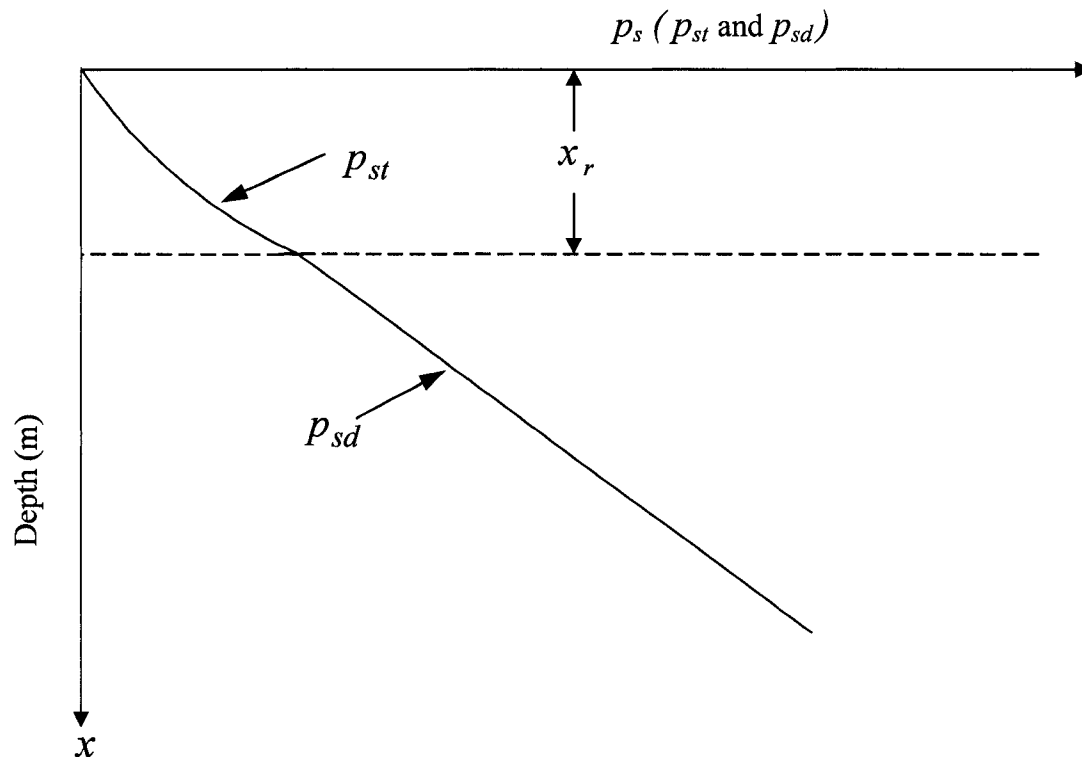


Figure 3-6 Variability of ultimate soil resistance p_s (p_{st} and p_{sd}) of qualitative type around laterally loaded piles embedded in sand.

At depth $x = x_r$, p_{st} and p_{sd} assure the continuity of ultimate soil pressure p_s . So equating them, the following relationship for x_r is established.

$$x_r = \frac{b \tan \beta \left[K_a \tan^7 \beta + K_o \tan \phi \tan^3 \beta \frac{1}{\tan(\beta - \phi)} \right]}{\frac{K_0 \tan \phi \sin \beta + \tan^2 \beta \sin \alpha}{\tan(\beta - \phi) \cos \alpha} + K_0 \tan \beta (\tan \phi \tan \beta - \tan \alpha)} \quad 3-20$$

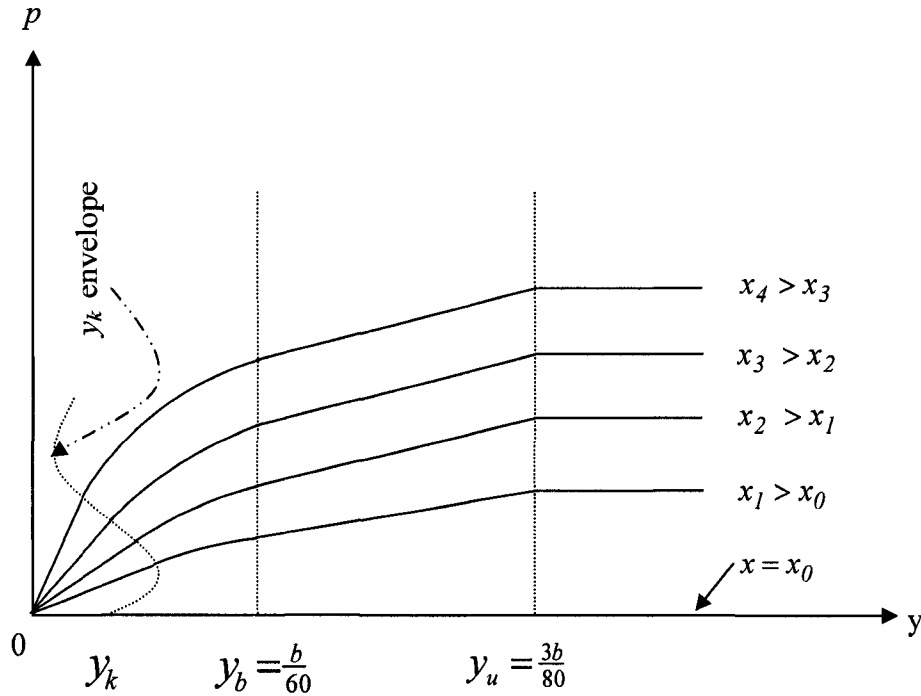


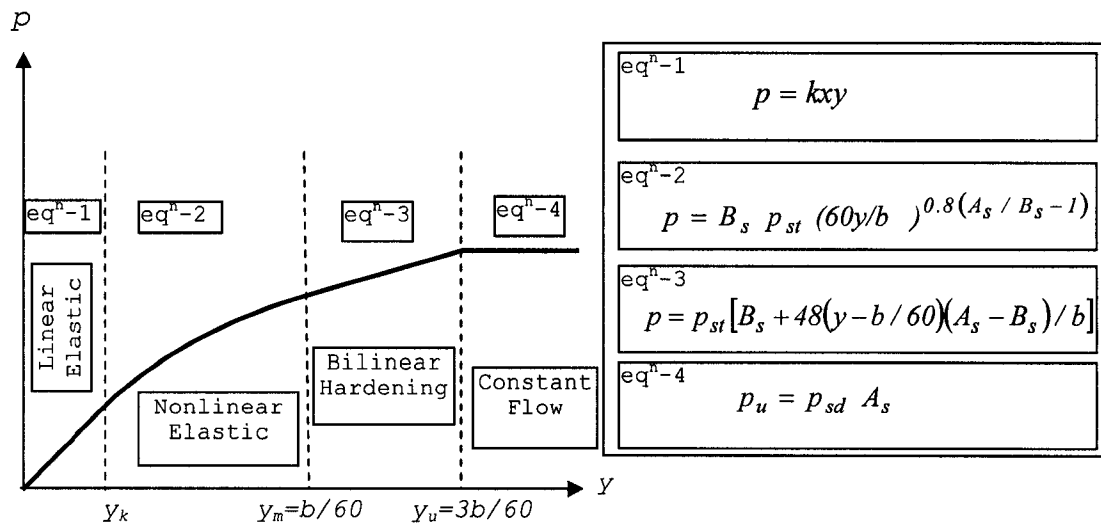
Figure 3-7 Family of p - y curves for different value of x .

A graphical presentation of ultimate soil pressure p_s with respect to depth x is given in Figure 3-6. For a constant value of x depending on the different value of deformation, y , starting from low to high, sand in the vicinity of the pile under lateral load passes through four phases. They are linear elastic, nonlinear elastic, bi-linear elastic and plastic flow phase. All four phases are represented by a p - y curve, uniquely for that value of depth x .

Choosing different values of depth x a series of p - y curves are required to model the sand around the pile throughout the length of the pile. A qualitative diagram showing a series

of such p - y curves are given in Figure 3-7. The components of p - y curves above x_r are summarized in Figure 3-8a. The components of p - y curves below x_r are summarized in Figure 3-8b.

$$p_{st} = \gamma x \left[\frac{K_0 x \tan \phi \tan \beta}{\tan(\beta - \phi) \tan \alpha} + \frac{\tan \beta}{\tan(\beta - \phi)} * (b + x \tan \beta \tan \alpha) + K_0 x \tan \beta (\tan \phi \sin \beta - \tan \alpha) - K_a b \right]$$



where γ = unit weight of sand; ϕ = angle of internal friction; $\alpha = \phi/2$; $\beta = 45 + \phi/2$; $K_a = \tan^2(45 - \phi/2)$; $k_0 = 0.4$ and b = width of pile at depth x .

Figure 3-8a Components of p - y curve above x_r .

$$P_{sd} = k_a b \gamma' (\tan^{\delta} \beta - 1) + k_0 \beta \gamma' x \tan \phi \tan \beta$$

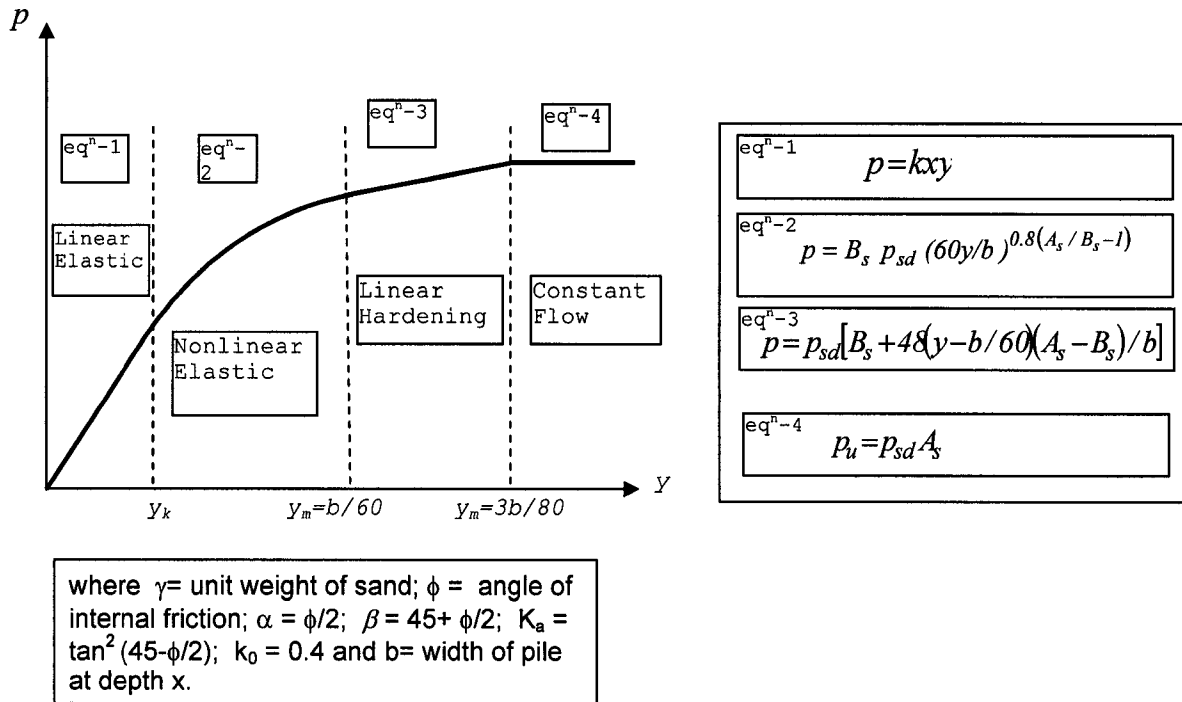


Figure 3-8b Components of p - y curve below x_r .

3.3 Computer program COM624P used in the investigation of single piles

For any horizontal force or bending moment applied to the pile, a deflection y and a soil resistance p can be calculated by solving the differential equation of beam using boundary conditions and p - y curves through iterations. But this would be a time consuming and difficult process because of the following reasons.

- Non-linear relationship exists between soil resistance and deflection.
- Deflection y is a non-linear function of load applied and soil response.

-
- c) There are many segments of p - y curves.
 - d) Pile deflection being substantial has to be considered in calculations.
 - e) Deflection and soil response depend on depth, x .
 - f) Depending on the pile length, soil strength, stiffness of pile and applied load the pile may deform in many different modes. For example the behavior of a long pile shows that the deflection oscillates back and forth about the axis of the undeformed pile so that there are a number of points of zero deflections.

These predicaments have been overcome through the use of computer program COM624P. The numerical investigations are conducted by the finite difference program COM624P of Wang and Reese (1993). The technology on which the program is based is the widely-used p - y curves method. The program solves the differential equation involving the pile-beam giving pile deflection, rotation, bending moment, and shear by using iterative procedure because of the non-linear response of the soil. This program can be used not only to analyze laterally loaded single pile with various pile head conditions and loadings, but also groups of pile by applying the p -multipliers to the pile. Through the use of COM624P a large number pile cases have been analyzed which would otherwise have not been possible.

CHAPTER IV

GROUP OF PILES

4.1 Introduction

In the field, piles are often arranged in groups, and the behaviour of a pile group differs substantially from that of a single pile. Evidently a group of piles can support a bigger load than a single pile. But piles loose efficiency when used in a group, that is, a single isolated pile carries more load than when used in a group. Deflections of piles in group are greater than deflections of single pile at the same load per pile. This is because of the pile-soil-pile interaction, that is, a pile being a member of a pile group shares the soil area of resistance with other pile or piles. All the member piles of a group are tied together by a rigid concrete pile cap at the ground surface. The response of a laterally loaded pile within a group of closely spaced piles is often substantially different than the response of a single isolated pile. Pile connection to the cap may be fully restrained, pinned or in between these two extremes. In this study, individual piles in a group are treated as single piles after ascertaining the portion, carried by the pile in question, of total load applied to the group as a whole. The member piles are represented as a beam supported laterally by soil, which is modeled using nonlinear load versus deflection curves, the $p-y$ curves. General arrangement of piles in a 3x3 group is shown in Figure 4-1.

The rows of pile stretch perpendicular to the line action of the force. The orientation of rows is shown in Figure 4-2. Measurement of displacement and stresses in full-scale and model pile group tests indicate that piles in the same group carry unequal lateral loads,

because of their location within the group and the spacing between them. This unequal distribution of load among the rows of piles is caused by the shadowing. In closely spaced piles of a group there occurs the overlapping of areas of resistance and as a result unequal reduction of soil resistance. The closer the piles are the more pronounced the effect of shadowing is. For spacing of $6D$, D being the diameter of pile, the shadowing effect is very small and often neglected. So, piles in a group with spacing $6D$ or more usually are treated as single piles.

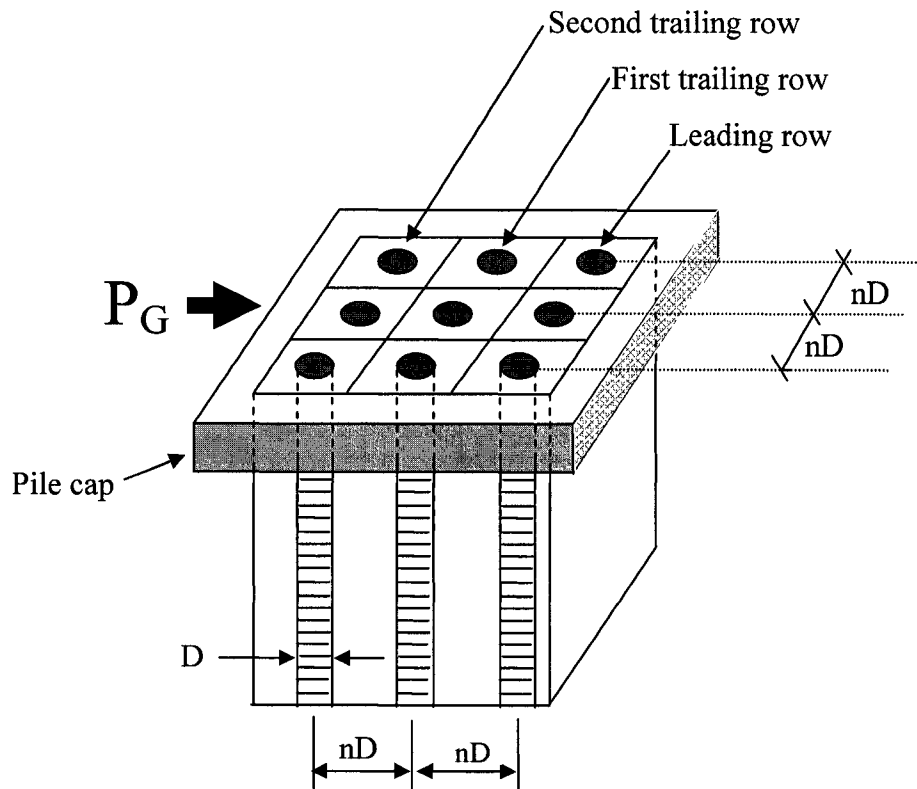


Figure 4-1 3x3 pile group and pile cap in a group of piles.

Piles in the leading row experience the greatest amount of soil reaction followed by that of 1st trailing row and then 2nd. In this research the member piles in the groups are modeled by the same method p - y that is used for single piles, except that p -values in the p - y are reduced multiplying by a p -multiplier, f_m to account for reduced efficiencies caused by pile-soil-pile interaction.

4.2 p -multiplier, f_m employed to model pile group

The concept of p -multiplier was introduced by Brown et al. (1985). They proposed the p -multiplier through large-scale test on pile group and isolated pile embedded in dense sand. Later on different researchers worked on p -multipliers and a number of papers have been published on this. In this research p -multipliers f_m , proposed by Mokwa and Duncan (2001) are employed. Mokwa and Duncan (2001) studied results from eleven experimental research work to determine p -multipliers f_m , for pile group of different pile sizes and different pile spacing. Twenty nine separate tests were performed by different research teams in all of these eleven studies. Mokwa and his team ascertained the value of p -multipliers through back analysis using results from instrumented pile-group and single pile load tests.

When a pile group is laterally loaded, the lateral load resistance of any pile in the group is equal to the product of load resistance of a single pile, that can be obtained dividing total load applied to the pile group by number of piles in the group, and p -multiplier assigned to the pile in question by virtue of its position in the group and spacing of the piles in the

group. When a pile group is laterally loaded, the lateral load resistance p of any pile in the group is equal to the product of load resistance of a single pile p_{sp} and p -multiplier denoted as f_m assigned to the pile.

$$P_{gp} = f_m P_{sp}$$

4-1

where:

P_{gp} = the lateral load resistance of a pile in a group that is p -value for the pile in the group,

P_{sp} = the lateral load resistance of a single pile that is p -value for a single pile,

f_m = p -multiplier.

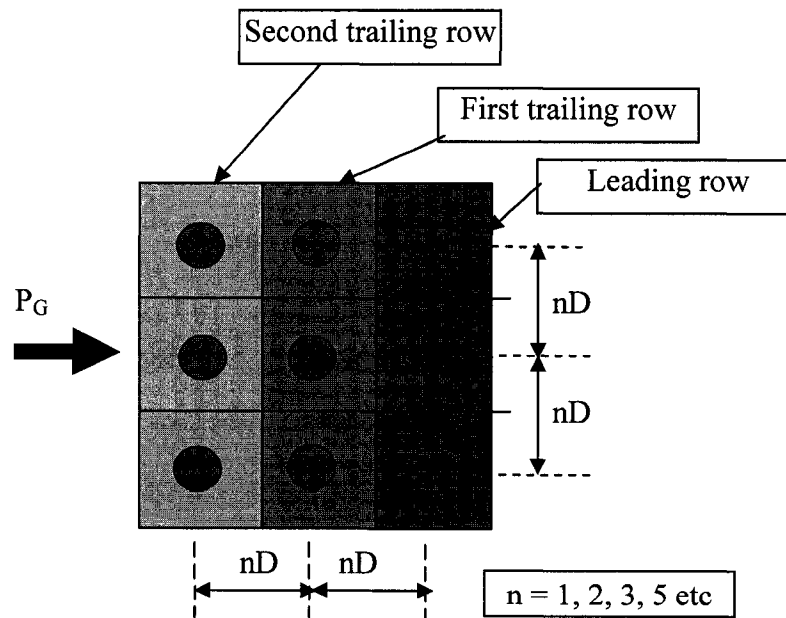


Figure 4-2 Orientation of rows in a plan of group of piles.

Mokwa and Duncan (2001) presented the recommended p -multiplier values as functions of pile spacing and pile location within the group in form of a chart shown in Figure 4-4. As suggested, the bending moment computed for the leading row corner piles should be increased if the spacing normal to the direction of load is less than $3D$. The values of p -multipliers, f_m for leading row through 3rd trailing row are shown in Figure 4-4 for pile spacing $1D$ to $6D$. For pile spacing $6D$ higher f_m value is 1. The value of f_m is essentially the same for third, fourth and subsequent trailing rows.

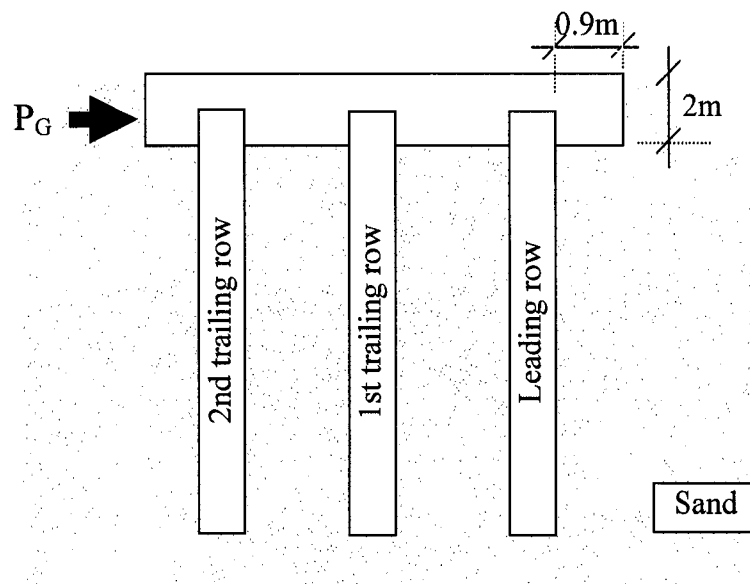


Figure 4-3 Geometrical characteristics of the pile group.

4.3 Efficiency of pile group

Mokwa and Duncan (2001) have shown relation between f_m and group efficiency. Overall efficiency G_e of a group, as they defined is the ultimate lateral capacity of the group of n number of piles divided by lateral capacity of a single pile times n .

$$G_e = \frac{(P_s)_g}{n(P_s)_s} \quad 4-2$$

where:

n - number of columns,

G_e - the pile group efficiency,

$(P_s)_g$ - the ultimate lateral load capacity of the pile group,

$(P_s)_s$ - the lateral load capacity of single pile.

Equation 4-2, when written in terms of f_m becomes

$$G_e = \frac{\sum_{i=1}^{N_r} f_{mi}}{N_r}$$

where

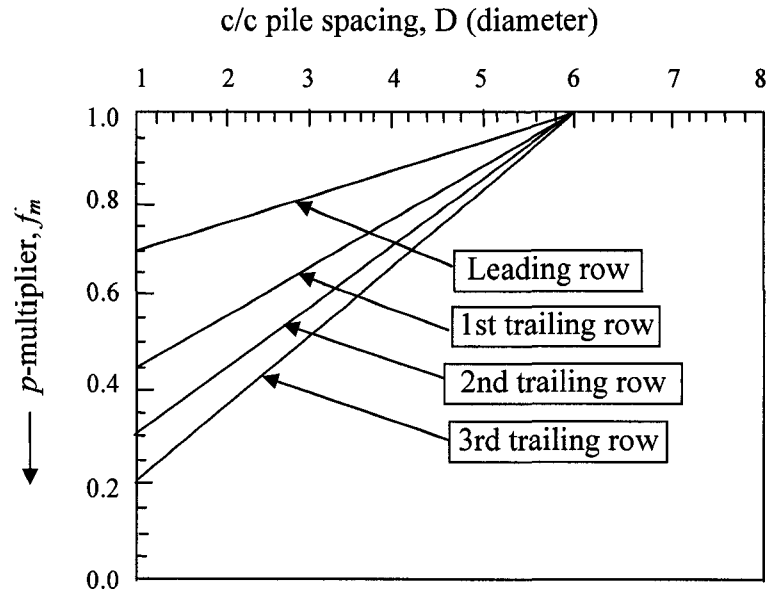
N_r - the number of rows,

f_{mi} - the p-multiplier f_m for i th row.

4.4 Computer program FB Pier used in the investigation of group of piles

The numerical analyses have been conducted by FB Pier (FTD & FHA, 2001) computer program. The University of Florida in collaboration with Bridge Software Institute, Florida Department of Transportation and Federal Highway Administration developed FB-Pier. Like COM624P this soft ware employs p - y model of soil and finite element method. With FB-Pier structures like single pile/shaft, group of pile/shaft, pile bent,

sound wall, retaining wall, high mast lighting and signs and bridge pier etc can be analyzed.



Notes:

- (1) the term row used in this chart refers to piles aligned perpendicular to the direction of applied load.
- (2) Use the f_m values recommended for the third trailing row for all rows beyond the third trailing row.
- (3) Bending moments and shear forces computed for the leading row corner piles should be adjusted as follows:

<u>side by side spacing</u>	<u>corner pile factor</u>
3D	1.0
2D	1.2
1D	1.6

Figure 4-4 Proposed p-multiplier design curves (Mokwa and Duncan, 2001).

It (FB Pier) is a non-linear, finite element analysis, soil-structure interaction program. Lateral load applied to the pile cap is regarded as applied to the pile group and is denoted by P_G whereas lateral force imposed on individual member pile as a result of P_G applied to the pile group is denoted by P_g . The pile structure of a member pile is discretized into 50 elements. For every value of P_G applied to the cap of primary pile group, the solution by FB Pier is in terms of suitable lateral forces P_g applied to each member pile, the deflection lines and the internal forces.

CHAPTER V

THEORITICAL FORMULATION OF SENSITIVITY

5.1 Introduction

This chapter deals with the formulation of sensitivity analysis of nonlinear pile-soil system embedded in sand. The purpose of sensitivity analysis in civil engineering is to determine how sensitive is the structural response to the changes of the design variables. In case of piles subjected to horizontal forces, top lateral displacement and flexural rotation at the pile head are the structural responses crucial for determination of performance of piles. The pile-soil system is subjected to lateral loading. The behaviour of the pile is simulated by means of 1D beam element, whereas the sand's response to lateral loading is described by means of p - y model. The physical parameters of the pile-soil system are taken as the design variables. The sensitivity of the maximum generalized deformations is formulated based on the principle of virtual work. The pile-soil model subjected to horizontal loading is investigated in the frame work of sensitivity theory by means of adjoint method for nonlinear system. The unknown variations of generalized deformations resulted from the imposed variation of design variables of the pile-soil system are determined in reference to the physical relationship. The first variation of the performance functional caused by the changes of the design variables defines the sensitivity of maximum generalized displacement due to the changes of the physical parameters of the pile-soil system. It is expressed in terms of sensitivity operators which are the sensitivity integrands. The complex pattern of the distributions of sensitivity integrands of the pile-soil system along the pile axis for variable in discrete fashion

horizontal forces is associated with the ability of the soil to develop many physical phases within the soil medium. Design variables are defined as a group of parameters that have potential for change in a possible range in order to improve or optimize a structure (Haftka et al. 1990). Under certain limitations design variables are subject of variation by the engineers to ensure best possible performance of the system under consideration. The pile stiffness and soil strength parameters are taken as the design variables. For this case of laterally loaded pile embedded in sand all of design parameters are identified and listed below.

- 1) The pile stiffness EI ,
- 2) Width of pile b ,
- 3) Angle of internal friction of sand ϕ ,
- 4) Submerged unit weight of soil γ ,
- 5) The coefficient of subgrade reaction k ,
- 6) The coefficient of active lateral earth pressure K_a of Rankine type.

5.2 Sensitivity analysis of laterally loaded single piles embedded in sand

The pile-soil system subjected to lateral loading is shown in Figure 5.1.

The condition of equality of the lateral deflections at the pile-soil interface is guaranteed by the solution of the following equation, the pile-soil system must satisfy:

$$EIy^{IV} + p(y) = 0 \tag{5-1}$$

where:

$p(y)$ = the soil reaction that depends on the lateral deflection y .

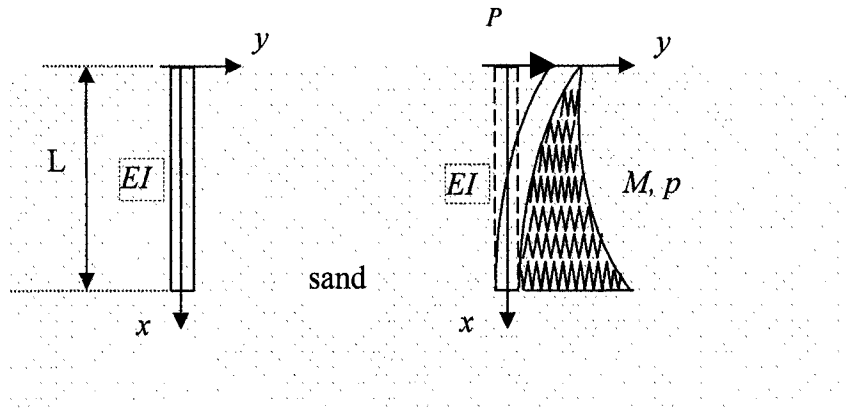


Figure 5-1 The geometry of pile-soil system before and after deflection.

In general, the behaviour of pile-soil system is affected by the magnitude of load applied as well as the physical parameters involved to characterize the structural response of the pile structure and soil medium. The behaviour of the pile structure subjected to bending moment M is described as:

$$EIy'' = -M \quad 5-2$$

where:

y'' - curvature of beam (pile).

The p - y relationships of the sand adjacent to pile has been defined in Chapter III. Depending upon the magnitude of deflection y the soil against a pile structure may be in four physical phases. They are: linear elastic ($0 \leq y \leq y_k$), nonlinear elastic

($y_k \leq y \leq y_m$), bilinear elastic ($y_m \leq y \leq y_u$) and plastic flow ($y \geq y_u$). Soil resistances that develop in the corresponding phases are given by the following equations.

For linear elastic ($0 \leq y \leq y_k$) phase, the soil resistance (Equation 3-15) is given as:

$$p = kxy$$

For nonlinear elastic ($y_k \leq y \leq y_m$) phase, soil resistance (Equation 3-14) is the following:

$$p = B_s p_s (60y/b)^{0.8(A_s/B_s-1)}$$

For bilinear elastic ($y_m \leq y \leq y_u$) phase, soil resistance (Equation 3-16) is written as:

$$p = p_s [B_s + 48(y - b/60)(A_s - B_s)/b]$$

For plastic flow ($y \geq y_u$) phase, soil resistance (Equation 3-5) is specified as:

$$p = p_s A_s$$

All strength parameters involved in physical relationships of pile-soil system are considered to form the design variables \bar{s} defined as:

$$\bar{s} = [EI, k, \gamma', \phi, K_a, b]^T \quad 5-3$$

The changes in the behaviour of pile-soil system when subjected to constant value of load can be generated by the changes of the design variables vector $\delta\bar{s}$. The causes of changes of \bar{s} can originate from various sources such as:

- Some changes of \bar{s} can be associated with imperfections in determination of soil parameters during in the field operations.

-
- The geometric properties of the infrastructure may undergo physical deterioration in course of time which is known as the aging process.
 - The environmental changes (climate effect, hazardous conditions) have also adverse impact on the material characteristics of soil.

Any change in at least one of the design variables leads to changes of the performance of the structure even if it is subjected to constant load. The increase of deformations of the supporting system has detrimental effect on the performance of superstructure. Consequently the increased deformeability of the system results in diminution of safety of the entire system. Thus, the analysis of maximum generalized deformations caused by the changes of the design variables which are considered as spatial functions is of substantial importance during design process to undertake suitable preventive measures. This results in generation of the deflection, y whereas the static equilibrium equations are satisfied. It is postulated that due to the changes of the physical strength parameters represented by $\delta\bar{s}$ an additional generalized deformations δy and $\delta\theta$ are generated. Their maximum values are located on the pile head of the pile-soil system, at $x = 0$, and are equal to δy_t and $\delta\theta_t$. They are arranged in the vector of increment of generalized displacements $\delta\bar{g}$ given as:

$$\delta\bar{g} = [\delta y_t, \delta\theta_t]^T \quad 5-4$$

The vector of increments of design variable $\delta\bar{s}$ is defined as follows:

$$\delta\bar{s} = [\delta(EI), \delta k, \delta\gamma', \delta\phi, \delta K_a, \delta b]^T \quad 5-5$$

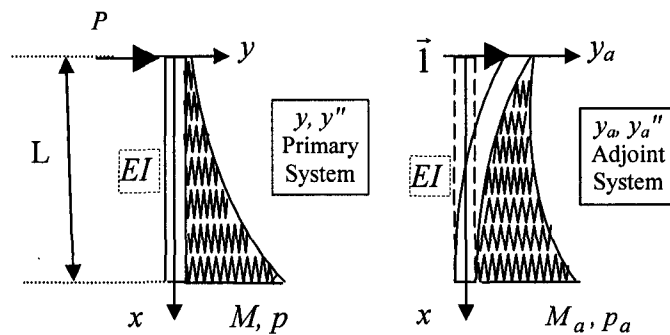


Figure 5-2 The geometry of pile-soil system (primary system), type of load, boundary conditions and the adjoint system.

The determination of δy_t or $\delta \theta_t$ is established based on the principle of virtual work (Washizu, 1976) applied with respect to the increment of deformation. It requires the suitable generalized unit load $\bar{1}$ be applied to the auxiliary structure called the adjoint structure (Dems and Mroz, 1983). There is a condition that requires the adjoint structure be in the state of deformation identical to primary structure. In case of soil-structure interaction system of linear elastic type, the adjoint system is also linear elastic which implies that state of deformations and internal forces generated by a unit generalized load $\bar{1}$ applied is independent of the deformation of the primary structure (Budkowska (1997)). But in case of nonlinear elastic soil-structure systems such as the one under investigation in this research linear extrapolation is not applicable. In general, the increment of maximum generalized deformations $\delta \bar{g}$ is determined in the scope of the principle of virtual work as follows:

$$\bar{I} \cdot \delta \bar{g} = - \int_0^l M_a \delta y'' dx + \int_0^l p_a \delta y dx \quad 5-6$$

where

\bar{I} = generalized unit load that corresponds to the type of deformation type,

M_a, p_a = the bending moment and the soil reaction of the adjoint system generated by application of unit generalized load \bar{I} ,

$\delta y, \delta y''$ = variations of deformations imposed of the primary structure.

The variations of δy and $\delta y''$ can determined from relationship of the pile structure and the supporting soil. The pile structure of primary system when subjected to changes in design variables $\delta \bar{s}$ results in development of change in bending moment δM given as:

$$\delta M = \frac{\partial M}{\partial y''} \delta y'' + \frac{\partial M}{\partial EI} \delta(EI) \quad 5-7$$

Similar relationship can be written for increment of soil reaction δp . Thus:

$$\delta p = \frac{\partial p}{\partial y} \delta y + \frac{\partial p}{\partial \bar{s}} \delta \bar{s} \quad 5-8$$

However, the primary system is subjected to constant load; therefore the increments of internal forces must vanish. This condition allows for determination of unknown $\delta y''$ and δy from Equations 5-7 and 5-8 respectively. Thus,

$$\delta y'' = - \frac{\partial y''}{\partial M} \frac{\partial M}{\partial(EI)} \delta(EI) \quad 5-9$$

$$\delta y = - \frac{\partial y}{\partial p} \frac{\partial p}{\partial \bar{s}} \delta \bar{s} \quad 5-10$$

If one or more of the strength parameters are varied keeping applied load P unchanged there will be change in the pile deflection y through out the length of the pile. All soil's physical strength parameters are included in vector of variation of design variables and shown in Definition 5-5 as follows.

$$\delta \bar{s} = [\delta k, \delta \gamma', \delta \phi, \delta K_a, \delta b]^T \quad 5-11$$

Applying the Equation 5-11 into Equation 5-10, the extended form of Equation 5-10 takes the shape:

$$\delta y = - \frac{\partial y}{\partial p} \frac{\partial p}{\partial k} \delta k - \frac{\partial y}{\partial p} \frac{\partial p}{\partial \gamma'} \delta \gamma' - \frac{\partial y}{\partial p} \frac{\partial p}{\partial \phi} \delta \phi - \frac{\partial y}{\partial p} \frac{\partial p}{\partial K_a} \delta K_a - \frac{\partial y}{\partial p} \frac{\partial p}{\partial b} \delta b \quad 5-12$$

Substituting Equations 5-12 and 5-9 into Equation 5-6 results in the following:

$$\begin{aligned} \bar{I} \cdot \delta \bar{g} = & \int_0^l M_a \frac{\partial y''}{\partial M} \frac{\partial M}{\partial (EI)} \delta (EI) dx - \int_0^l p_a \frac{\partial y}{\partial p} \frac{\partial p}{\partial k} \delta k dx - \int_0^l p_a \frac{\partial y}{\partial p} \frac{\partial p}{\partial \gamma'} \delta \gamma' dx \\ & - \int_0^l p_a \frac{\partial y}{\partial p} \frac{\partial p}{\partial \phi} \delta \phi dx - \int_0^l p_a \frac{\partial y}{\partial p} \frac{\partial p}{\partial K_a} \delta K_a dx - \int_0^l p_a \frac{\partial y}{\partial p} \frac{\partial p}{\partial b} \delta b dx \end{aligned} \quad 5-13$$

Multiplying and dividing each term of equation 5-13 corresponding to a each design variable by the design variable itself, the following equation appears:

$$\begin{aligned} \bar{I} \cdot \delta \bar{g} = & \int_0^l M_a \frac{\partial y''}{\partial M} \frac{\partial M}{\partial (EI)} \delta(EI) \frac{EI}{EI} dx - \int_0^l p_a \frac{\partial y}{\partial p} \frac{\partial p}{\partial k} \delta k \frac{k}{k} dx - \int_0^l p_a \frac{\partial y}{\partial p} \frac{\partial p}{\partial \gamma} \delta \gamma \frac{\gamma}{\gamma} dx \\ & - \int_0^l p_a \frac{\partial y}{\partial p} \frac{\partial p}{\partial \phi} \delta \phi \frac{\phi}{\phi} dx - \int_0^l p_a \frac{\partial y}{\partial p} \frac{\partial p}{\partial K_a} \delta K_a \frac{K_a}{K_a} dx - \int_0^l p_a \frac{\partial y}{\partial p} \frac{\partial p}{\partial b} \delta b \frac{b}{b} dx \end{aligned} \quad 5-14$$

Rearranging Equation 5-14, the following can be written:

$$\begin{aligned} \bar{I} \cdot \delta \bar{g} = & \int_0^l y_a'' y'' \delta(EI) \frac{EI}{EI} dx - \int_0^l p_a \frac{\partial y}{\partial p} \frac{\partial p}{\partial k} k \delta k \frac{1}{k} dx - \int_0^l p_a \frac{\partial y}{\partial p} \frac{\partial p}{\partial \gamma} \gamma \delta \gamma \frac{1}{\gamma} dx \\ & - \int_0^l p_a \frac{\partial y}{\partial p} \frac{\partial p}{\partial \phi} \phi \delta \phi \frac{1}{\phi} dx - \int_0^l p_a \frac{\partial y}{\partial p} \frac{\partial p}{\partial K_a} K_a \delta K_a \frac{1}{K_a} dx - \int_0^l p_a \frac{\partial y}{\partial p} \frac{\partial p}{\partial b} b \delta b \frac{1}{b} dx \end{aligned} \quad 5-15$$

To simplify the terms in each integrand, the following relationships are defined:

$$S_{EI} = [y'' y_a'' EI] \quad 5-16$$

$$S_k = \left[p_a \frac{\partial y}{\partial p} \frac{\partial p}{\partial k} k \right] \quad 5-17$$

$$S_{\gamma'} = \left[p_a \frac{\partial y}{\partial p} \frac{\partial p}{\partial \gamma'} \gamma' \right] \quad 5-18$$

$$S_{\phi} = \left[p_a \frac{\partial y}{\partial p} \frac{\partial p}{\partial \phi} \phi \right] \quad 5-19$$

$$S_{K_a} = \left[p_a \frac{\partial y}{\partial p} \frac{\partial p}{\partial K_a} K_a \right] \quad 5-20$$

$$S_b = \left[p_a \frac{\partial y}{\partial p} \frac{\partial p}{\partial b} b \right] \quad 5-21$$

where S_{EI} , P_k , S_{γ} , S_{ϕ} , S_{K_a} and S_b = the sensitivity operators affecting generalized

maximum deflections due to the changes of the design variables EI , k , γ , ϕ , K_a , b ;

and

$$\delta(EI)_N = \frac{\delta EI}{EI} \quad 5-22$$

$$\delta k_N = \frac{\delta k}{k} \quad 5-23$$

$$\delta \gamma_N = \frac{\delta \gamma}{\gamma} \quad 5-24$$

$$\delta(K_a)_N = \frac{\delta K_a}{K_a} \quad 5-25$$

$$\delta b_N = \frac{\delta b}{b} \quad 5-26$$

are the normalized variations of the design variables.

Introducing the above to Equation 5-15 a more compact form is obtained as shown below.

$$\bar{I} \cdot \delta \bar{g} = \int_0^l S_{EI} \delta(EI)_N dx - \int_0^l S_k \delta k_N dx - \int_0^l S_\gamma' \delta \gamma_N' dx - \int_0^l S_\phi \delta \phi_N dx - \int_0^l S_{K_a} \delta(K_a)_N dx - \int_0^l S_b \delta b_N dx \quad 5-27$$

Multiplication of the terms in each integrands of Equation 5-15 by corresponding design variable makes the sensitivity operators of same unit. Through the same operation each component of the variation of design variable vector $\delta \bar{g}$ has been normalized against the corresponding initial values of design variable. As a result of this operation all the sensitivity integrands at right side of Equation 5-27 becomes of the same unit as the term at left hand side of the equation and normalized changes in design variables become dimensionless fractions which renders the equation more easily usable.

The left hand side of Equation 5-16 that is $\delta\bar{g}$ contains two components, namely δy_t and $\delta\theta_t$. In former case, the internal forces M_a and p_a are those that are generated by application of $\bar{P} = \bar{1}$ to the adjoint pile–soil system, whereas in latter case M_a and p_a are the outcomes of application of $\bar{M} = \bar{1}$ to the adjoint system. The presented theoretical formulation of sensitivity analysis of laterally loaded piles embedded in the p - y sand located below the water table forms the basis for numerical investigations.

5.3 Sensitivity analysis of laterally loaded pile group

Pile groups consisting of 9 piles arranged in three rows has been investigated. The pile members in 3x3 pile group are distributed into three rows, namely leading row, first trailing row and second trailing row. The behaviour of member piles in a group has been described in Chapter IV. The group behaviour of member piles has been modeled by employment of p -multipliers proposed by Mokwa and Duncan (2001). With the use of p -multipliers any member of a group can be extracted from the group and analyzed as single isolated pile. The analysis of laterally loaded pile group is done by means of FB Pier computer program (2001). Output from this software gives the deflection, soil response and internal force of each member pile separately due to the application of lateral load P_G applied to the pile cap. Using these output data from FB Pier any member pile can be extracted from the group and analyzed as single isolated pile. The formulation derived in Section 5.2 is also applicable to member piles of a pile group.

5.4 Primary and adjoint structure

In this research sensitivity analysis of laterally loaded single pile and group of piles, embedded in sand below water table has been performed. The top horizontal displacement and the angle of flexural rotation at the top of the pile are considered as the structural response for both single and group of piles. The sensitivity of the deformation at the top of the pile with the changes of design variables has been formulated using variational calculus. Sensitivity investigations have been performed by adjoint system method. The nonlinear load-deformation behaviour of laterally loaded pile is path independent. For an investigation of such a system the adjoint system is most effective (Kleiber et al. 1997).

In this study the actual structural system on which the real loadings are applied is termed as primary structure. So, it is the primary structure on which the actual deformations and the internal forces develop. On the other hand adjoint structure is a imaginary structure on which a virtual unit force is applied in order to be able to apply the principle of virtual work on the system. For a linear system the state of deformation of adjoint structure is immaterial but for a nonlinear system the adjoint structure is required to be in the same state of deformation and bounded by same boundary conditions as the primary structure is (Budkowska, 1997). Depending on the type of structural response whose sensitivity is sought following a suitable unit load is applied on the adjont structure. Primary and adjoint structures with suitable unit load that have employed in this research are shown below.

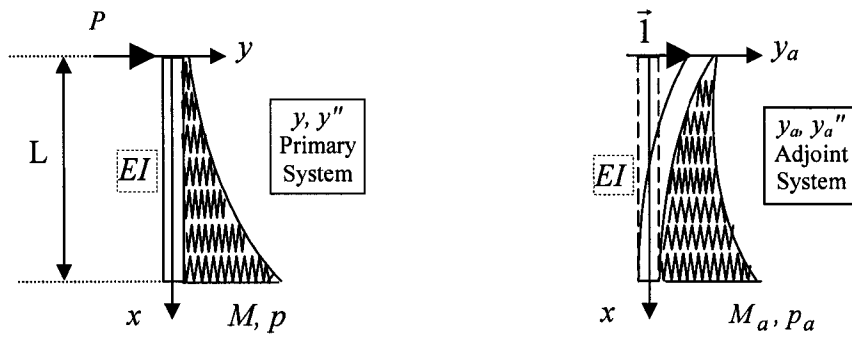


Figure 5-3 The primary and adjoint system for determination of sensitivity of top lateral deflection δy_t , when the primary structure is subjected to lateral force P .

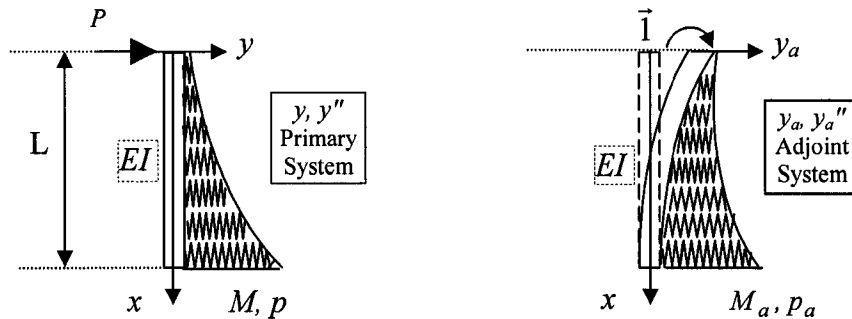


Figure 5-4 The primary and adjoint system for determination of sensitivity of top flexural rotation $\delta\theta_t$, when the primary structure is subjected to lateral force P .

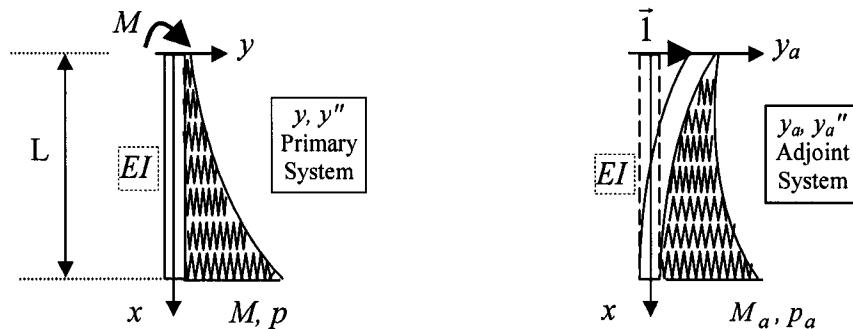


Figure 5-5 The primary and adjoint system for determination of sensitivity of top lateral deflection δy_t , when the primary structure is subjected to bending moment M .

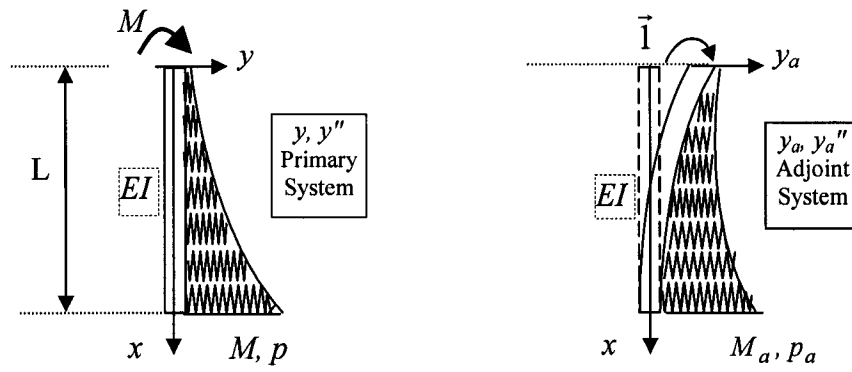


Figure 5-6 The primary and adjoint system for determination of sensitivity of top flexural rotation $\delta\theta_t$, when the primary structure is subjected to bending moment M .

CHAPTER VI

ASSESSMENT OF SENSITIVITY

6.1 Assessment of sensitivity factors affecting the first variation of maximum generalized deformation due to changes of the design variables

Let us refer to Equation 5-27,

$$\bar{l} \cdot \delta \bar{g} = - \int_0^l S_{EI} \delta(EI)_N dx - \int_0^l S_k \delta k_N dx - \int_0^l S_\gamma \delta \gamma'_N dx - \int_0^l S_\phi \delta \phi_N dx - \int_0^l S_{K_a} \delta(K_a)_N dx - \int_0^l S_b \delta b_N dx \quad 5-27$$

which defines the sensitivity of the changes of pile head deformation due to changes of the design variables. Using this equation it is possible to assess the changes in the maximum generalized deformation by integrating the terms on the right hand side over the length of the pile. The normalized changes in design variables are dimensionless and scalars. It is worth noting that Equation 5-27 is written in symbolic fashion. The term $\delta \bar{g}$ contains two components which are maximum lateral deflection δy_t and maximum flexural rotation $\delta \theta_t$. Each of the six terms of the Equation 5-27 is connected to variable soil phases that develop along the axis of the pile depending on the lateral deflection y of the pile. Equation 5-27 is used to determine δy_t and $\delta \theta_t$ when the pile system is subjected to either horizontal force P and bending moment M . The graphical presentation of the sensitivity intergrands are considered as an important part of sensitivity investigation. They enable one to assess effectively the result of the changes of the specific design variables one or more at a time on the deformation of the pile-soil system. They are also able to indicate the location and size of soil phases. The examinations of sensitivity

integrands allows Equation 5-27 be applied with respect to various soil phases that develops as a result of an increased load. Therefore it is possible to evaluate quantitatively the contribution of changes of design variables connected to each soil phase in the change of top generalized deformation. Equation 5-27 can be written in the following fashion.

$$\bar{I} \cdot \delta \bar{g} = A_{EI} \delta(EI)_N = A_k \delta k_N + A_{\gamma'} \delta \gamma'_N + A_{\phi} \delta \phi_N + A_{K_a} \delta(K_a)_N + A_b \delta b_N \quad 6-1$$

where

$$A_{EI} = \int_0^l S_{EI} dx \quad 6-2$$

$$A_k = \int_0^l S_k dx \quad 6-3$$

$$A_{\gamma'} = \int_0^l S_{\gamma'} dx \quad 6-4$$

$$A_{\phi} = \int_0^l S_{\phi} dx \quad 6-5$$

$$A_{K_a} = \int_0^l S_{K_a} dx \quad 6-6$$

$$A_b = \int_0^l S_b dx \quad 6-7$$

where A_{EI} , A_k , $A_{\gamma'}$, A_{ϕ} , A_{K_a} and A_b are the sensitivity factors of maximum general deformation connected to changes of design EI , k , γ' , ϕ , K_a and b respectively.

The quantitative assessment of $\delta \bar{g}$ associated with each soil phase can be obtained with the assumption that all variations of the design variables are constant. It is important aspect of this research to identify the influence of changes of each design variable compared to total changes in maximum generalized deformation. Denoting the total sensitivity as A_{tot} Equation 6-1 can be rewritten in the following form.

$$\bar{l} \cdot \delta \bar{g} = A_{tot} \left(\frac{A_{EI}}{A_{tot}} \delta(EI)_N + \frac{A_k}{A_{tot}} \delta k_N + \frac{A_\gamma}{A_{tot}} \delta \gamma_N + \frac{A_\phi}{A_{tot}} \delta \phi_N + \frac{A_{K_a}}{A_{tot}} \delta(K_a)_N + \frac{A_b}{A_{tot}} \delta b_N \right) \quad 6-8$$

where

$$(A_{tot}) = (A_{EI} + A_k + A_\gamma + A_\phi + A_{K_a} + A_b) \quad 6-9$$

From Equation 6-8,

$$\bar{l} \cdot \delta \bar{g} = A_{tot} (F_{EI} \delta(EI)_N + F_k \delta k_N + F_\gamma \delta \gamma_N + F_\phi \delta \phi_N + F_{K_a} \delta(K_a)_N + F_b \delta b_N) \quad 6-10$$

where

$$F_{EI} = \frac{A_{EI}}{A_{tot}} \quad 6-11$$

$$F_k = \frac{A_k}{A_{tot}} \quad 6-12$$

$$F_{\gamma'} = \frac{A_{\gamma'}}{A_{tot}} \quad 6-13$$

$$F_\phi = \frac{A_\phi}{A_{tot}} \quad 6-14$$

$$F_{K_a} = \frac{A_{K_a}}{A_{tot}} \quad 6-15$$

$$F_b = \frac{A_b}{A_{tot}} \quad 6-16$$

F_{EI} , F_k , $F_{\gamma'}$, F_ϕ , F_{K_a} and F_b are relative sensitivity factors connected with the corresponding design variable. They show in fraction contribution of change of any design variable compared to total change produced in the maximum generalized deflection.

For any arbitrary horizontal force or bending moment the relative sensitivity factors $F_{(\dots)}$ can be applied for each phase of soil deformation. Let us consider an arbitrary load P_t or M_t due to which the pile underwent lateral deformation creating soil phases e.g. the linear elastic, the non-linear elastic, the bi-linear elastic and the plastic flow phase. The corresponding portions of soil phases along the length of the pile are denoted as l_P, l_{BL}, l_{NL} and l_L . They are shown in Figure 6-1.

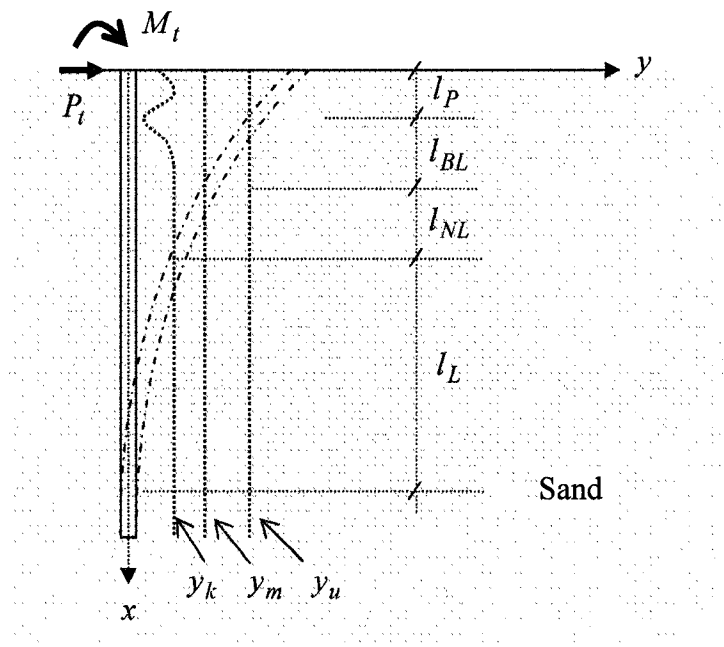


Figure 6-1 Qualitative length of pile involved in different soil phases.

Splitting the sensitivity operators phase wise Equation 5-16 can be written as:

$$\begin{aligned}
\bar{l} \cdot \delta \bar{g} = & \left[\int_{l_p} (0) dx \right]_P \\
& + \left[\int_{l_{BL}} \{ S_{EI}(\delta EI)_N - S_\phi(\delta \phi)_N - S_{K_a}(\delta K_a)_N - S_\gamma(\delta \gamma)_N - S_b(\delta b)_N \} dx \right]_{BL} \\
& + \left[\int_{l_{NL}} \{ S_{EI}(\delta EI)_N - S_\phi(\delta \phi)_N - S_{K_a}(\delta K_a)_N - S_\gamma(\delta \gamma)_N - S_b(\delta b)_N \} dx \right]_{NL} \\
& + \left[\int_{l_L} \{ S_{EI}(\delta EI)_N - S_k(\delta k)_N + (0) + (0) + (0) \} dx \right]_L
\end{aligned} \tag{6-17}$$

Introducing $(A_{tot})_{BL}$ = total sensitivity associated with the bilinear phase of soil

$$(A_{tot})_{BL} = (A_{EI} + A_\gamma + A_\phi + A_{K_a} + A_b)_{BL} \tag{6-18}$$

Total change in maximum generalized deformation vector $\delta \bar{g}$ due to change in all the design variables occurring in all the soil deformation phases can be split into portion connected to individual phases. Thus,

$(\delta \bar{g})_{BL}$ = that portion of $\delta \bar{g}$ associated with development of bilinear phase of soil

$$\delta \bar{g} = (\delta \bar{g})_{BL} + (\delta \bar{g})_{NL} + (\delta \bar{g})_L \tag{6-19}$$

$$(\delta \bar{g})_{BL} = \frac{(A_{tot})_{BL}}{(A_{tot})_{BL}} (A_{EI}(\delta EI)_N + A_\phi(\delta \phi)_N + A_{K_a}(\delta K_a)_N + A_\gamma(\delta \gamma)_N + A_b(\delta b)_N)_{BL} \tag{6-20}$$

$$(\delta\bar{g})_{BL} = (A_{tot})_{BL} \left(\frac{A_{EI}}{A_{tot}} (\delta EI)_N + \frac{A_{\phi}}{A_{tot}} (\delta\phi)_N + \frac{A_{K_a}}{A_{tot}} (\delta K_a)_N + \frac{A_{\gamma}}{A_{tot}} (\delta\gamma)_N + \frac{A_b}{A_{tot}} (\delta b)_N \right)_{BL}$$

6-21

$$(\delta\bar{g})_{BL} = (A_{tot})_{BL} (F_{EI} (\delta EI)_N + F_{\phi} (\delta\phi)_N + F_{K_a} (\delta K_a)_N + F_{\gamma} (\delta\gamma)_N + F_b (\delta b)_N)_{BL}$$

6-22

where $F_{(...)}_{BL}$ are relative sensitivity factors associated with bilinear soil phase (BL).

Similarly, for non-linear soil phase (NL) the following relationship is developed:

$$(\delta\bar{g})_{NL} = (A_{tot})_{NL} (F_{EI} (\delta EI)_N + F_{\phi} (\delta\phi)_N + F_{K_a} (\delta K_a)_N + F_{\gamma} (\delta\gamma)_N + F_b (\delta b)_N)_{NL}$$

6-23

For linear soil phase (L) the relation is:

$$(\delta\bar{g})_L = (A_{tot})_L (F_{EI} (\delta EI)_N + F_k (\delta k)_N)_L$$

6-24

Equation 6-24 does not contain $F_{\gamma'}$, F_{ϕ} , F_{K_a} and F_b because their values are zero for linear elastic phase. In other words changes in design variables γ' , ϕ , K_a and b are not capable of producing changes in maximum generalized deformation where the pile is in the state of deformation of linear elastic phase. Equation 5-27 can further be modified in form in order to show typical characteristics of sensitivity analysis that have some significance in engineering practice. Considering a pile subjected to horizontal force applied to pile head, horizontal force P applied to the pile head, the sensitivity of lateral pile head deflection y_t can be written as,

$$\bar{l} \cdot \delta y^P = -\int_0^l S_{EI}^{Py} \delta(EI)_N dx - \int_0^l S_k^{Py} \delta \kappa_N dx - \int_0^l S_{\gamma'}^{Py} \delta \gamma'_N dx - \int_0^l S_{\phi}^{Py} \delta \phi_N dx - \int_0^l S_{K_a}^{Py} \delta(K_a)_N dx - \int_0^l S_b^{Py} \delta b_N dx$$

6-25

Equation 6-25 holds true for any arbitrary specific value of top horizontal force $P = P_i$ but due to non-linearity of the pile-soil system the determined integrands cannot be extended. Writing equation 6-25 in terms of sensitivities of design variables:

$$\bar{l} \cdot \delta y^P = A_{EI}^{Py} \delta(EI)_N + A_k^{Py} \delta \kappa_N + A_{\gamma'}^{Py} \delta \gamma'_N + A_{\phi}^{Py} \delta \phi_N + A_{K_a}^{Py} \delta(K_a)_N + A_b^{Py} \delta b_N$$

6-26

Equation 6-26 can further be modified in order to show typical characteristics of sensitivity analysis that have significance in engineering practices.

Now varying one design variable at a time and keeping the rest unchanged we get following series of equations.

$$\bar{l} \cdot \delta y^P = A_{EI}^{Py} \delta(EI)_N$$

6-27

$$\bar{l} \cdot \delta y^P = A_k^{Py} \delta \kappa_N$$

6-28

$$\bar{l} \cdot \delta y^P = A_{\gamma'}^{Py} \delta \gamma'_N$$

6-29

$$\bar{l} \cdot \delta y^P = A_{\phi}^{Py} \delta \phi_N$$

6-30

$$\bar{l} \cdot \delta y^P = A_{K_a}^{Py} \delta(K_a)_N$$

6-31

$$\bar{l} \cdot \delta y^P = A_b^{Py} \delta b_N$$

6-32

It is worth noting that all variations of the design variables in Equation 5-27 are scalars as they are normalized against initial values and expressed in percentage or fractions.

Studying the consistency of unit of the Equations 6-27 to 6-32, we can find the following relationship:

$$\bar{I} [kN] \cdot \delta y_{EI}^{Py} [m] = A_{EI}^{Py} [kNm] \cdot \delta(EI)_N [\%] \quad 6-33$$

Consequently, accounting for $\bar{I} = 1kN$, equation 6-33 can be written for arbitrary force P_i having the value P_i as:

$$\delta y_{EI}^{Piy} [m] = \frac{A_{EI}^{Piy} [kNm] \cdot \delta(EI)_N [\%]}{\bar{I} [kN]} \quad 6-34$$

which is interpreted as the sensitivity of lateral deflection expressed in meter caused by changes of δEI when the applied force P_i has the value of P_i .

6.2 Regression analysis of sensitivity of $\delta y_{(\cdot)}^{Piy}$ due to the change of the design variables when the pile structure is subjected to variable lateral force P_i .

Due to the non-linear load-deformation of laterally loaded pile system, the sensitivity of maximum general deformation at any specific load cannot be linearly extended for any other load. To account for this in the sensitivity investigation sensitivities due to change of a particular design variable are determined for an applied forces varied in discrete fashion.

For different values of P_i the graphical representation of Equation 6-34 is shown symbolically in Figure 6-2. The curve of Figure 6-2 enables one to determine sensitivity $\delta y_{EI}^{P_i}$ of top lateral deflection due to δEI for arbitrary value of applied load P_i .

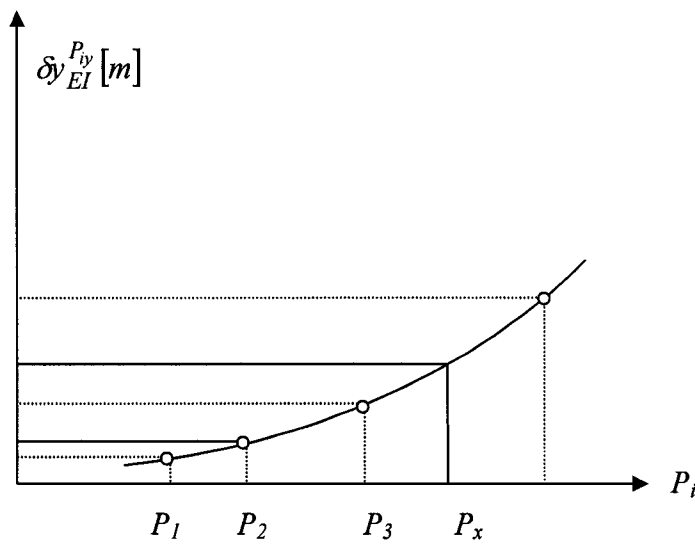


Figure 6-2 Graphical representation of sensitivity δy_i expressed in m .

Similarly, the expressions like Equation 6-34 can be written for other design variables and are shown below.

$$\delta y_k^{P_{iy}} [m] = \frac{A_k^{P_{iy}} [kNm] \cdot \delta(k)_N [\%]}{\bar{I} [kN]} \quad 6-35$$

$$\delta y_{\gamma}^{Piy} [m] = \frac{A_{\gamma}^{Piy} [kNm] \cdot \delta(\gamma)_N [\%]}{\bar{I} [kN]} \quad 6-36$$

$$\delta y_{\phi}^{Piy} [m] = \frac{A_{\phi}^{Piy} [kNm] \cdot \delta(\phi)_N [\%]}{\bar{I} [kN]} \quad 6-37$$

$$\delta y_{K_a}^{Piy} [m] = \frac{A_{K_a}^{Piy} [kNm] \cdot \delta(K_a)_N [\%]}{\bar{I} [kN]} \quad 6-38$$

$$\delta y_b^{Piy} [m] = \frac{A_b^{Piy} [kNm] \cdot \delta(b)_N [\%]}{\bar{I} [kN]} \quad 6-39$$

The graphs similar to one shown in Figure 6-2 can be made for other design variables using the above expressions. With the help of these graphs sensitivity of maximum generalized deformation connected to any design variable due to the change of the design variable can be estimated. Through this regression analysis pattern of change of sensitivities with changes of applied lateral loads can be assessed. Since the changes of sensitivities with variable values of applied load is nonlinear, the value of $\delta y_{(.)}^{(.)}$ at a particular value of load cannot be extended linearly for a different value of applied load. Using the graphical representation of sensitivity connected to change of any particular design variable, the value of $\delta y_{(.)}^{(.)}$ at any value of applied can be calculated.

CHAPTER VII

CHARACTERISTIC LENGTH OF PILE

7.1 Introduction

The length of the pile that is employed in the analysis of laterally loaded pile is an important consideration. The deformed shape of a long pile shows that the deflection oscillates back and forth about the axis of the lower portion of the pile so that there is at least one point of zero deflection. On the other hand with too short length of the pile even a single point of inflection may not at all form. So a length called critical penetration comes into consideration. At a penetration less than critical the top of the pile will experience additional deflection because the bottom of the pile is deflecting.

7.2 Relative stiffness factor

The determination of the length of long pile embedded in p - y soil is based on the approach proposed by Evans and Duncan (1982). It is based on the concept of relative stiffness factor T , proposed by Matlock and Reese (1960), which for the frictional soil with $\phi \neq 0$ is given as:

$$T = \sqrt[3]{\frac{y_t EI}{A_y H_t}} \quad 7-1$$

where:

$A_y = 2.43$ for a free head pile,

$A_y = 0.93$ for a fixed head pile,

EI = the bending stiffness of the pile,

H_t = horizontal forces applied at the pile top of the pile.

Equation 7-1 is applicable to free or fixed head pile under horizontal forces. For bending moment equation 7-2 is applicable.

$$T = \sqrt[2]{\frac{y_t EI}{B_y M_t}} \quad 7-2$$

where:

$B_y = 1.62$

M_t = moment applied at the top of pile.

The horizontal force H_t can be assessed for a given y_t by the method proposed by Evans and Duncan (1982). They defined characteristic shear load H_c and characteristic moment M_c as follows:

$$H_c = \lambda B^2 ER_I \left(\frac{\sigma_p}{ER_I} \right)^m (\epsilon_{50})^n \quad 7-3$$

and

$$M_c = \lambda B^3 ER_I \left(\frac{\sigma_p}{ER_I} \right)^m (\epsilon_{50})^n \quad 7-4$$

where:

λ = dimensionless parameter that depends on stress-strain behavior of soil,

$\lambda = 1.0$ for plastic clay and sand,

b = the width of the pile,

R_I = the moment of inertia ratio,

σ_p = the representative passive pressure of soil,

ε_{50} = the strain at which 50% of the soil strength is mobilized,

m = exponent dependent of type of load and type of soil,

n = exponent dependent of type of load and type of soil,

E - Young's modulus of the pile material.

The representative passive pressure of soil σ_p for cohesionless soil is defined as:

$$\sigma_p = 2C_{p\phi} \gamma b \tan^2\left(45^\circ + \frac{\phi}{2}\right) \quad 7-5$$

where:

$C_{p\phi}$ = the passive pressure factor equal to $\frac{\phi}{10}$,

ϕ = friction angle, in degrees, of soil located between ground surface and a depth of
8 pile diameter,

γ = unit weight of soil located between ground surface and a depth of 8 pile
diameters.

The moment of inertia ratio defined as:

$$R_I = \frac{I}{\frac{\pi b^4}{64}} \quad 7-6$$

where:

I - moment of inertia of pile section.

For solid circular section, R_I has a value 1.0, and for solid square section 1.7

Value of ε_{50} can be determined by triaxial compression test. Typically for medium dense sand $\varepsilon_{50} = 0.002$ and for clay $\varepsilon_{50} = 0.01$

Table 7-1 Values of exponents m and n for Equations 7- 3 and 7-4

Soil type	For H_c		For M_c	
	m	n	m	n
cohesive	0.683	-0.22	0.46	-0.15
cohesionless	0.57	-0.22	0.40	-0.15

7.3 Definition of short and long pile

If the embedded length of the pile is greater than $5T$ the pile is considered as a long pile.

A pile is said to be long if the deflected shape of the pile is such that the bottom end of the pile does not move laterally or rotate; in other words the end of the pile is considered to be fixed at the bottom. And if embedded length is less than $4T$ it is a short pile. For lengths (embedded) between $4T < l < 5T$ a pile is either considered as long or short depending on the relative stiffness of the pile. For relatively flexible piles, such as timber piles, an embedded length of at least 20 diameters is considered long otherwise short. For

relatively stiff piles, such as those of steel or concrete, the minimum length to be $35D$ to regarded as long pile.

CHAPTER VIII

NUMERICAL INVESTIGATION

8.1 Properties of pile-soil system

For numerical investigation the case of piles embedded in sand located below water table will be investigated. The structural pile-soil system subjected to lateral loading is shown in Figure 8-1. It is embedded in sand located below the water table. Its physical behaviour is described by $p-y$ model of Cox, Reese and Grubbs (1974). The pile-soil system forms interaction system that has the same deformations at the pile-soil interface. The sand surrounding the pile is considered as nonlinear springs with coefficient of subgrade reaction k .

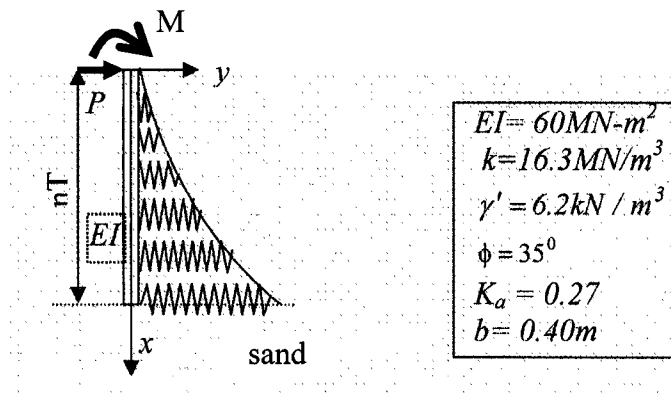


Figure 8-1 Geometry of pile, soil properties and type of load.

With application of theoretical formulation of sensitivity analysis numerical investigation has been performed and shown below.

Piles properties:

Width of pile, $b = 0.4 \text{ m}$

Area of cross section of pile, $A = 0.015 \text{ m}^2$

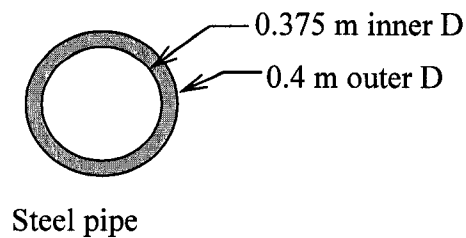


Figure 8-1a Cross section of pile.

Moment of inertia, $I = 2.9 \times 10^{-4} \text{ m}^4$,

Moment of inertia ratio (dimension less), $R_I = \frac{I}{\frac{\pi b^4}{64}} = 0.23$,

Young's modulus of the pile material, $E = 2 \times 10^8 \text{ kN/m}^2$,

Flexural moment capacity of pile section = $\frac{I}{r} f_y = .0003 * 350 \times 10^3 / .2 = 525 \text{ kN-m}$,

Soil properties:

Friction angle, $\phi = 35^\circ$,

Submerged unit weight of soil, $\gamma' = 6.2 \text{ kN}$,

Strain at which 50% of the soil(sand) strength is mobilized, $\epsilon_{50} = .002$,

Passive pressure factor, $C_{p\phi} = \frac{\phi}{10} = 3.5$,

8.2 Determination of relative stiffness factor of pile

Representative passive pressure of soil, $\sigma_p = 2C_{p\phi} \gamma' b \tan^2\left(45 + \frac{\phi}{2}\right) = 64 \text{ kN/m}^2$,

Exponent, $m = 0.57$; for horizontal force,

Exponent, $n = -0.22$; for horizontal force,

$\lambda = 1.0$,

$$\begin{aligned} H_c &= \lambda B^2 ER_l \left(\frac{\sigma_p}{ER_l} \right)^m (\epsilon_{50})^n \\ &= (1.0)(0.4)^2 (2.0 * 10^8)(.228) \left(\frac{64}{(20. * 10^8)(.228)} \right)^{0.57} (0.002)^{-0.22} \\ &= 13200 \text{ kN} \end{aligned}$$

$$\frac{y_t}{b} = .05 \text{ (arbitrary)}$$

$$\frac{H_T}{H_c} = .006 \text{ (from chart of Evans and Duncan, 1982),}$$

$$y_t = .05 \times 0.4 = .02 \text{ m}$$

$$H_t = 79.2 \text{ kN}$$

$$T_p = \sqrt[3]{\frac{y_t EI}{A_y H_t}} = 1.8 \text{ m (stiffness factor for pile under lateral load at top).}$$

Exponent, $m = 0.4$; for bending moment,

Exponent, $n = -0.15$; for bending moment,

$$\begin{aligned} M_c &= \lambda B^3 ER_I \left(\frac{\sigma_p}{ER_I} \right)^m (\epsilon_{50})^n \\ &= (1.0)(.4)^3 (2 * 10^8)(.228) \left(\frac{64}{(2 * 10^8)(.228)} \right)^{.4} (.002)^{-.15} \\ &= 33800 \text{ kN-m,} \end{aligned}$$

$$\frac{y_t}{b} = 0.03 \text{ (arbitrary),}$$

$$\frac{M_T}{H_c} = .0045 \text{ (from chart of Evans and Duncan, 1982),}$$

$$y_t = .03 \times 0.4 = .012 \text{ m,}$$

$$M_t = 152 \text{ kN,}$$

$$T_m = \sqrt[2]{\frac{y_t EI}{A_y H_t}} = 1.7 \text{ m (stiffness factor for pile under moment at top).}$$

8.3 Development of p-y curve

The sand around the pile is modeled by p-y curves proposed by Cox et al. (1974). With

the values of soil parameters shown in Article 8.1 p - y curves at different depths x have been constructed and shown in Figure 8-2.

unit weight of sand = $\gamma' = 6.2$ kN,

angle of internal friction = $\phi = 35^\circ$,

$\alpha = \phi/2 = 15.5^\circ$,

$\beta = 45 + \frac{\phi}{2} = 45 + \frac{35}{2} = 62.5^\circ$,

K_a = the coefficient of active lateral earth pressure of Rankine's type equal to

$$= \tan^2 (45 - 35/2) = 0.27,$$

$k_0 = 0.4$ coefficient earth pressure at rest = 0.4,

b = width of pile = 0.4m,

$$x_r = \frac{b \tan \beta \left[K_a \tan^7 \beta + k_0 \tan \phi \tan^3 \beta \frac{1}{\tan(\beta - \phi)} \right]}{\frac{K_0 \tan \phi \sin \beta + \tan^2 \beta \sin \alpha}{\tan(\beta - \phi) \cos \alpha} + K_0 \tan \beta (\tan \phi \tan \beta - \tan \alpha)}$$

$$x_r = 6.7m$$

$$p_{st} = \gamma' x \left[\frac{K_0 x \tan \phi \tan \beta}{\tan(\beta - \phi) \tan \alpha} + \frac{\tan \beta}{\tan(\beta - \phi)} (b + x \tan \beta \tan \alpha) + K_0 x \tan \beta (\tan \phi \sin \beta - \tan \alpha) - K_a b \right]$$

$$p_{st} = 18.42x^2 + 8.48x$$

$$p_{sd} = K_a b \gamma' (\tan^8 \beta - 1) + K_0 b \gamma' x \tan \phi \tan \beta$$

$$p_{sd} = 132.955x,$$

Ultimate soil resistance p_s which consists of p_{st} and p_{sd} above and below x_r

respectively is shown in Figure 8-2.

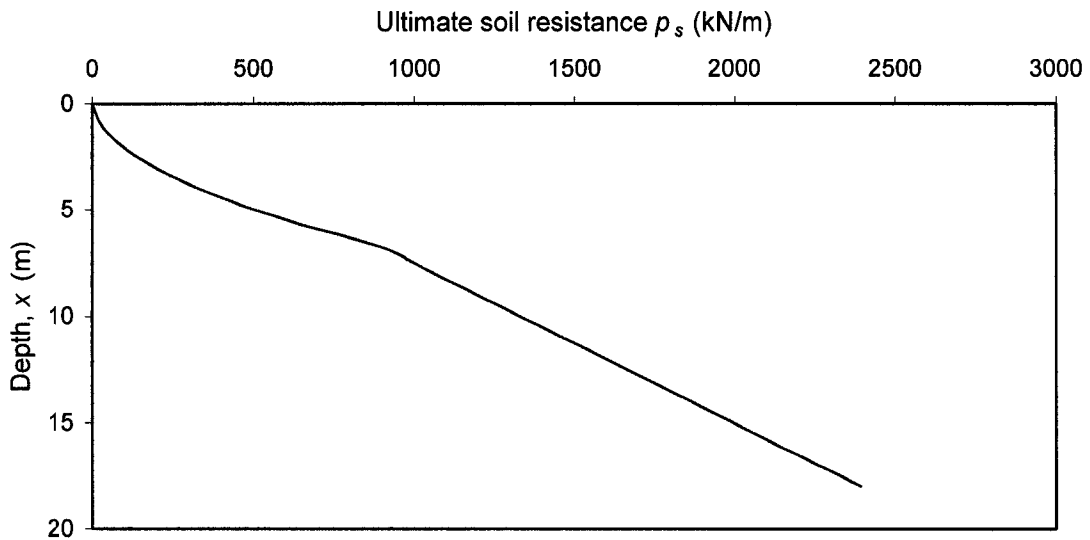


Figure 8-2 Ultimate soil resistance.

Using equations, shown in Figure 3-8, p - y curves have been constructed. Microsoft Excel has been used for organization and calculation. A group of p - y curves are shown in Figure 8-3.

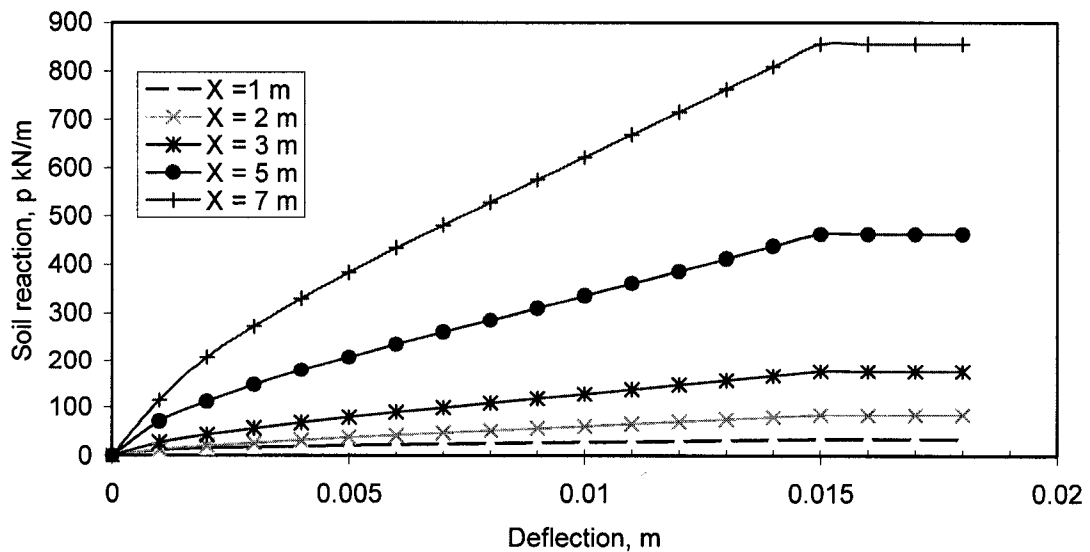


Figure 8-3 p - y curves at different depth, x .

The initial part of $p-y$ curves in Figure 8-3 are straight indicating linear elastic zone followed by nonlinear portion indicated nonlinear elastic, and then by linear portion indicating bilinear hardening and finally horizontal portion indicates constant flow. As the depth increases the $p-y$ curves moves upwards that shows increase in soil response with depth for same value of deflection.

Table 8-1 Length, boundary condition and types of sensitivity investigated for single isolated pile category.

SINGLE PILES			
Boundary conditions	Pile length L	Deformation type under study	Load steps
Free head pile under lateral load	2.0T _p , 2.5T _p , 3T _p , 3.5T _p , 4.5T _p , 5.0T _p , 6.0T _p , 7.0T _p , 8.0T _p , 9.0T _p , 10T _p	Deflection & flexural rotation	Varied
Fixed head pile under lateral load	2.0T _p , 2.5T _p , 3T _p , 3.5T _p , 4.5T _p , 5.0T _p , 6.0T _p , 7.0T _p , 8.0T _p , 9.0T _p , 10T _p	Deflection	Varied
Free head pile under bending moment	2.0T _m , 2.5T _m , 3T _m , 3.5T _m , 4.5T _m , 5.0T _m , 6.0T _m , 7.0T _m , 8.0T _m , 9.0T _m , 10T _m	Deflection & flexural rotation	Varied

8.4 Sensitivity analysis of single piles

Investigation of sensitivity affecting maximum lateral deflection and angle of flexural rotation of short and long piles with different boundary conditions and subjected to horizontal forces and bending moment has been performed. Table 8-1 shows the full range of piles investigated in this category.

Figures 8-4 to 8-12 show result of results of sensitivity analysis of short free headed single pile of length $2T = 3.5$ m subjected to horizontal forces varied in discrete fashion. These figures represent sensitivity of top lateral deflection δy_t .

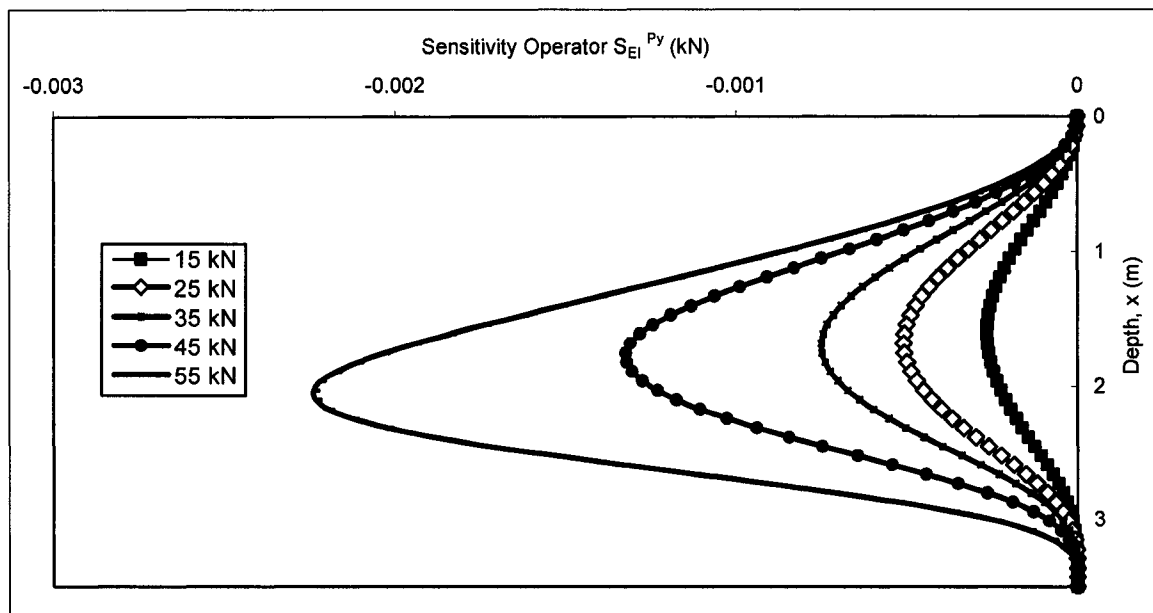


Figure 8-4 Distribution of sensitivity operators S_{EI}^{Py} affecting the change of δy_t due to the variation of design variable δEI for the pile of length, $2.0T_p = 3.5$ m subjected to variable horizontal forces.

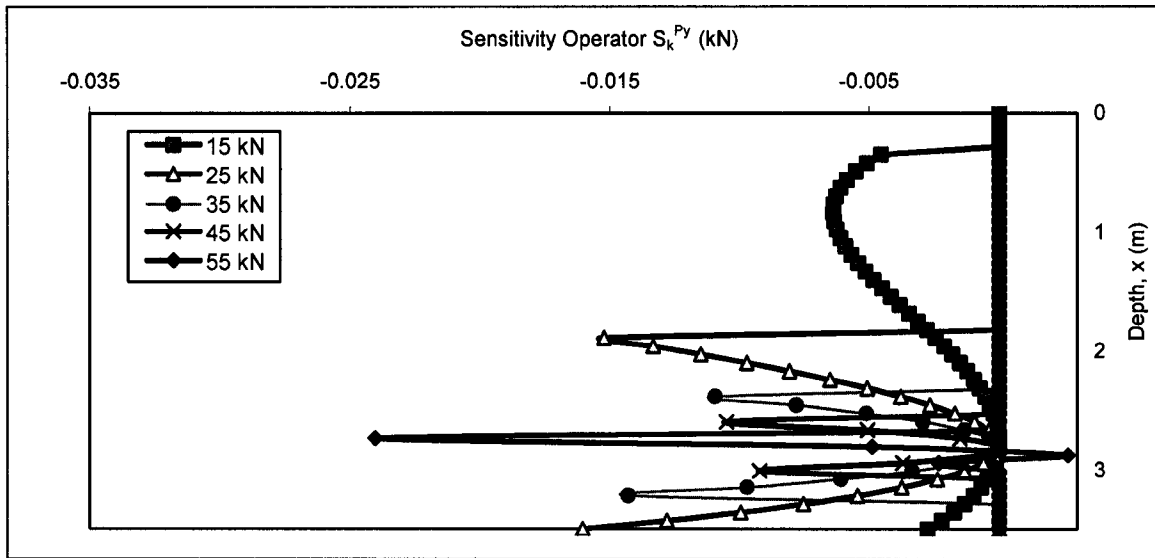


Figure 8-5 Distribution of sensitivity operators S_k^{Py} affecting the change of δy_t due to the variation of design variable δk for the pile of length, $2.0T_p = 3.5$ m subjected to variable horizontal forces.

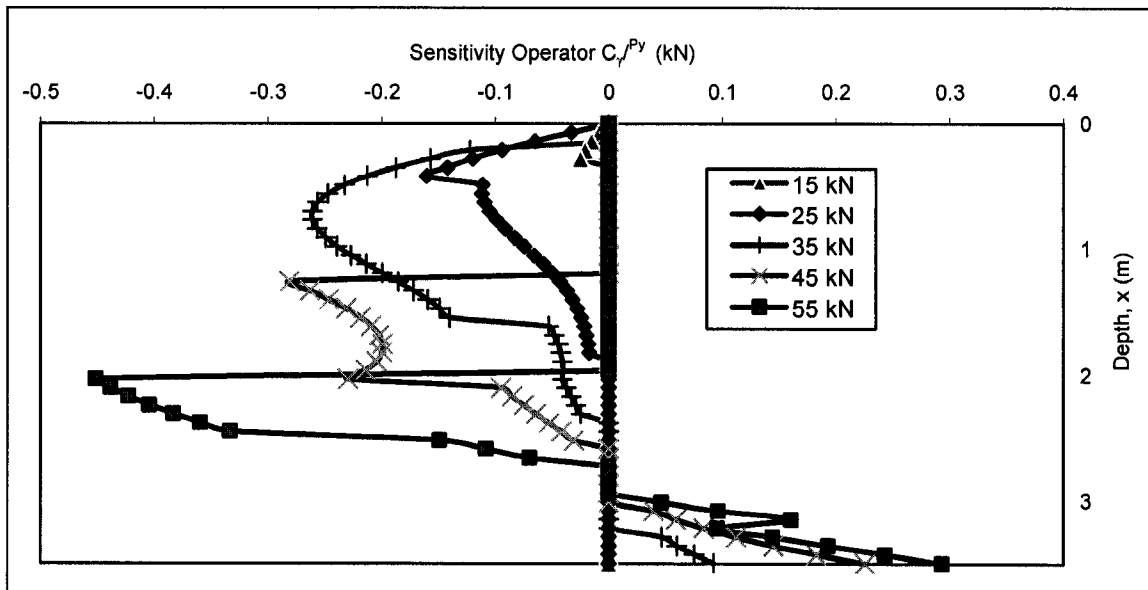


Figure 8-6 Distribution of sensitivity operators $S_{\gamma'}^{Py}$ affecting the change of δy_t due to the variation of design variable $\delta \gamma'$ for the pile of length, $2.0T_p = 3.5$ m subjected to variable horizontal forces.

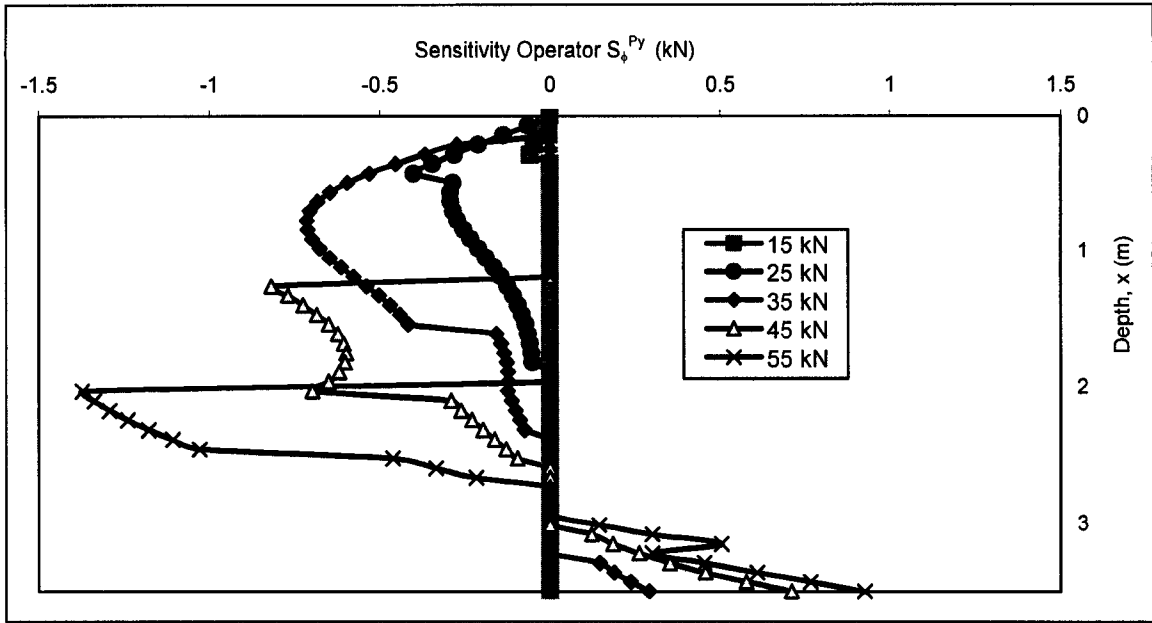


Figure 8-7 Distribution of sensitivity operators S_{ϕ}^{Py} affecting the change of δy_t due to the variation of design variable $\delta\phi$ for the pile of length, $2.0T_p = 3.5$ m subjected to variable horizontal forces.

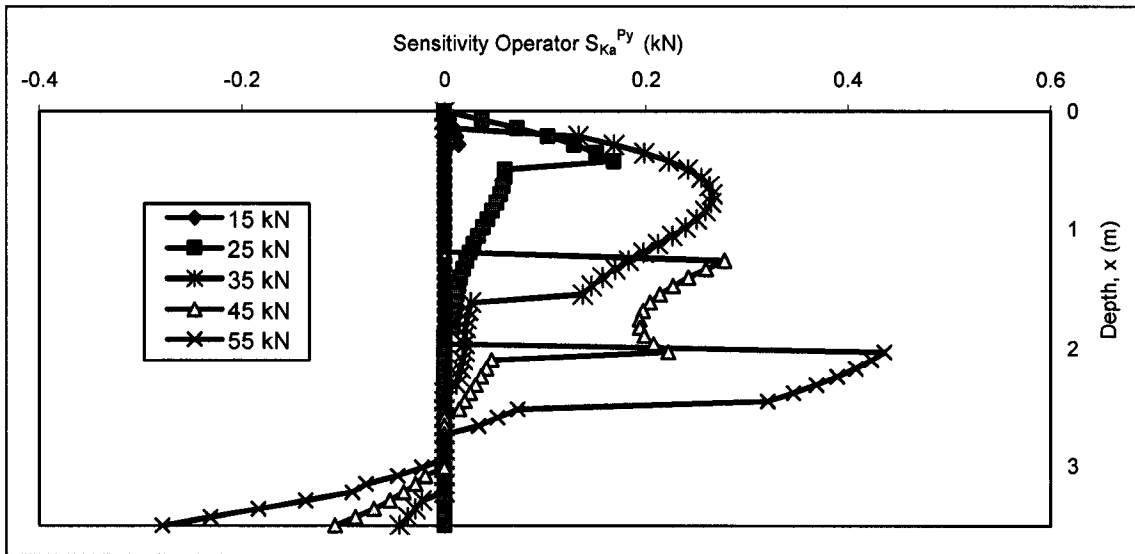


Figure 8-8 Distribution of sensitivity operators $S_{K_a}^{Py}$ affecting the change of δy_t due to the variation of design variable δK_a for the pile of length, $2.0T_p = 3.5$ m subjected to variable horizontal forces.

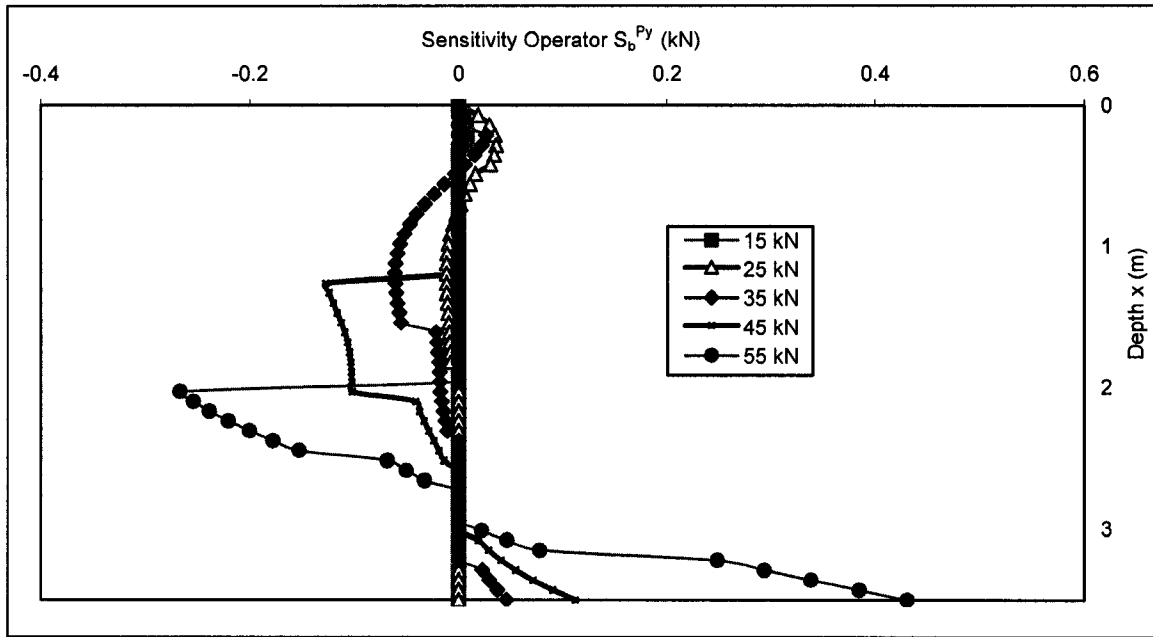


Figure 8-9 Distribution of sensitivity operators S_b^{Py} affecting the change of δy_t due to the variation of design variable δK_a for the pile of length, $2.0T_p = 3.5$ m subjected to variable horizontal forces.

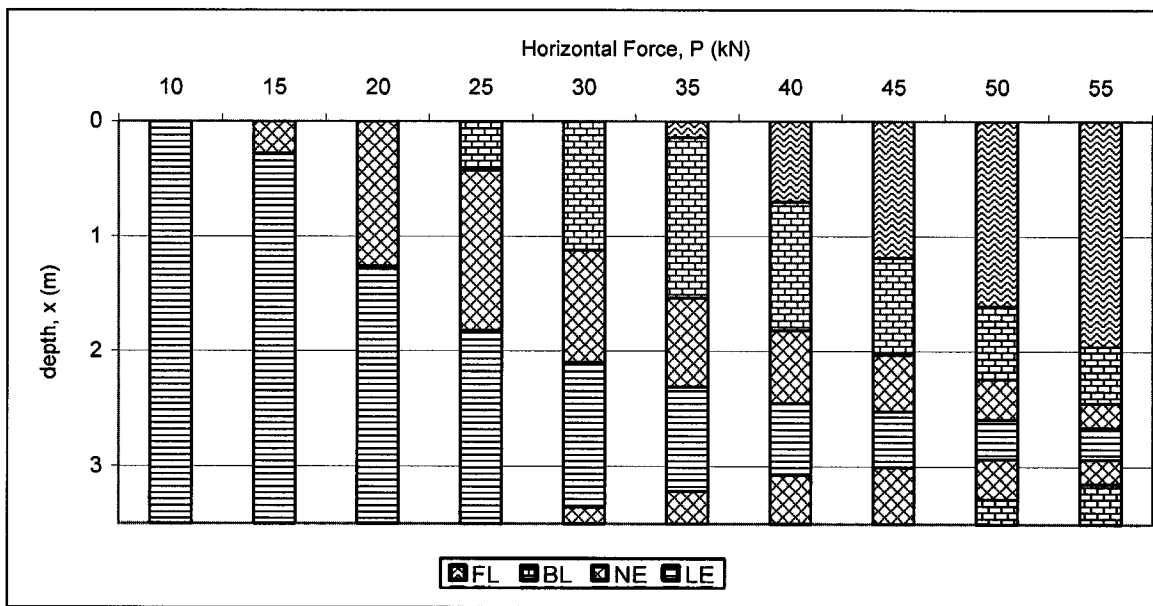


Figure 8-10 Quantitative assessment of location and size of soil phases developed with depth determined based on the distributions of sensitivity operators of δy_t for pile (free head) of length, $2.0T_p = 3.5$ m, subjected to variable horizontal forces, P .

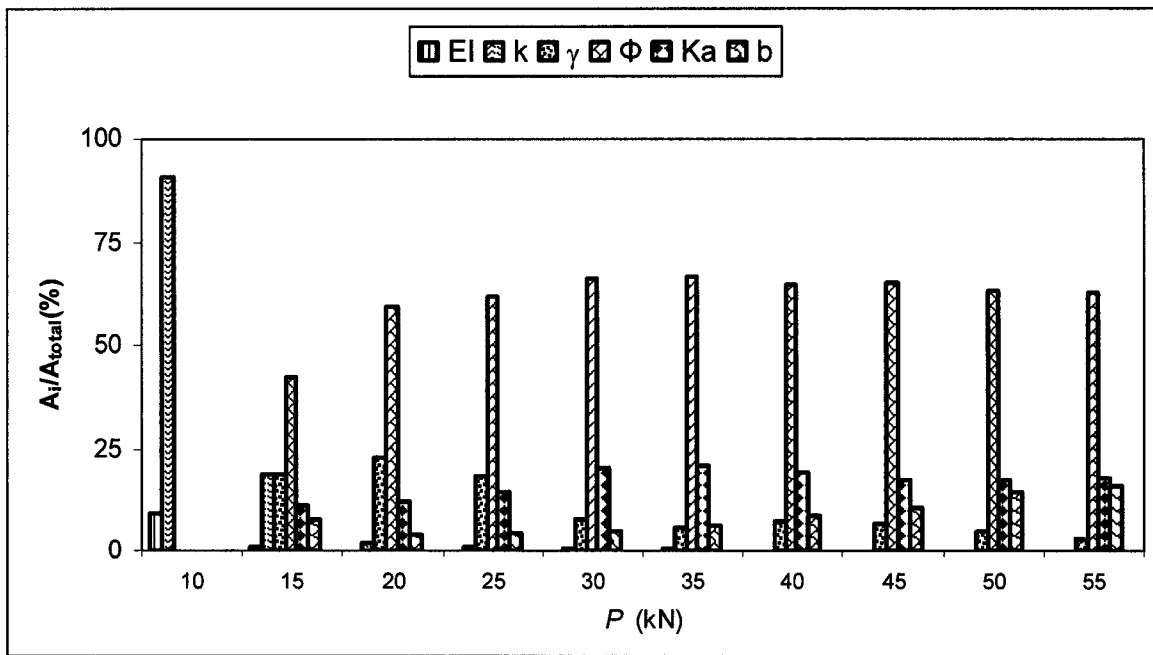


Figure 8-11 Quantitative assessment (in %) of sensitivity of top lateral displacement δy_t due to design variables for pile (free head) length of, $2.0T_p = 3.5$ m subjected to variable horizontal forces P .

Sensitivity factors connected to the design variables has been evaluated for different value of applied load varied in discrete fashion. Graphical representation of sensitivities of δy_i^P (..) when the pile of length $2T_p = 3.5$ m is subjected to variable P ; is shown in figure 8-12.

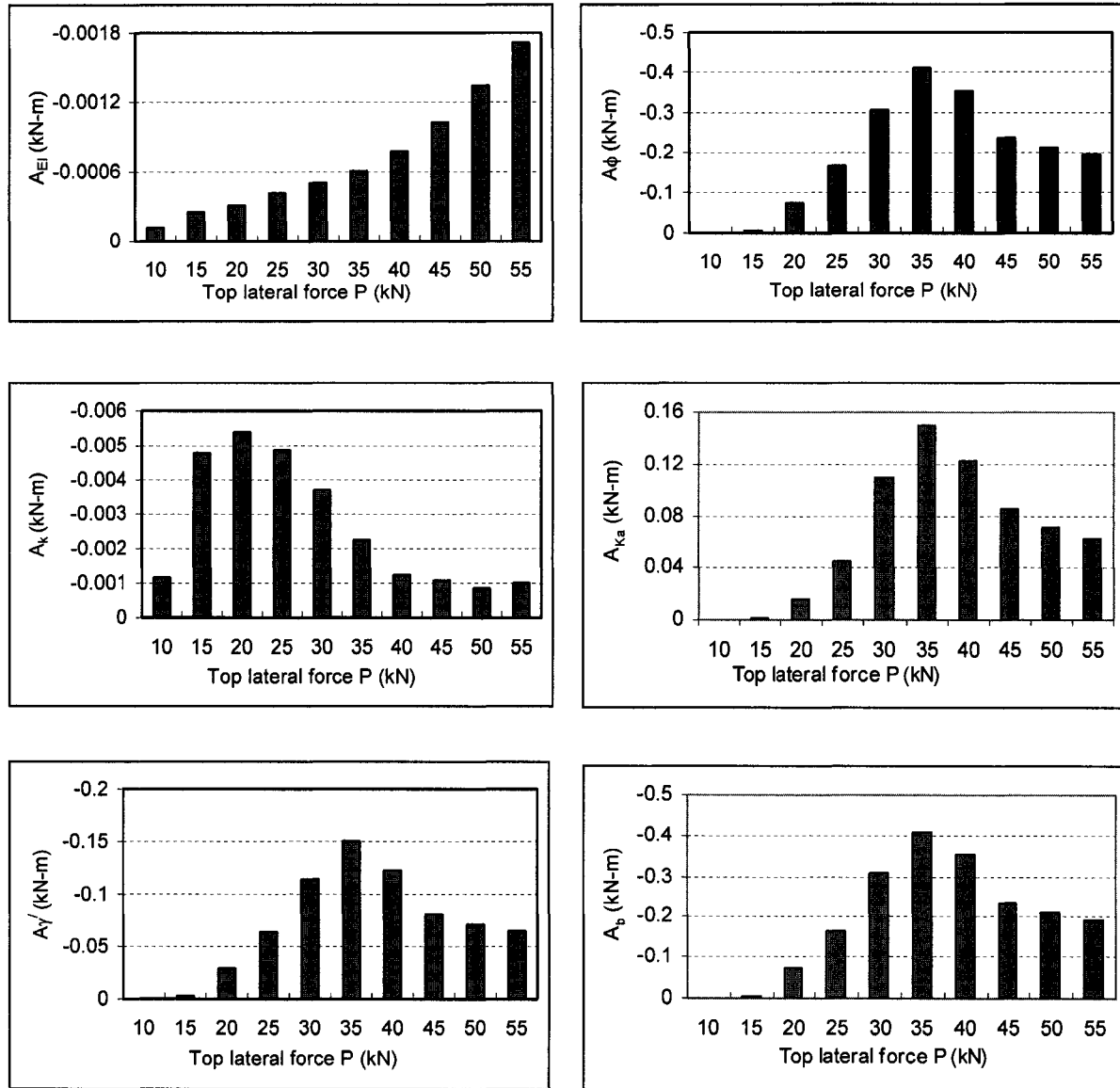


Figure 8-12 The quantitative assessment of sensitivity factors A_{EI}^{Py} , A_k^{Py} , $A_{\gamma'}^{Py}$, A_{ϕ}^{Py} , $A_{K_a}^{Py}$ and A_b^{Py} affecting the top lateral deformation y_i of free head pile of length $2T_p = 3.5$ m subjected to force P due to the changes of design variables EI , k , γ' , ϕ , K_a and b .

Figures 8-4 to 8-12 show the results of sensitivity analysis on a short pile hinge-connected to the pile cap subjected to horizontal forces varied in discrete fashion. Distribution of sensitivity operator S_{EI}^{Py} plotted against depth x is shown in Figure 8-4. For this length of pile and boundary condition, changes in design variable EI throughout the length of the pile are capable of producing changes in top lateral deflection y_t at all values of applied load. This is because change in EI is capable of producing changes in top lateral deflection irrespective of soil phase and EI is a pile property which is directly related to the flexural property of the pile. Sensitivity operator connected to the design variable EI follows the pattern of bending moment distribution along the pile due to the application of lateral load. Value of S_{EI}^{Py} is maximum at the middle portion of the pile and gradually reduces to become zero at either ends. The negative values of S_{EI}^{Py} indicate that increase in EI decreases y_t . Therefore, EI is a strengthening parameter of pile-soil system which improves the performance of the pile.

Distribution of sensitivity operator S_k^{Py} plotted against depth x is shown in Figure 8-5. At a value of applied horizontal force 15 kN, this operator has zero value near the top of the pile for a portion of about 0.2 m. This is because at this load this length of pile passes out of linear elastic phase. S_k^{Py} has nonzero value only where the deflection of pile is such that p - y soil remains in state of linear elastic phase. As the load increases longer portion of pile from top moves out of linear elastic phase and S_k^{Py} curves move downwards accordingly. The pile deflects in the opposite direction near the lower end of the pile. At higher values of applied loads tip of the pile moves out of the linear elastic

phase, this is why S_k^{Py} curves show zero values near the tip of the pile at higher values of applied load. For this length and boundary condition of pile design variable k is a strengthening parameter. At higher value of applied load the pile top lateral deflection becomes less sensitive to change in k .

Distribution of sensitivity operator $S_{\gamma'}^{Py}$ plotted against depth x is shown in Figure 8-6.

At 15 kN, 25 kN and 35 kN the curves for sensitivity operator $S_{\gamma'}^{Py}$ begin from zero and display nonzero values because at these values of applied loads the pile top remains in either nonlinear or bilinear phase. At 15 kN the small length of pile moves out of linear elastic phase where nonzero value of $S_{\gamma'}^{Py}$ curve is apparent. For the rest of the length of the pile deflection remains less than y_k , so, the pile-soil system remain is state of linear elastic phase where $S_{\gamma'}^{Py}$ is zero. At relatively higher values of applied loads, increase in value of γ' at regions above the point of zero deflection strengthens the pile-soil system whereas increase in γ' below point of zero deflection weakens the system.

Distribution of sensitivity operator S_{ϕ}^{Py} shows the same pattern as $S_{\gamma'}^{Py}$ and shown in Figure 8-7. The only difference is that values of S_{ϕ}^{Py} are higher than the corresponding values of $S_{\gamma'}^{Py}$.

Distribution of sensitivity operator $S_{K_a}^{Py}$ follows the same pattern of $S_{\gamma'}^{Py}$ and S_{ϕ}^{Py} . As shown in Figure 8-8 the values of $S_{K_a}^{Py}$ are opposite in sign to $S_{\gamma'}^{Py}$ or S_{ϕ}^{Py} and different in magnitude. Increase in value of K_a at regions above the point of zero deflection

weakens the pile-soil system whereas increase in K_a below point of zero deflection strengthens the system.

Distribution of sensitivity operator S_b^{Py} plotted against depth x is shown in Figure 8-9. Increase in value of b near the top of the pile weakens the system, strengthens at the middle part of the pile and again weakens the system near the tip of the pile.

Figure 8-10 shown formation of soil phase along the length of the pile with the increase in horizontal forces for free head pile of length $2.0 T_p = 3.5$ m subjected to variable horizontal force. At 10 kN the whole length of the pile is in linear elastic phase. With increase in applied load deflection increases and other phases develops along the length of the pile.

Figure 8-11 shows distribution of the relative sensitivity factors at different values of applied load. At 10 kN only F_{EI}^{Py} and F_k^{Py} have nonzero values because at this value of applied load, entire length of the pile is in linear elastic phase. At higher values of applied loads, relative sensitivity factors connected to all design variables have nonzero values, but F_ϕ^{Py} has remarkably high values.

Figure 8-12 shows distribution of the sensitivity factors with increase in values of applied load. For this length and boundary condition of the pile, A_{EI} increases in nonlinear fashion with increase in values of applied load. For other sensitivity factors their values increase and decrease again with increase in vales of applies load.

Results of sensitivity investigation on free head short pile subjected to variable bending moment M_i are shown in Figures 8-13 to 8-21.

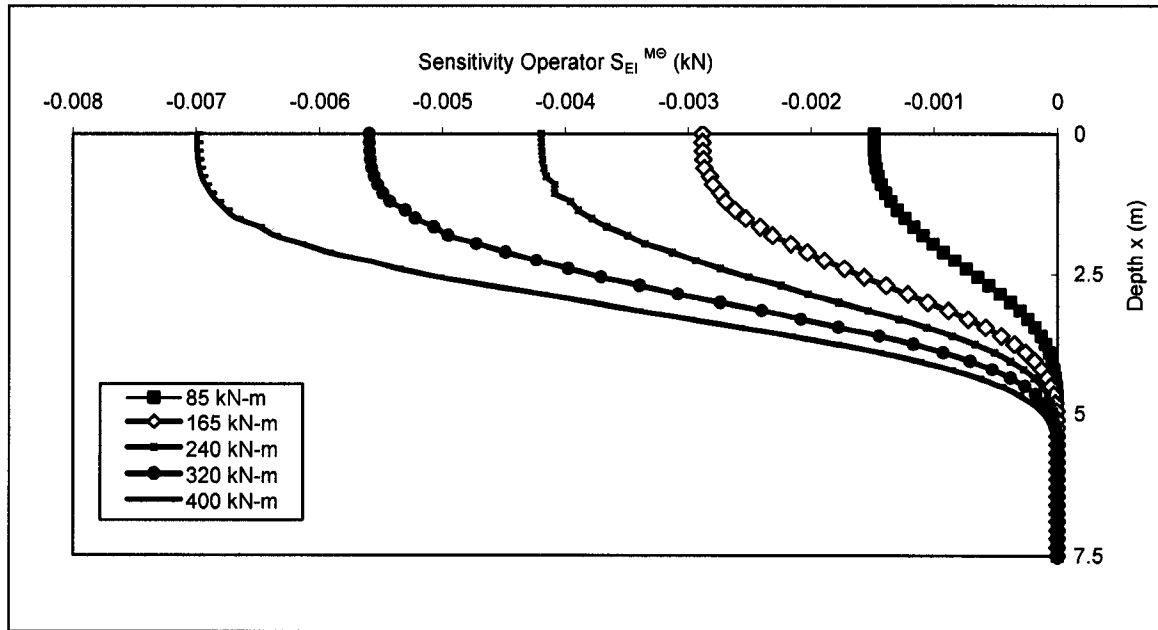


Figure 8-13 Distribution of sensitivity operators $S_{EI}^{M\theta}$ affecting the change of $\delta\theta_i$ due to the variation of design variable δEI for the free head pile of length, $4.5T_m = 7.5$ m subjected to variable bending moment M_i .

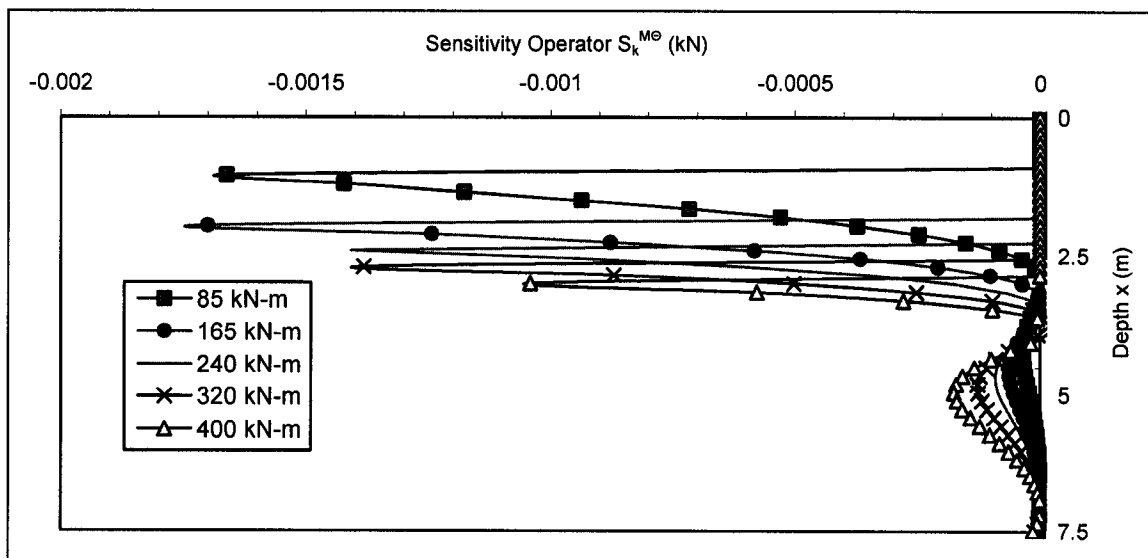


Figure 8-14 Distribution of sensitivity operators $S_k^{M\theta}$ affecting the change of $\delta\theta_i$ due to the variation of design variable δk for the free head pile of length, $4.5T_m = 7.5$ m subjected to variable bending moment M_i .

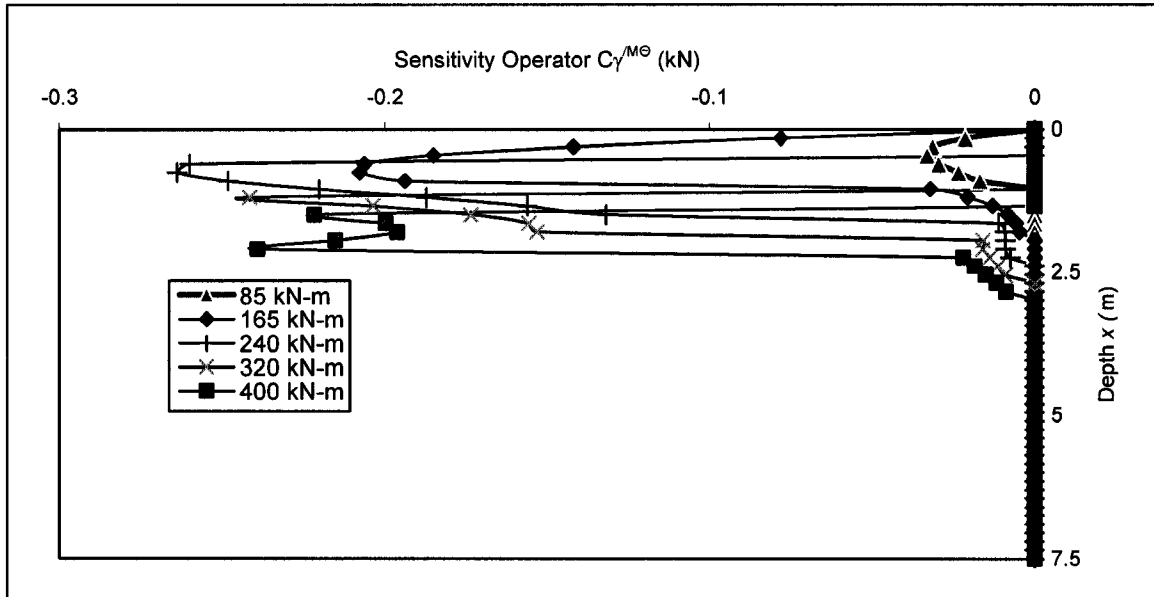


Figure 8-15 Distribution of sensitivity operators $S_{\gamma}^{M\theta}$ affecting the change of $\delta\theta_t$ due to the variation of design variable $\delta\gamma'$ for the free head pile of length, $4.5T_m = 7.5$ m subjected to variable bending moment M_i .

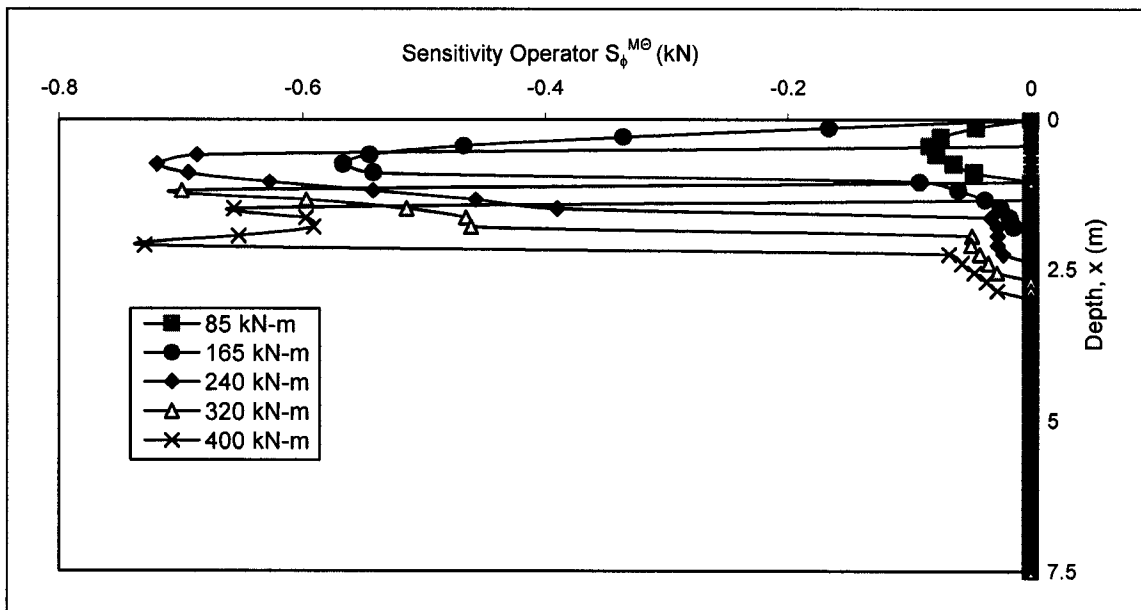


Figure 8-16 Distribution of sensitivity operators $S_{\phi}^{M\theta}$ affecting the change of $\delta\theta_t$ due to the variation of design variable $\delta\phi$ for the free head pile of length, $4.5T_m = 7.5$ m subjected to variable bending moment M_i .

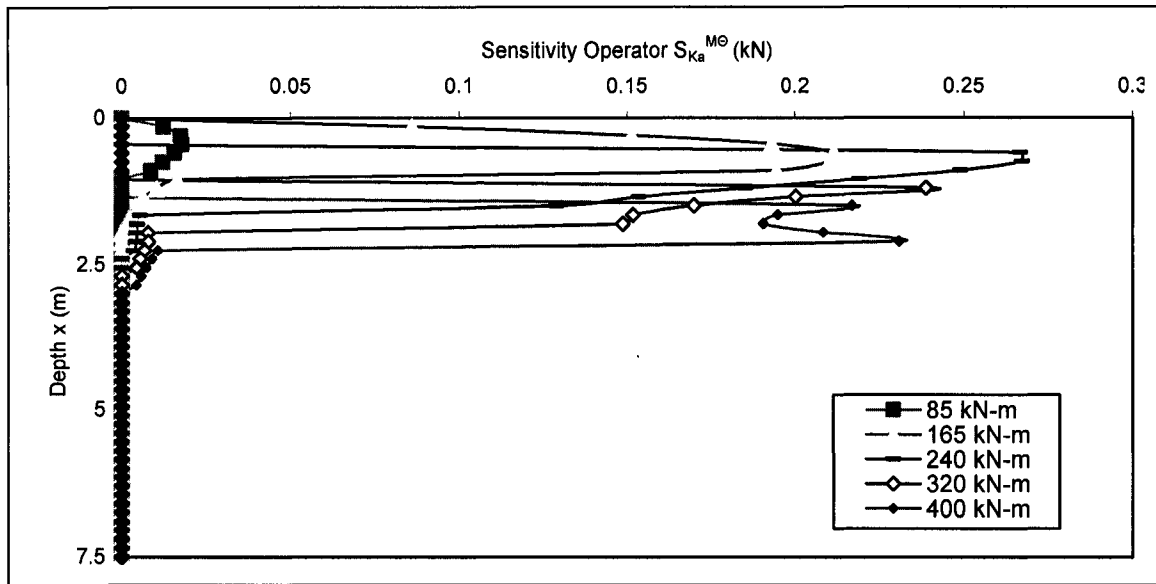


Figure 8-17 Distribution of sensitivity operators $S_{K_a}^{M\theta}$ affecting the change of $\delta\theta_t$ due to the variation of design variable δK_a for the free head pile of length, $4.5T_m = 7.5$ m subjected to variable bending moment M_i .

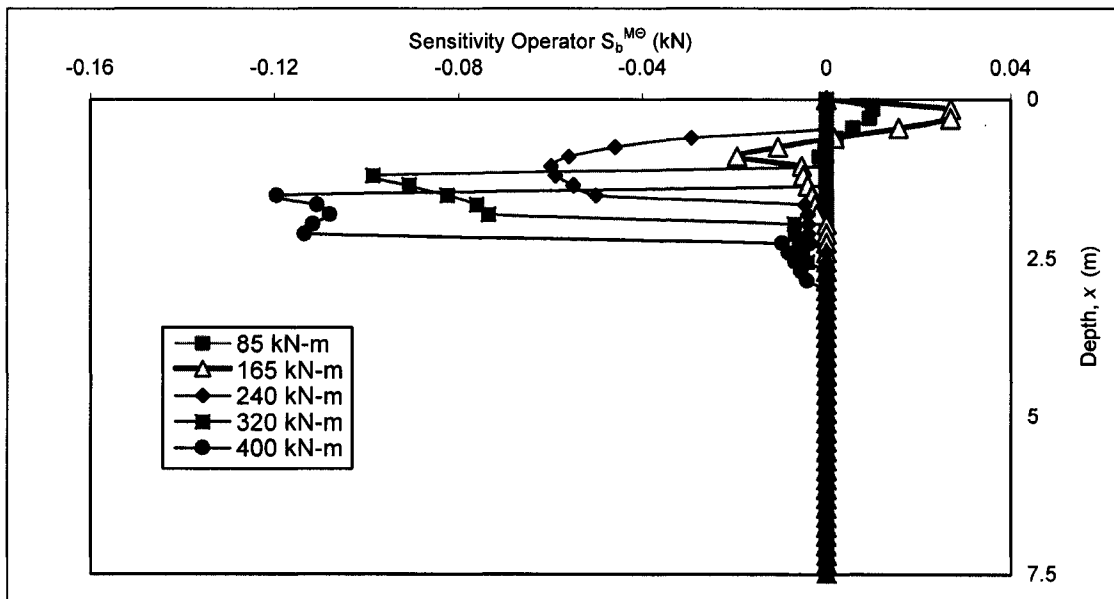


Figure 8-18 Distribution of sensitivity operators $S_b^{M\theta}$ affecting the change of $\delta\theta_t$ due to the variation of design variable δ_b for the free head pile of length, $4.5T_m = 7.5$ m subjected to variable bending moment M_i .

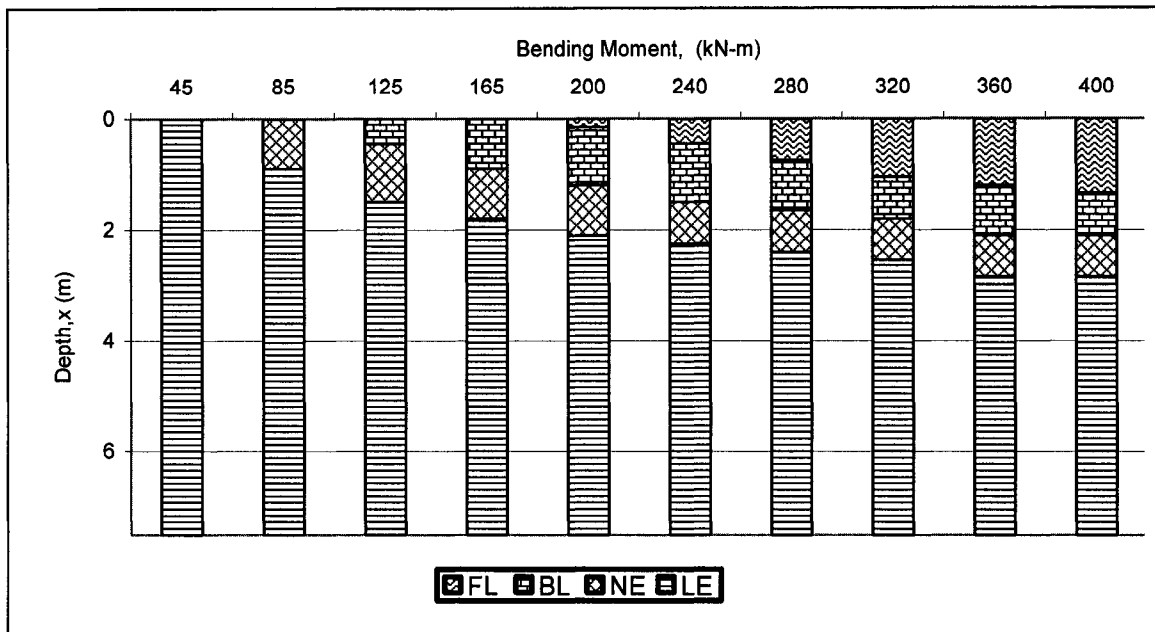


Figure 8-19 Quantitative assessment of location and size of soil phases developed with depth determined based on the distributions of sensitivity operators of $\delta\theta_i$ for free head pile of length, $4.5T_m = 7.5$ m, subjected to variable bending moment, M_i .

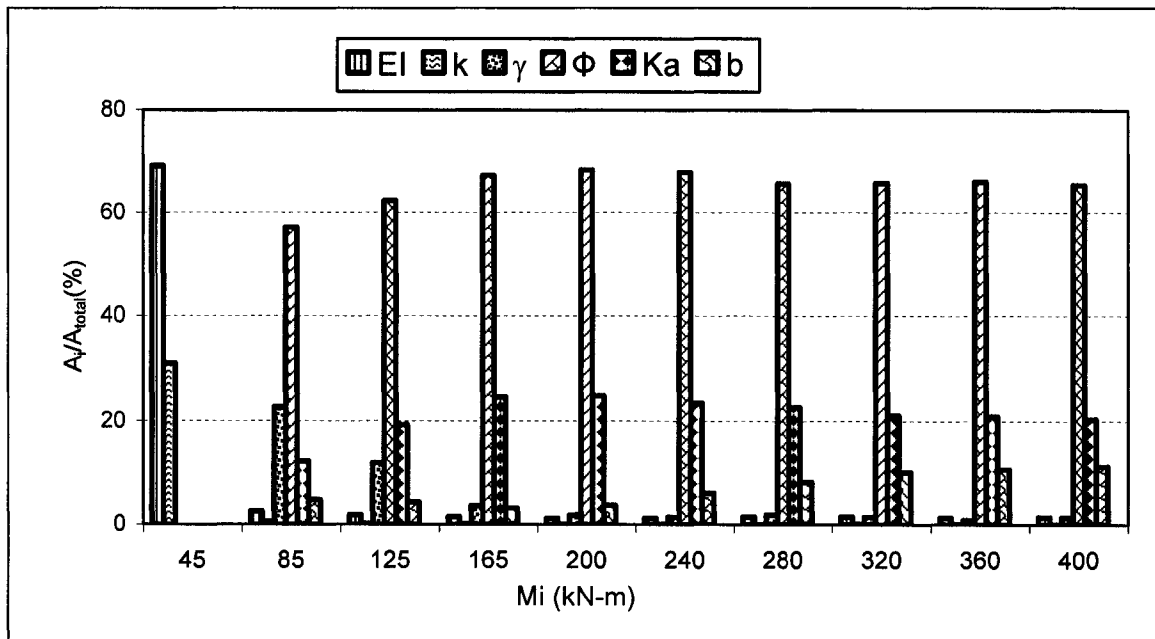


Figure 8-20 Quantitative assessment (in %) of sensitivity of top lateral displacement due to design variables for free head pile of length $4.5T_m = 7.5$ m subjected to variable bending moments, M_i .

Sensitivity factors connected to the design variables has been evaluated in different value of applied load varied in discrete fashion. Graphical representation of sensitivity of $\delta\theta_t^{M\theta}$ when the pile of length $4.5T_m = 7.5$ m is subjected to variable M_i is shown in Figure 8-21.

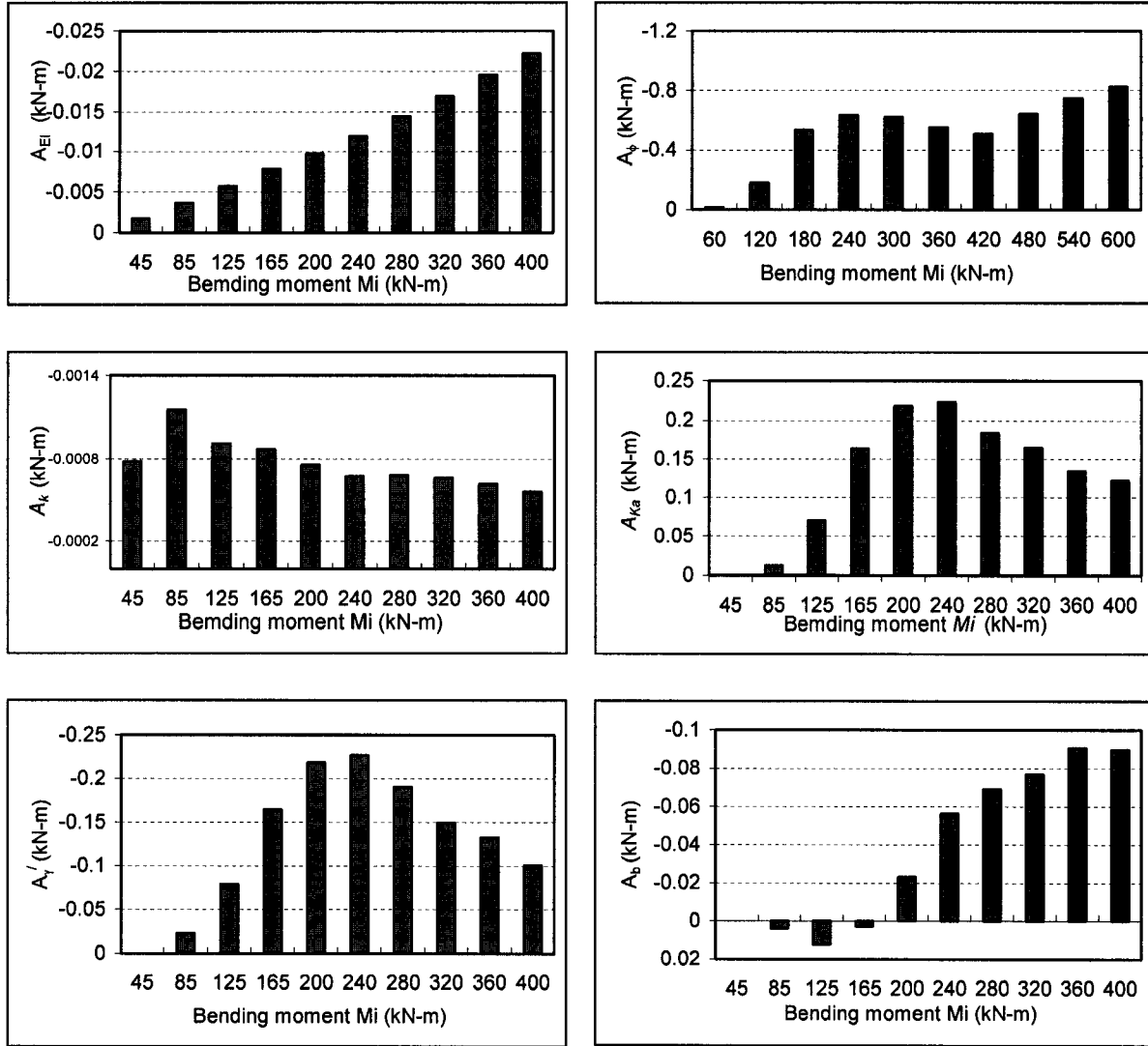


Figure 8-21 The quantitative assessment of sensitivity factors $A_{EI}^{M\theta}$, $A_k^{M\theta}$, $A_{\gamma'}^{M\theta}$, $A_{\phi}^{M\theta}$, $A_{K_a}^{M\theta}$ and $A_b^{M\theta}$ affecting the top angle of flexural rotation θ_t of free head pile of length $4.5T_m = 7.5$ m subjected to bending moment M due to the changes of design variables EI , k , γ' , ϕ , K_a and b .

Figures 8-13 to 8-21 shows the distribution of sensitivity operators, sensitivity factors and relative sensitivity factors and soil phase along the length of the pile for free headed pile subjected to bending moment applied to the pile head varied in discrete fashion. Distribution of $S_{EI}^{M\theta}$ affecting the sensitivity of flexural rotation at the top of the pile θ_t , shows higher values near the top of the pile because of the concentrated bending moment applied to the pile cap. Values of $S_{EI}^{M\theta}$ decreases with depth and become almost zero at a depth of 5 m. Distribution of the sensitivity operators also shows that top flexural rotation of pile is more sensitive to change in flexural stiffness EI of pile at higher values of applied bending moment.

Figure 8-14 shows distribution of sensitivity operator $S_k^{M\theta}$ affecting the top flexural rotation of pile due to the changes in coefficient of subgrade reaction k . $S_k^{M\theta}$ curves show that θ_t is more sensitive to changes in k at upper part of the pile than to the changes at lower part of the pile. The zero values of $S_k^{M\theta}$ are because of soil is out of linear phase.

Distributions of sensitivity operator $S_{\gamma'}^{M\theta}$ affecting the top flexural rotation of pile due to the changes in submerged unit weight of soil are shown in Figure 8-15. $S_{\gamma'}^{M\theta}$ curves show nonzero values for top 2.5 m of the pile, which means that θ_t is sensitive to changes in unit weight of soil for a depth of about 2.5 m. Distributions of sensitivity operator $S_{\phi}^{M\theta}$, $S_{K_a}^{M\theta}$ and $S_b^{M\theta}$ follows the same pattern of $S_{\phi}^{M\theta}$, although each has different values for same depth and applied bending moment.

Figures 8-22 to 8-30 show result of results of sensitivity analysis of long fixed headed single pile of length $7T_p = 12.5$ m.

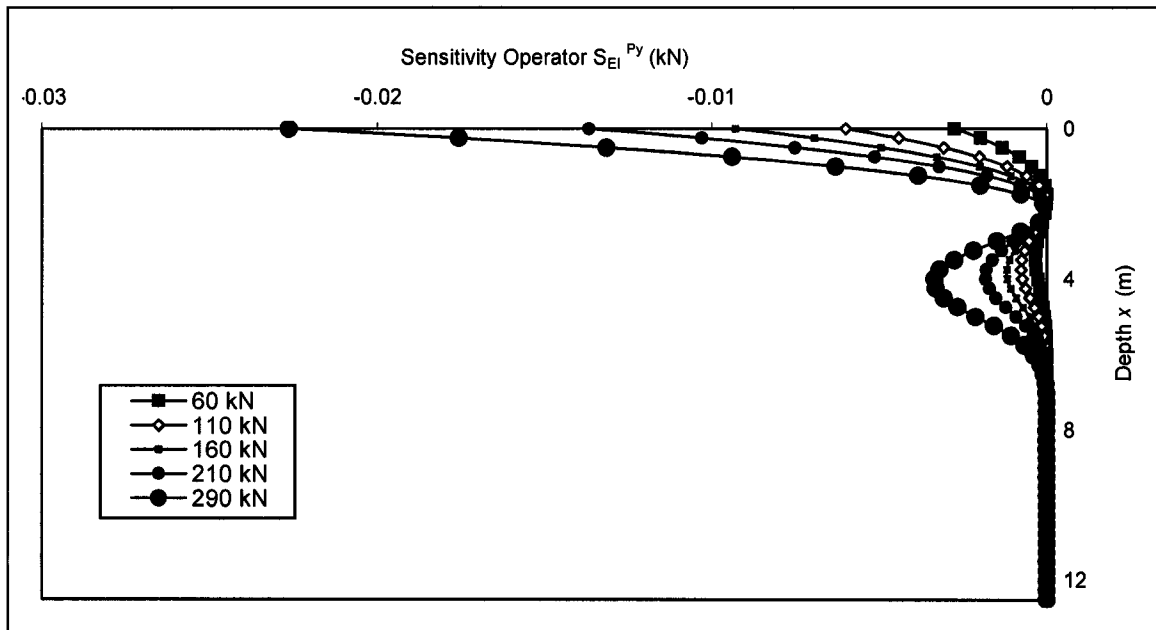


Figure 8-22 Distribution of sensitivity operators S_{EI}^{Py} affecting the change of δy_t due to the variation of design variable δEI for the fixed headed pile of length, $7.0T_p = 12.5$ m subjected to variable horizontal forces.

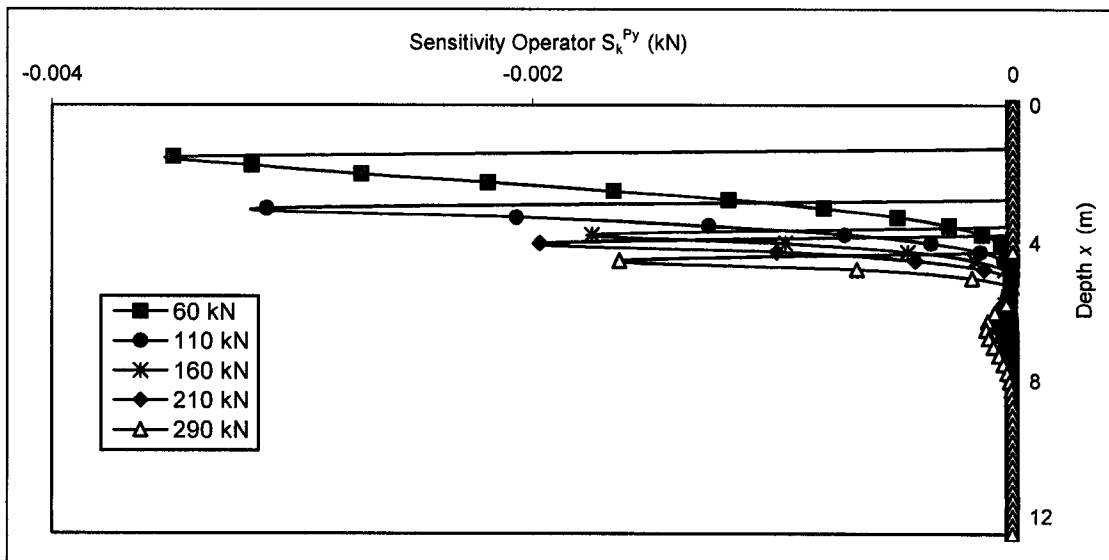


Figure 8-23 Distribution of sensitivity operators S_k^{Py} affecting the change of δy_t due to the variation of design variable δk for the fixed headed pile of length, $7.0T_p = 12.5$ m subjected to variable horizontal forces.

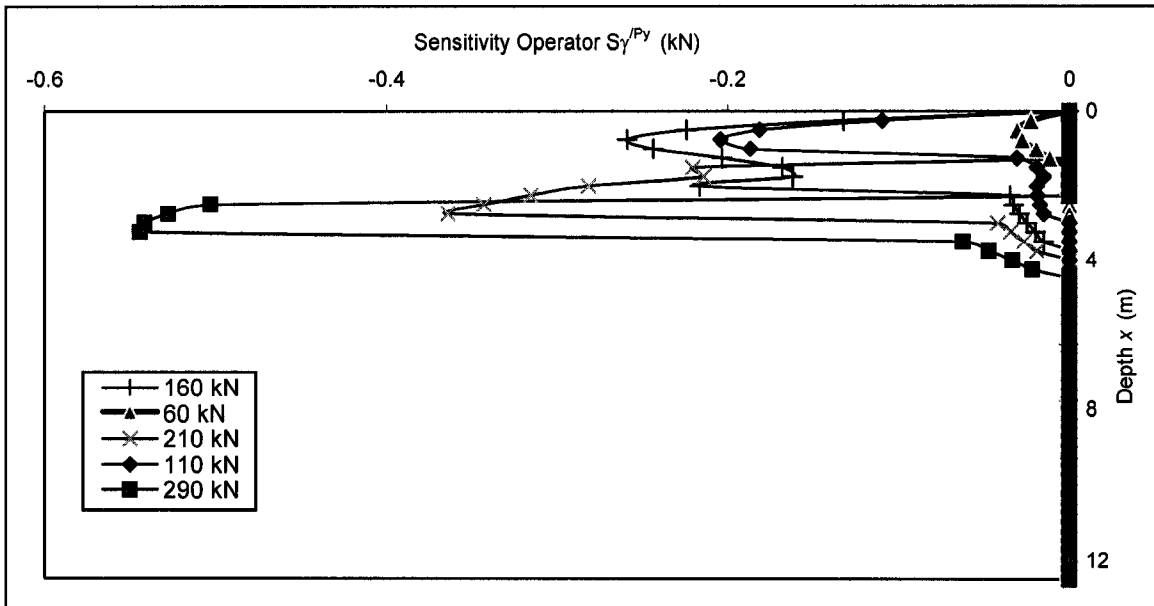


Figure 8-24 Distribution of sensitivity operators $S_{\gamma'}^{Py}$ affecting the change of δy_t due to the variation of design variable $\delta \gamma'$ for the fixed headed pile of length, $7.0T_p = 12.5$ m subjected to variable horizontal forces.

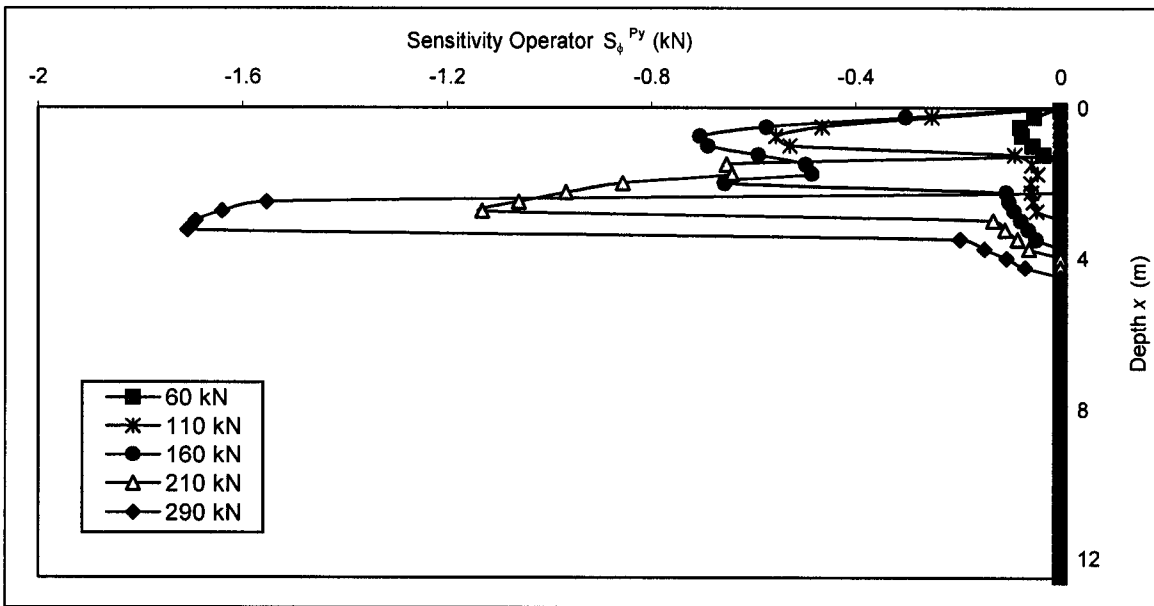


Figure 8-24 Distribution of sensitivity operators S_{ϕ}^{Py} affecting the change of δy_t due to the variation of design variable $\delta \phi$ for the fixed headed pile of length, $7.0T_p = 12.5$ m subjected to variable horizontal forces.

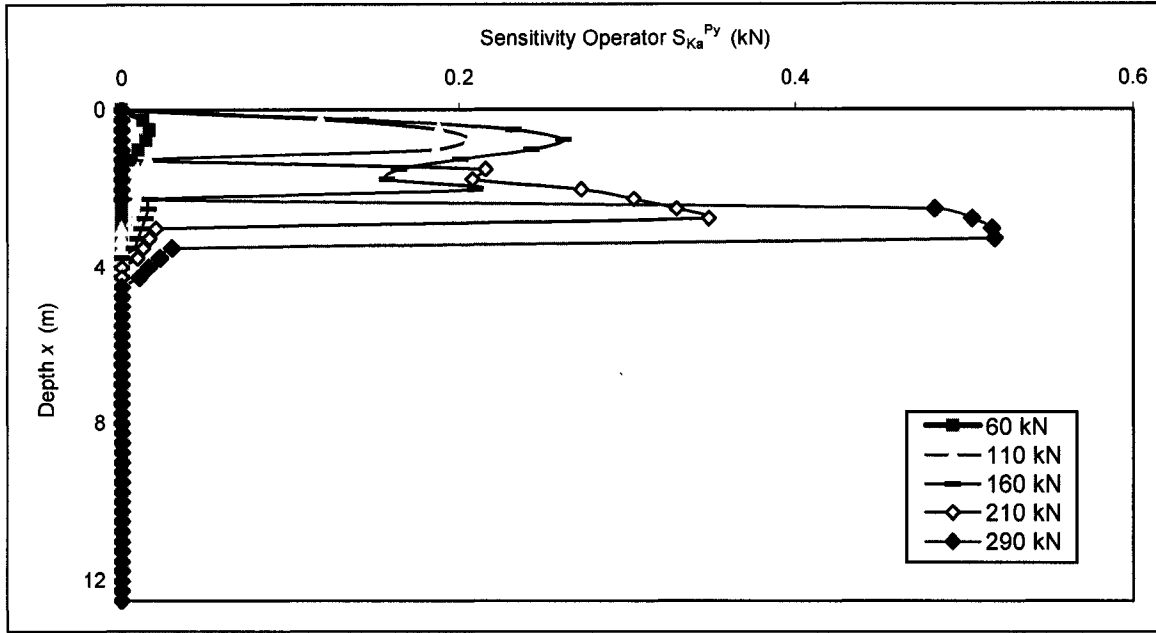


Figure 8-26 Distribution of sensitivity operators $S_{K_a}^{P_y}$ affecting the change of δy_t due to the variation of design variable δK_a for the fixed headed pile of length, $7.0T_p = 12.5$ m subjected to variable horizontal forces.

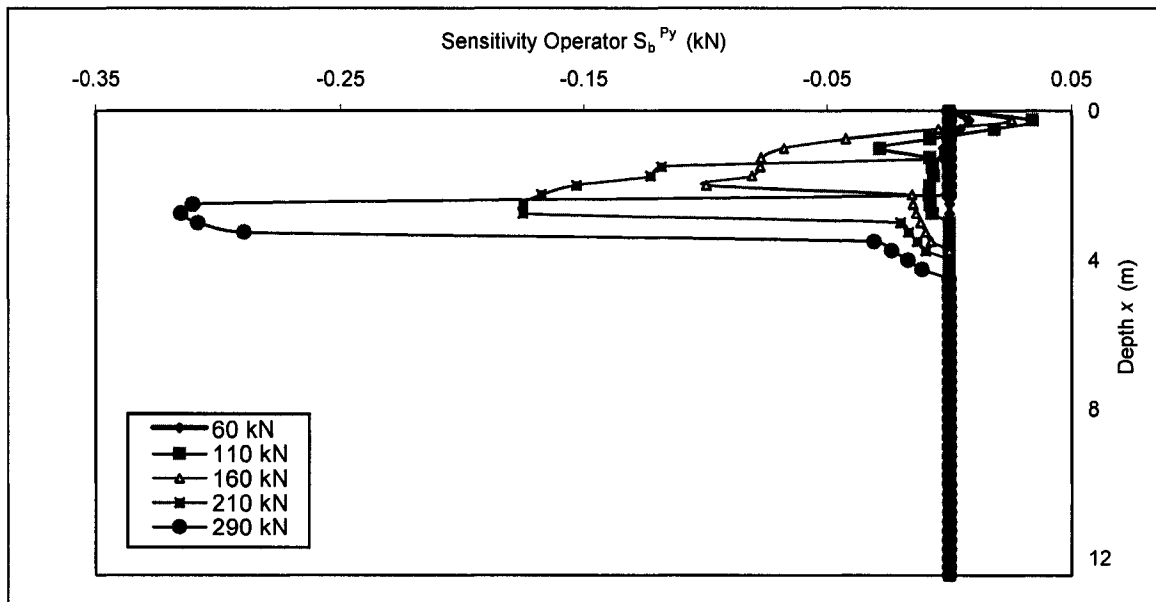


Figure 8-27 Distribution of sensitivity operators $S_b^{P_y}$ affecting the change of δy_t due to the variation of design variable δb for the fixed headed pile of length, $7.0T_p = 12.5$ m subjected to variable horizontal forces.

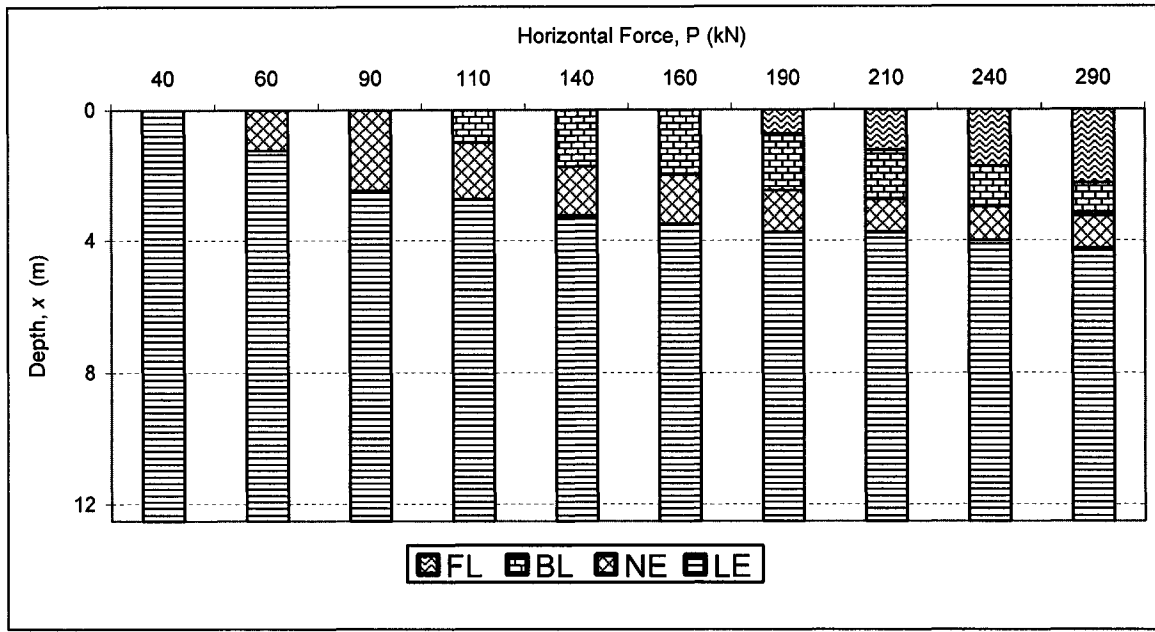


Figure 8-28 Quantitative assessment of location and size of soil phases developed with depth determined based on the distributions of sensitivity operators of δy_i for fixed headed pile of length, $7.0T_p = 12.5$ m, subjected to variable horizontal forces, P .

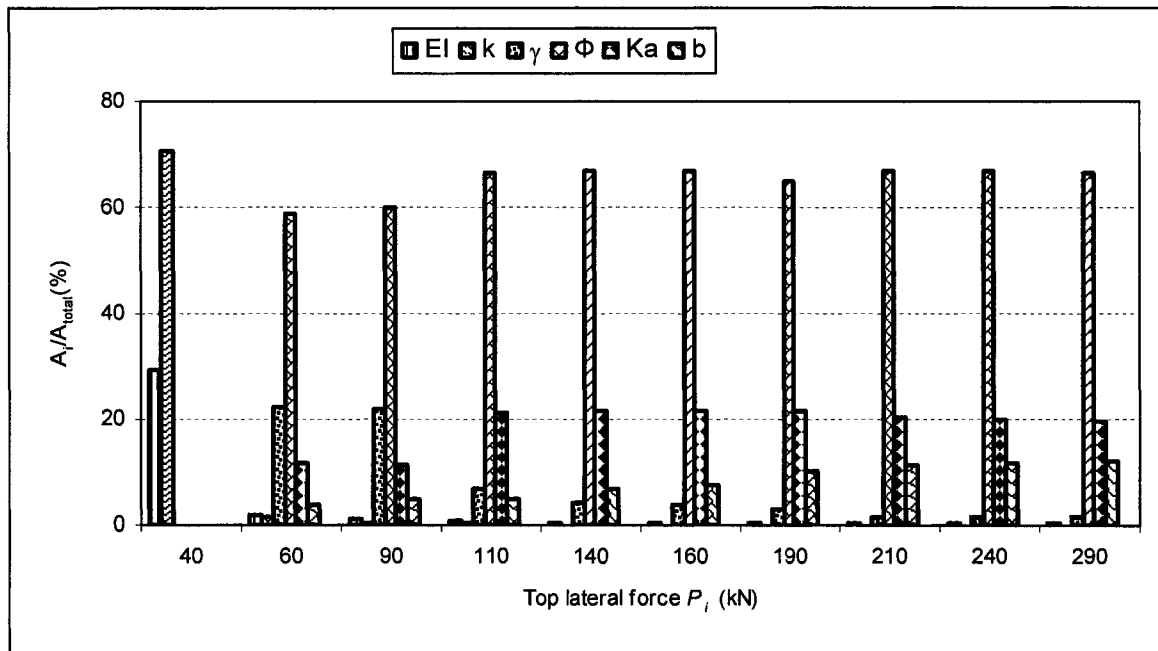


Figure 8-29 Quantitative assessment (in %) of sensitivity of top lateral displacement δy_i due to design variables the for fixed headed pile length of, $7.0T_p = 12.5$ m subjected to variable horizontal forces, P .

Sensitivity factors connected to the design variables has been evaluated in different value of applied load varied in discrete fashion. Graphical representation of sensitivity of δy_i^P when the pile of length $7T_p = 12.5$ m is subjected to variable P_i is shown in Figure 8-30.

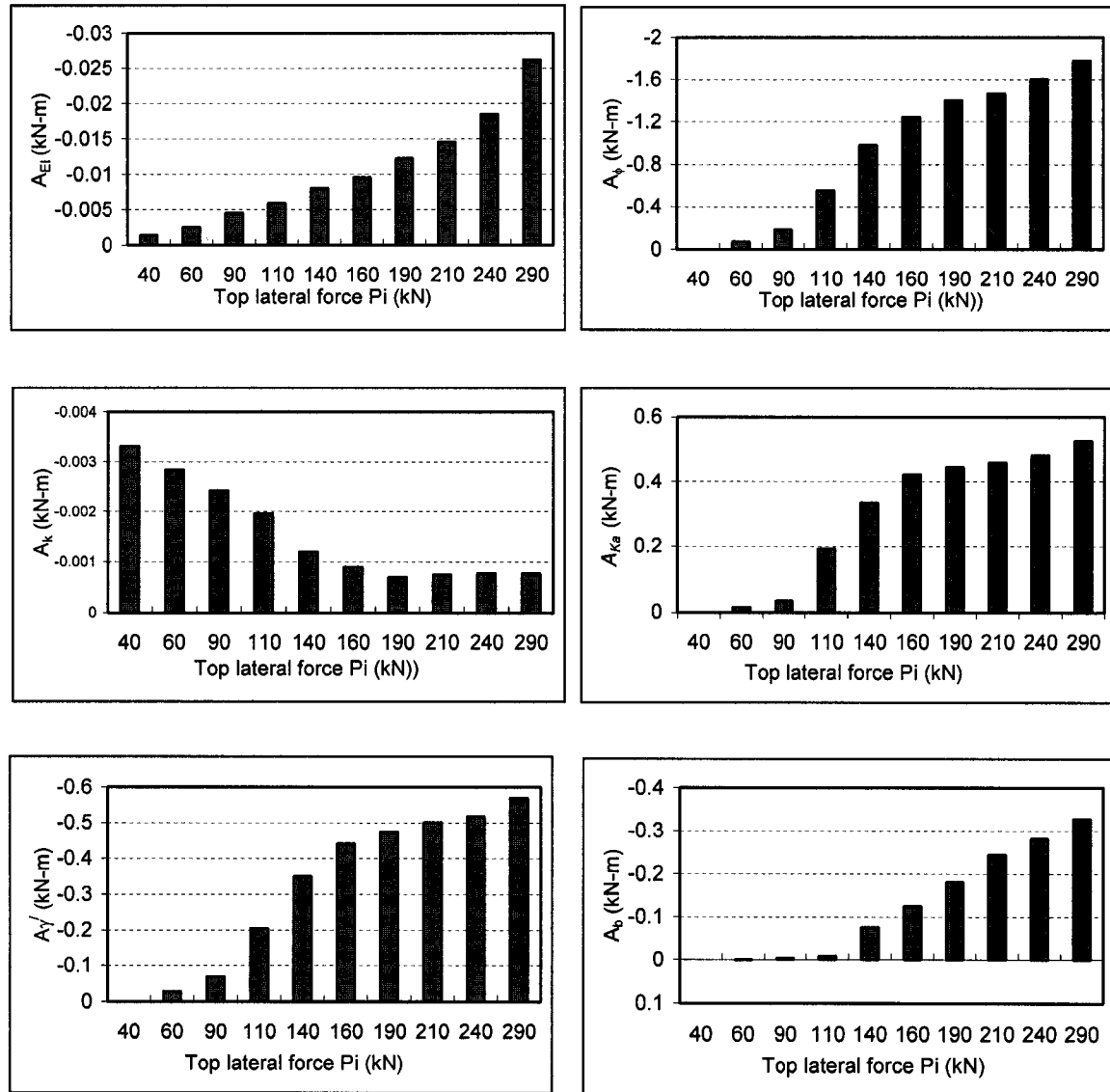


Figure 8-30 The quantitative assessment of sensitivity factors A_{EI}^{Py} , A_k^{Py} , $A_{\gamma'}^{Py}$, A_{ϕ}^{Py} , $A_{K_a}^{Py}$ and A_b^{Py} affecting the top lateral deformation y_i of of free head pile of length $7T_m = 12.5$ m subjected to force P due to the changes of design variables EI , k , γ' , ϕ , K_a and b .

Distribution of sensitivity operator, sensitivity factors, relative sensitivity factors and soil phase along the length of the fixed pile under different value of horizontal force varied in discrete fashion are shown in Figures 8-22 to 8-30. S_{EI}^{Py} curves have highest values at top of the pile where bending moment, developed at the pile cap due to fixicity of the pile to the pile cap, is maximum. S_{EI}^{Py} decreases as depth increases to become zero at depth of about 2 m before showing nonzero values between the depths 4 m to 8 m.

Distribution of sensitivity operators S_k^{Py} , $S_{\gamma'}^{Py}$, S_{ϕ}^{Py} , $S_{K_a}^{Py}$ and S_b^{Py} affecting the sensitivities of top lateral deflection y_t due the changes in design variables k , γ' , ϕ , K_a and b follow the same pattern of distribution of operators for free head short pile subjected to variable moment. For a short length at the top of pile S_b^{Py} shows positive values which indicates, increase in values of pile width b will decrease top lateral deflection y_t . But below that depth S_b^{Py} shows negative values upto a depth of about 4 m where width of pile is a strengthening parameter of pile-soil system.

Pile being long undergoes relatively smaller deflections at the lower zone of the pile length. Formation of nonlinear elastic and bilinear elastic phase concentrates at the upper part of the pile length which is shown in Figure 8-28.

Distribution of sensitivity factors are shown in Figure 8-30. Values of A_{EI} , $A_{\gamma'}$ and A_{ϕ} increases from lower positive value to highest as load increases, whereas A_k decreases.

Results of sensitivity investigation on free head long pile subjected to variable bending moment M_i are shown in Figures 8-31 to 8-39.

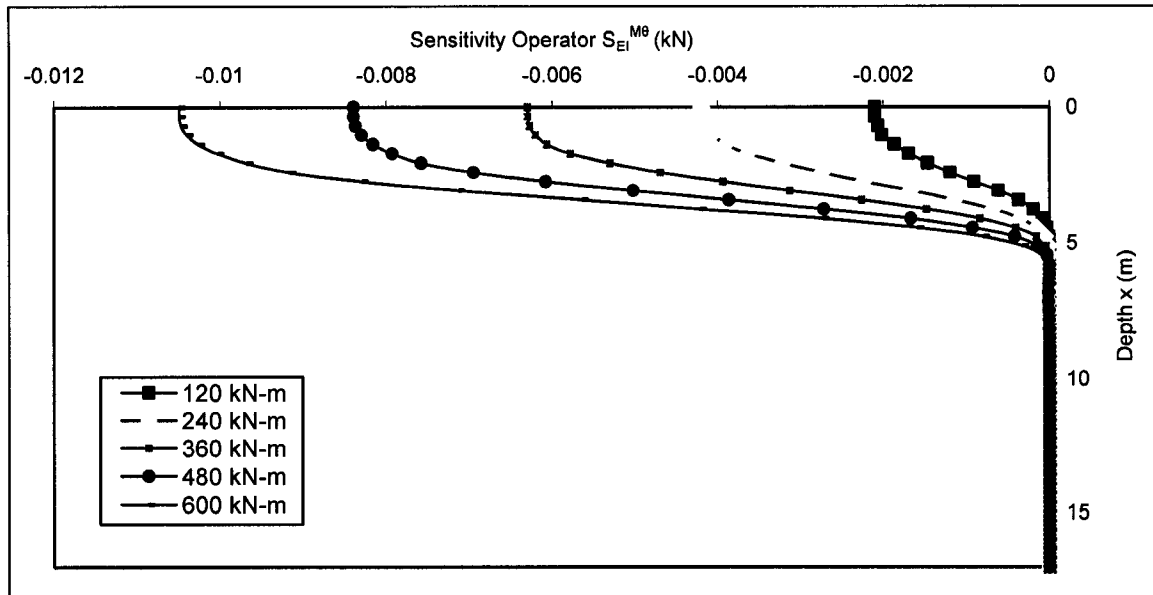


Figure 8-31 Distribution of sensitivity operators $S_{EI}^{M\theta}$ affecting the change of $\delta\theta_i$ due to the variation of design variable δEI for the free head pile of length, $10T_m = 17.0$ m subjected to variable bending moment M_i .

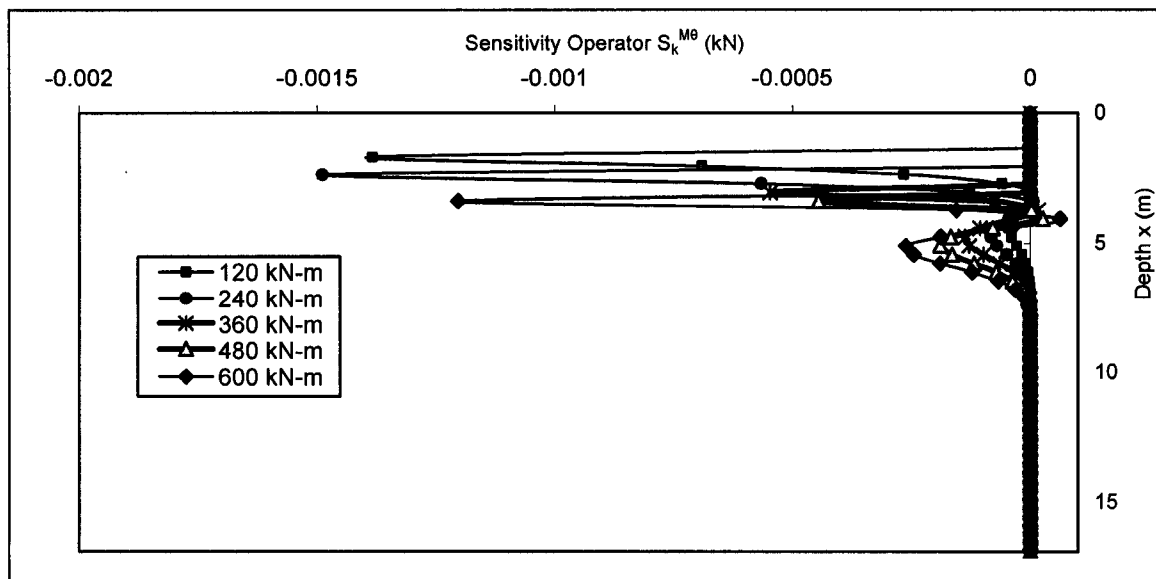


Figure 8-32 Distribution of sensitivity operators $S_k^{M\theta}$ affecting the change of $\delta\theta_i$ due to the variation of design variable δk for the free head pile of length, $10T_m = 17.0$ m subjected to variable bending moment M_i .

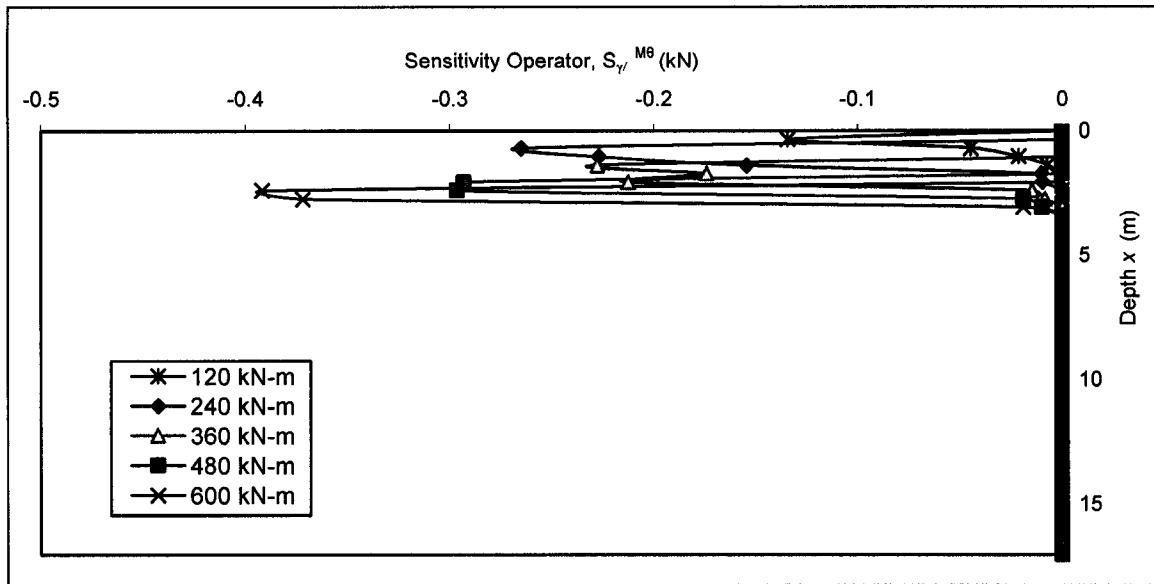


Figure 8-33 Distribution of sensitivity operators $S_{\gamma'}^{M\theta}$ affecting the change of $\delta\theta_t$ due to the variation of design variable $\delta\gamma'$ for the free head pile of length, $10T_m = 17.0$ m subjected to variable bending moment M_i

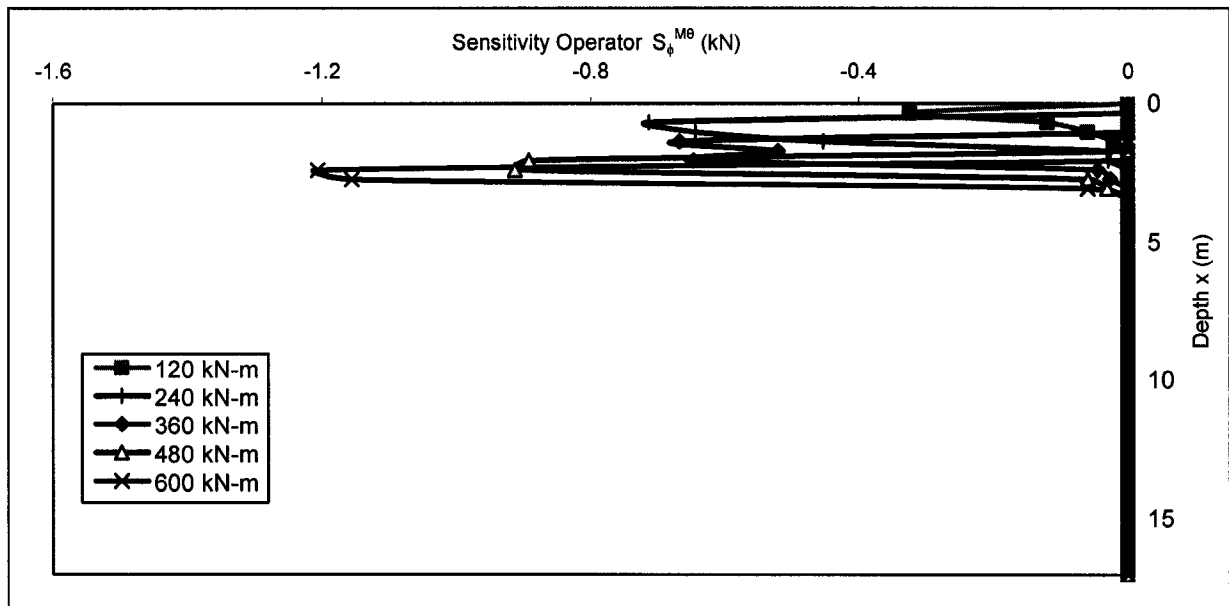


Figure 8-34 Distribution of sensitivity operators $S_{\phi}^{M\theta}$ affecting the change of $\delta\theta_t$ due to the variation of design variable $\delta\phi$ for the free head pile of length, $10T_m = 17.0$ m subjected to variable bending moment M_i .

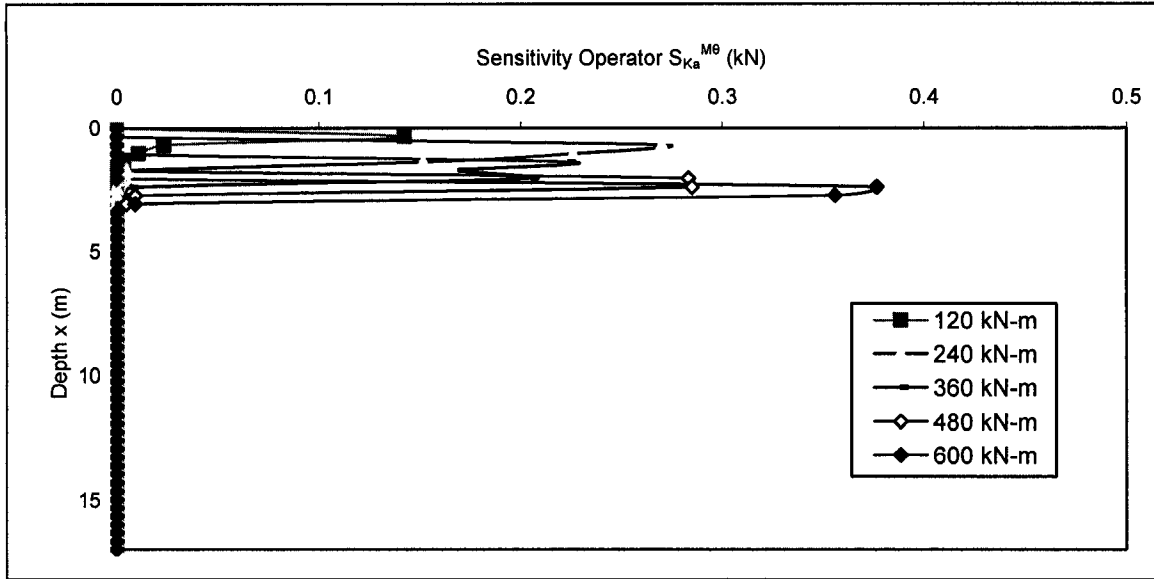


Figure 8-35 Distribution of sensitivity operators $S_{K_a}^{M\theta}$ affecting the change of $\delta\theta_t$ due to the variation of design variable δK_a for the free head pile of length, $10T_m = 17.0$ m subjected to variable bending moment M_i .

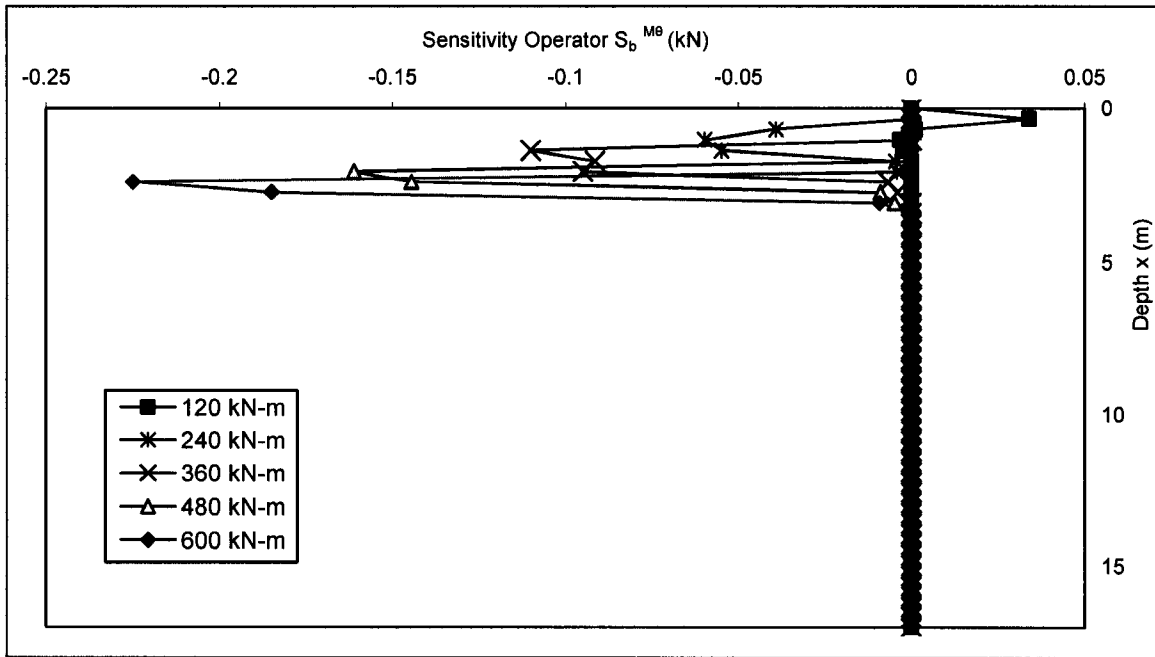


Figure 8-36 Distribution of sensitivity operators $S_{K_b}^{M\theta}$ affecting the change of $\delta\theta_t$ due to the variation of design variable δK_b for the free head pile of length, $10T_m = 17.0$ m subjected to variable bending moment M_i .

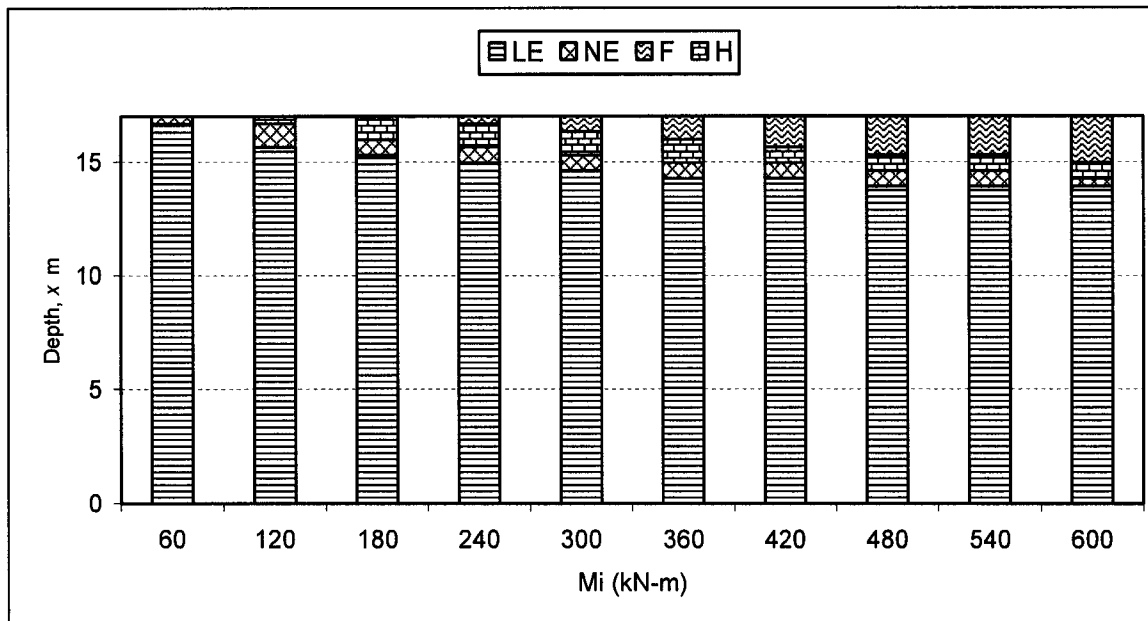


Figure 8-37 Quantitative assessment of location and size of soil phases developed with depth determined based on the distributions of sensitivity operators of $\delta\theta_i$ for free head pile of length, $10T_m = 17.0$ m, subjected to variable bending moment, M_i .

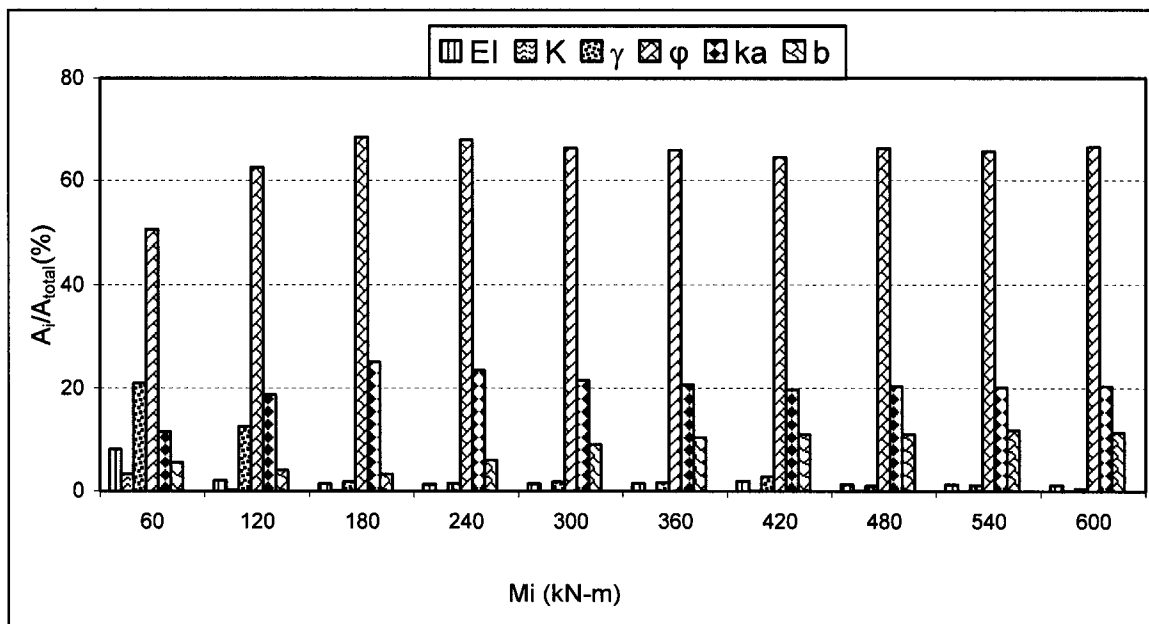


Figure 8-38 Quantitative assessment (in %) of sensitivity of top lateral displacement due to design variables for free head pile of length, $10T_m = 17.0$ m subjected to variable bending moments, M_i .

Sensitivity factors connected to the design variables has been evaluated in different value of applied load varied in discrete fashion. Graphical representation of sensitivities of $\delta\theta_{(\dots)}^M$ when the pile of length $10T_m = 17.0$ m is subjected to variable M_i is shown in figure 8-39.

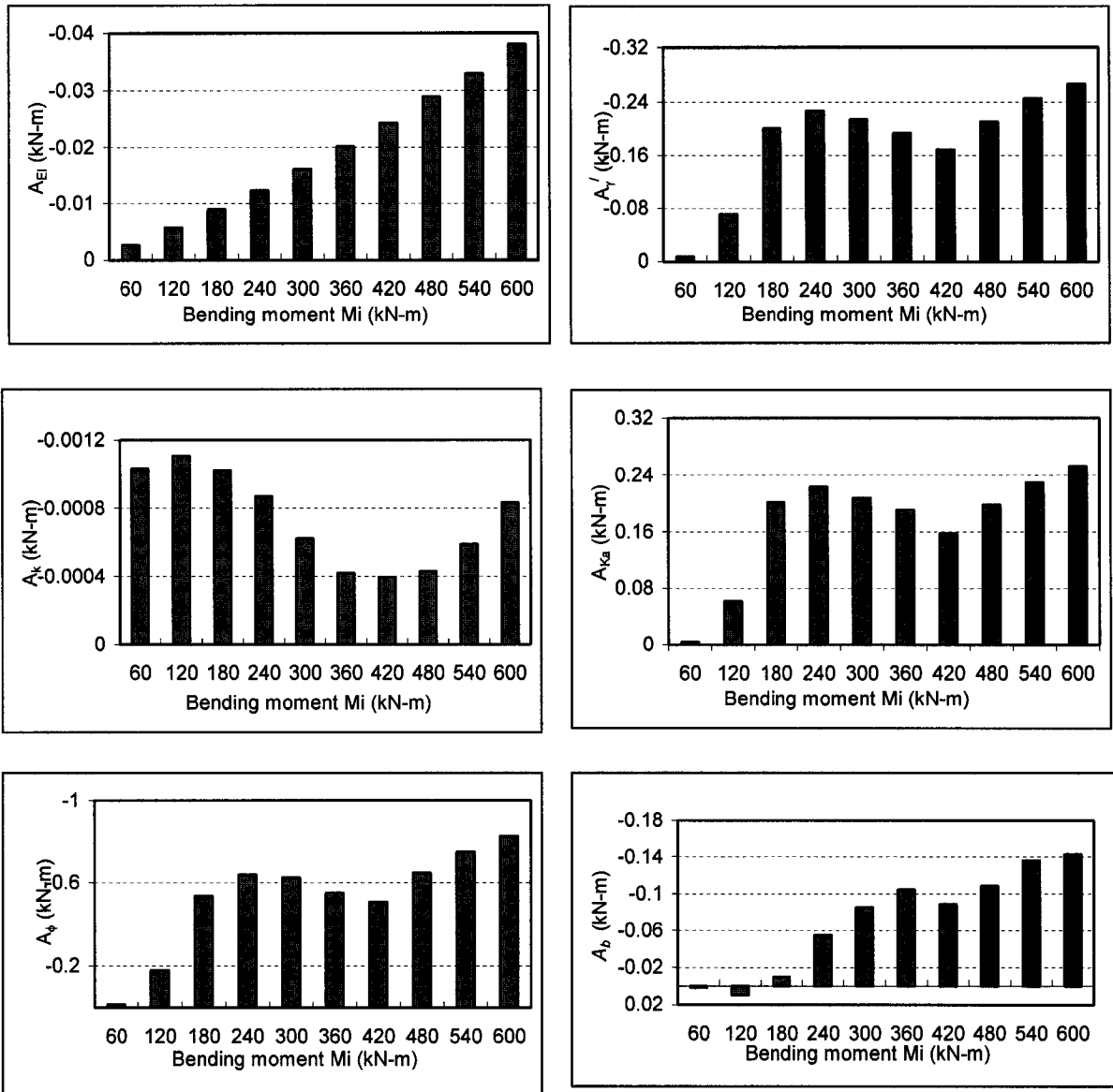


Figure 8-39 The quantitative assessment of sensitivity factors $A_{EI}^{M\theta}$, $A_k^{M\theta}$, $A_{\gamma'}^{M\theta}$, $A_{\phi}^{M\theta}$, $A_{K_a}^{M\theta}$ and $A_b^{M\theta}$ affecting the top angle of flexural rotation θ_t of free head pile of length $7T_m = 12.5$ m subjected to bending moment M due to the changes of design variables EI , k , γ' , ϕ , K_a and b .

Distribution of sensitivity operator, sensitivity factors, relative sensitivity factors affecting the angle of flexural rotation θ_t and soil phase along the length of the fixed pile under different value of bending moment varied in discrete fashion are shown in Figures 8-31 to 8-39. S_{EI}^{Py} curves have highest values at top of the pile where the bending moment is applied to the pile top. As the magnitude of moment decreases with depth, value of S_{EI}^{Py} also decreases to become zero at depth of about 5 m. For the length of the pile between depth 5 m and 15 m any change in design variable EI is not capable of producing changes in θ_t .

Distribution of sensitivity operators S_k^{Py} , $S_{\gamma'}^{Py}$, S_{ϕ}^{Py} , $S_{K_a}^{Py}$ and S_b^{Py} affecting the sensitivities of top lateral deflection y_t due the changes in design variables k , γ' , ϕ , K_a and b follow the same pattern of distribution of operators for free head short pile subjected to variable moment. For a short length at the top of pile S_b^{Py} shows positive at lower values of applied bending moment which indicates, increase in values of pile width b will decrease top lateral deflection y_t . Pile being long undergoes relatively smaller deflections at the lower zone of the pile length. Formation of nonlinear elastic and bilinear elastic phase concentrates at the upper part of the pile length which is shown in Figure 8-37. Distribution of sensitivity factors are shown in Figure 8-39. A_{EI} increases from lower positive value to highest as load increases. A_k decreases from higher positive value at lower loads to a minimum value before increasing again at higher values of applied moment. Starting from negative value, A_b increases to positive maximum value at higher loads.

8.5 Sensitivity analysis of group of piles

In this research laterally loaded pile groups composed of piles connected to the pile cap subjected to lateral load P_G varied in discrete fashion have been studied. Table 8-2 shows the full range of piles investigated in this category.

Table 8-2 Loading, boundary conditions and types of sensitivity investigated for group of piles pile investigated.

GROUP OF PILES			
Boundary conditions	Pile spacing	Deformation type under study	Load steps
Free head pile under lateral load	2D, 3D, 3D, 4D and 5D	Deflection & flexural rotation	Varied
Fixed head pile under lateral load	2D, 3D, 3D, 4D and 5D	Deflection	Varied
Free head pile under bending moment	2D, 3D, 3D, 4D and 5D	Deflection & flexural rotation	Varied

The theoretical formulation employed in numerical investigation of sensitivity analysis of single isolated pile has also been employed in investigation of group of pile. To compare between single isolated piles and group of pile it is clear that in case of a single pile there is pile-soil interaction whereas in a group of piles there is pile-soil-pile interaction. This group action is modeled by p-multipliers f_m proposed by Mokwa and Duncan (2001). The numerical investigations are conducted by FB Pier (FTD & FHA, 2001). Analysis of

group of pile by FB Pier allows of extraction of a member piles from the group and investigation as a single isolated pile after taking into account the necessary modifications for group action. The determination of the length of pile is based on the relative stiffness factor T proposed by Evans and Duncan (1982).

For every value of lateral load P_G applied to the group corresponding force P_g that is applied on the primary member pile structure is obtained from FB Pier analysis. The soil response along the length of the member pile is also available from FB Pier as output of analysis. The adjoint structure is modeled is such a fashion that a suitable load is imposed on group so that as result a force of unity gets applied in the sense of the sensitivity sought. In other words, P_G is selected in such a way that P_g becomes of unit value. The result of sensitivity investigation on group of piles of length $10T=18\text{m}$ in length arranged in 3×3 matrix form and embedded in sand are shown in Figures 8-41 to 8-59. All material strength parameters of the pile-soil system are taken as the design variables. The geometry and initial data of a member pile and surrounding sand, located under water table, employed for numerical studies are shown in Figure 8-40.

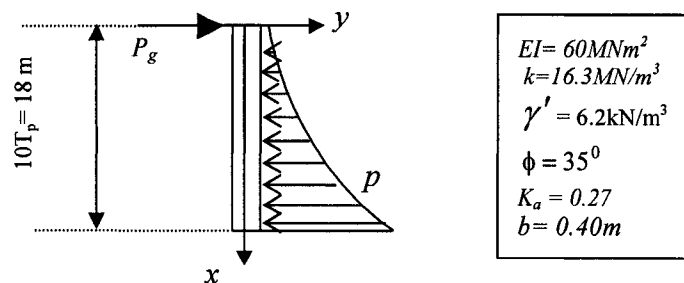


Figure 8-40 Geometry and initial numerical data employed in numerical investigations.

The pile group with concrete pile cap of thickness 1.85m and 9 member piles arranged in 3x3 matrix form with 5D, 4D, 3D and 2D pile spacing in both directions has been studied. The pile cap thickness of 1.85 m has been selected to ensure rigid behaviour of the concrete cap for maximum spacing, 5D of member piles. The distributions of sensitivity integrants G_{EI} , G_k , $G_{\gamma'}$, G_{ϕ} , G_{K_a} and G_b affecting δy_t due to the changes of the design variables EI , k , γ' , ϕ , K_a , and b when the primary structure is subjected to horizontal forces P_G , applied to the pile cap and varied in discrete fashion, are presented in Figures 8-42 to 8-59.

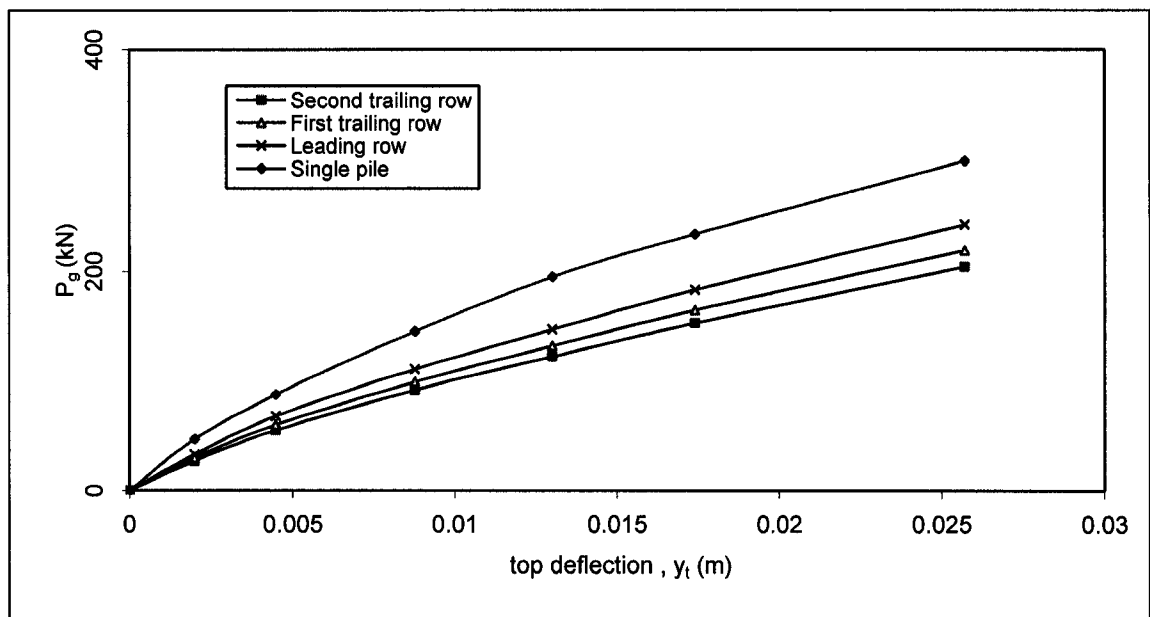


Figure 8-41 The comparison between horizontal forces P_g of piles of different row and single isolated pile for same value of pile cap deflection y_t .

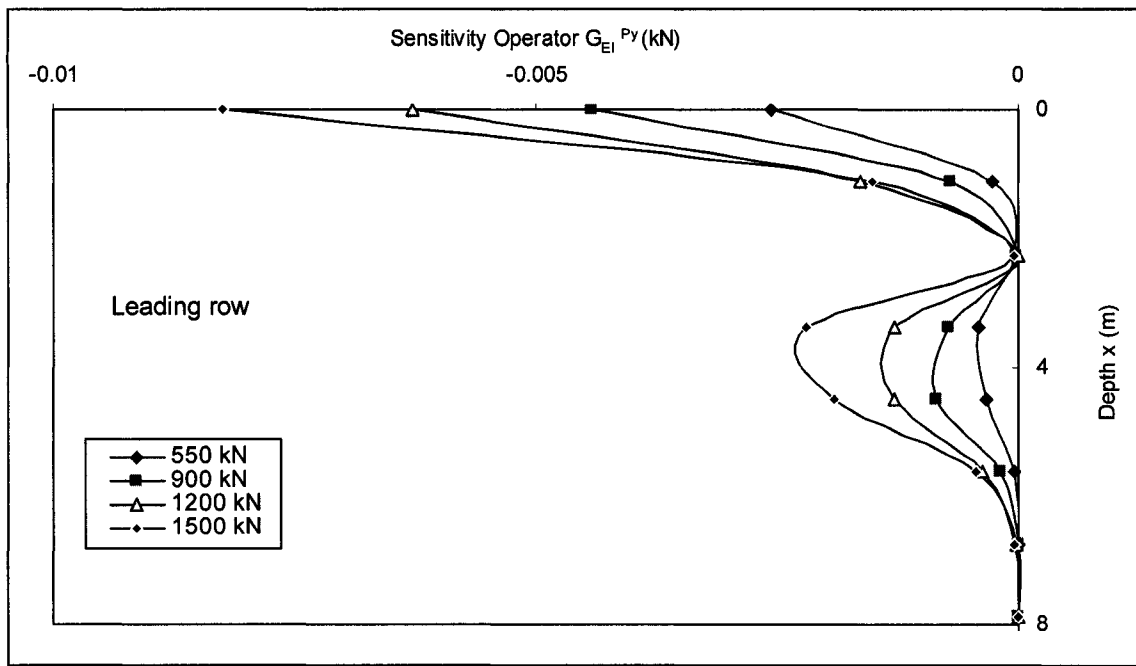


Figure 8-42 Distribution of sensitivity operators G_{EI}^{Py} affecting the change of δy_i due to the variation of design variable δEI for the pile of length, $10T=18\text{m}$, located at centre of leading row subjected to variable horizontal forces P_G applied to the group.

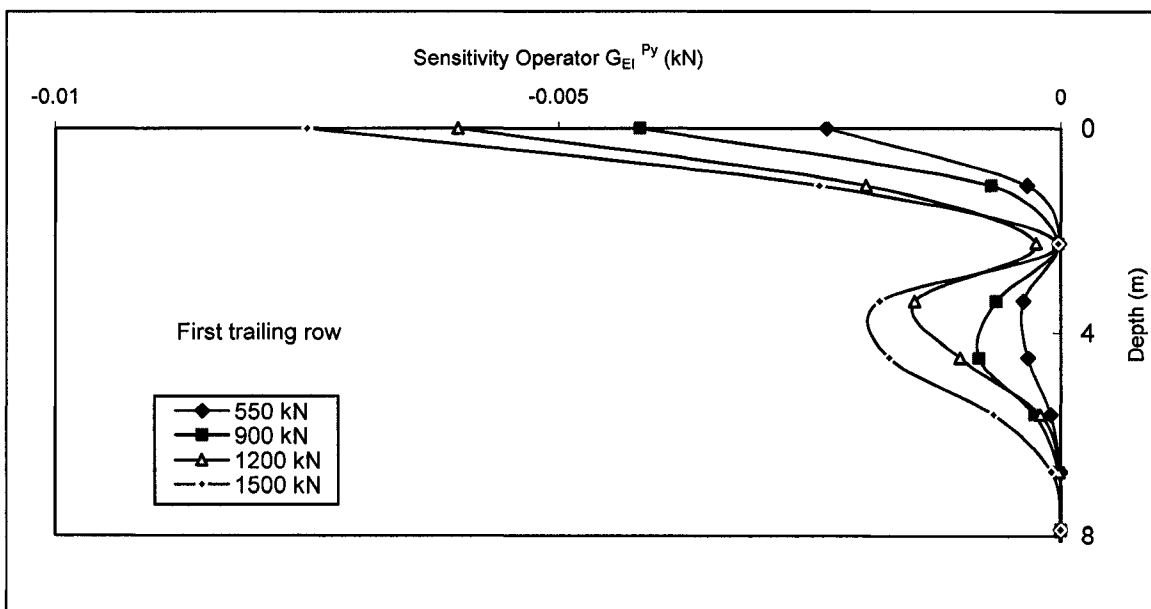


Figure 8-43 Distribution of sensitivity operators G_{EI}^{Py} affecting the change of δy_i due to the variation of design variable δEI for the pile of length, $10T=18\text{m}$, located at centre of first trailing row subjected to variable horizontal forces P_G applied to the group.

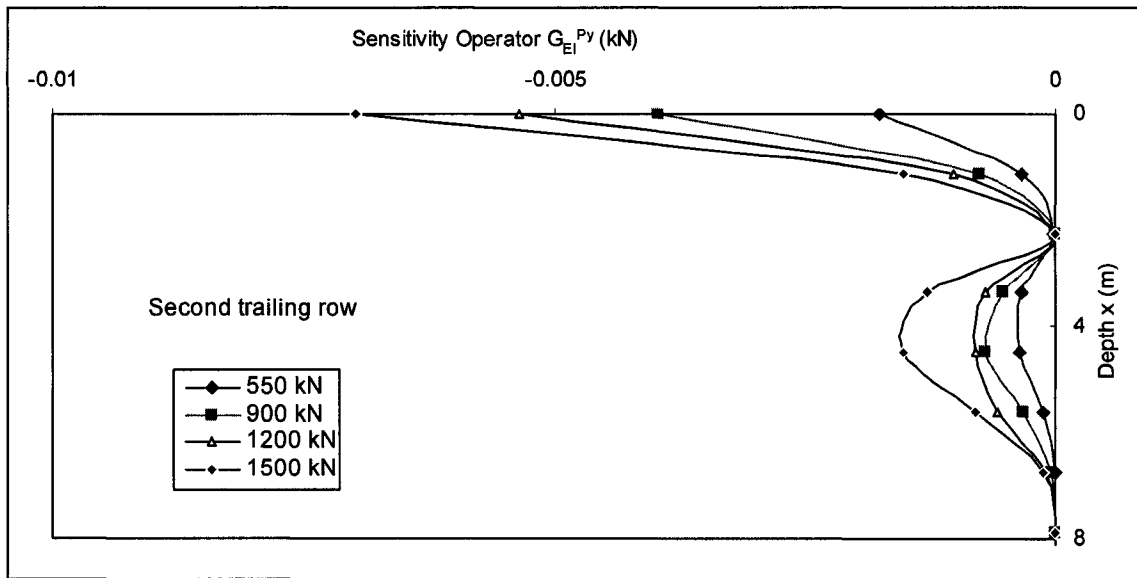


Figure 8-44 Distribution of sensitivity operators G_{EI}^{Py} affecting the change of δy_t due to the variation of design variable δEI for the pile of length, $10T=18\text{m}$, located at centre of second trailing row subjected to variable horizontal forces P_G applied to the group.

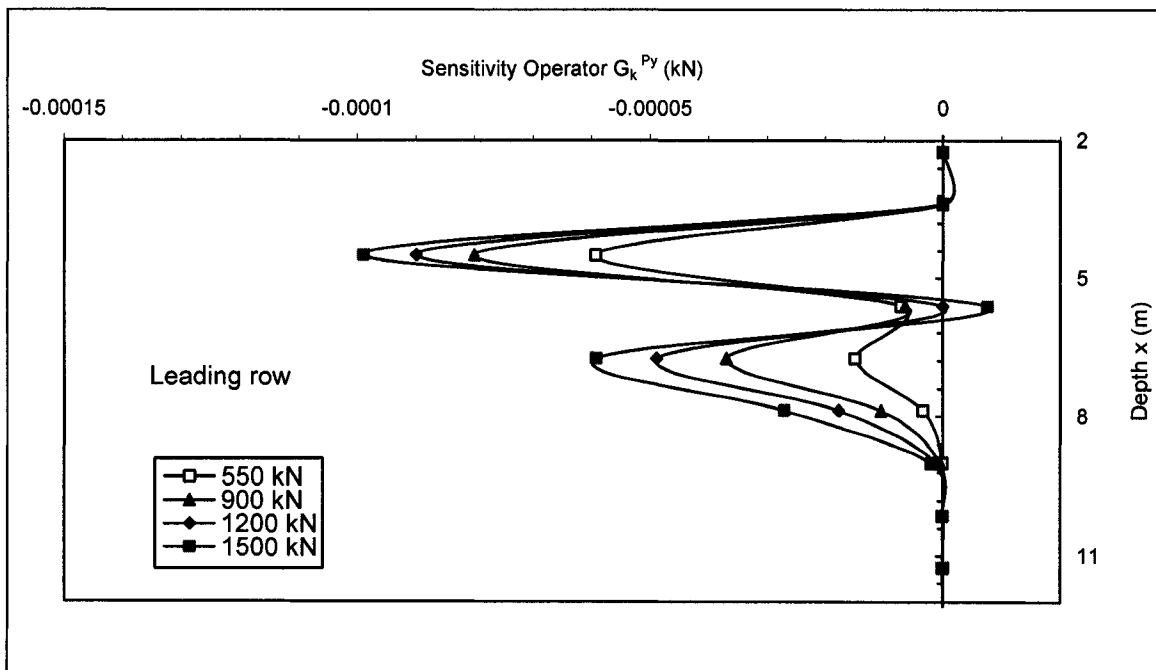


Figure 8-45 Distribution of sensitivity operators G_k^{Py} affecting the change of δy_t due to the variation of design variable δk for the pile of length, $10T=18\text{m}$, located at centre of leading row subjected to variable horizontal forces P_G applied to the group.

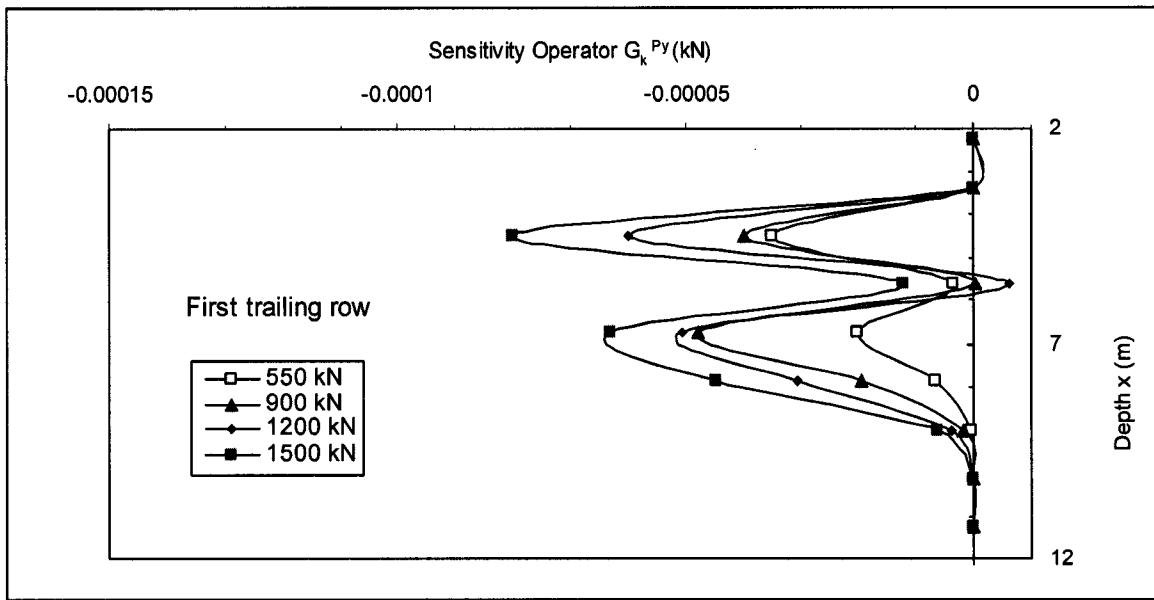


Figure 8-46 Distribution of sensitivity operators G_k^{Py} affecting the change of δy_t due to the variation of design variable δk for the pile of length, $10T=18\text{m}$, located at centre of first trailing row subjected to variable horizontal forces P_G applied to the group.

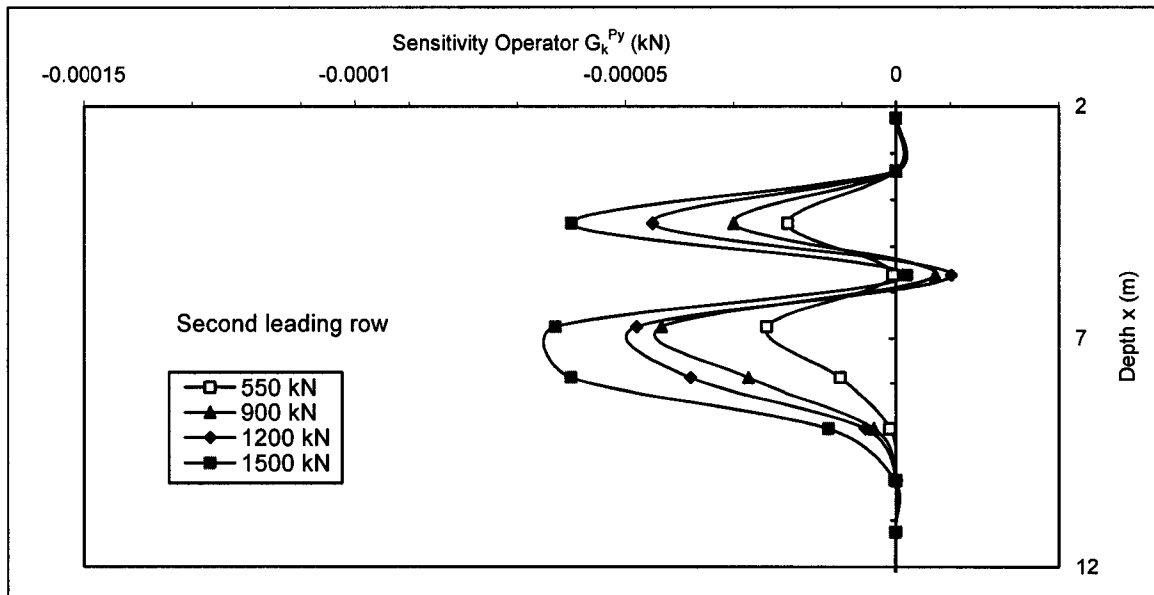


Figure 8-47 Distribution of sensitivity operators G_k^{Py} affecting the change of δy_t due to the variation of design variable δk for the pile of length, $10T=18\text{m}$, located at centre of second trailing row subjected to variable horizontal forces P_G applied to the group.

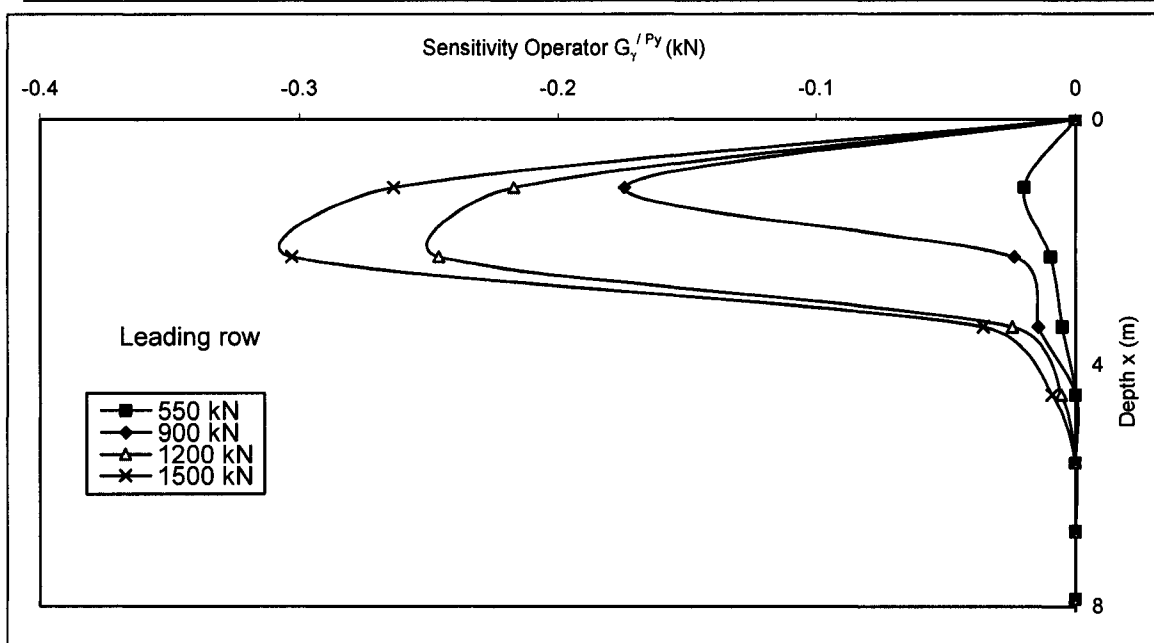


Figure 8-48 Distribution of sensitivity operators $G_{\gamma'}^{Py}$ affecting the change of δy_t due to the variation of design variable $\delta \gamma'$ for the pile of length, $10T=18\text{m}$, located at centre of leading row subjected to variable horizontal forces P_G applied to the group.

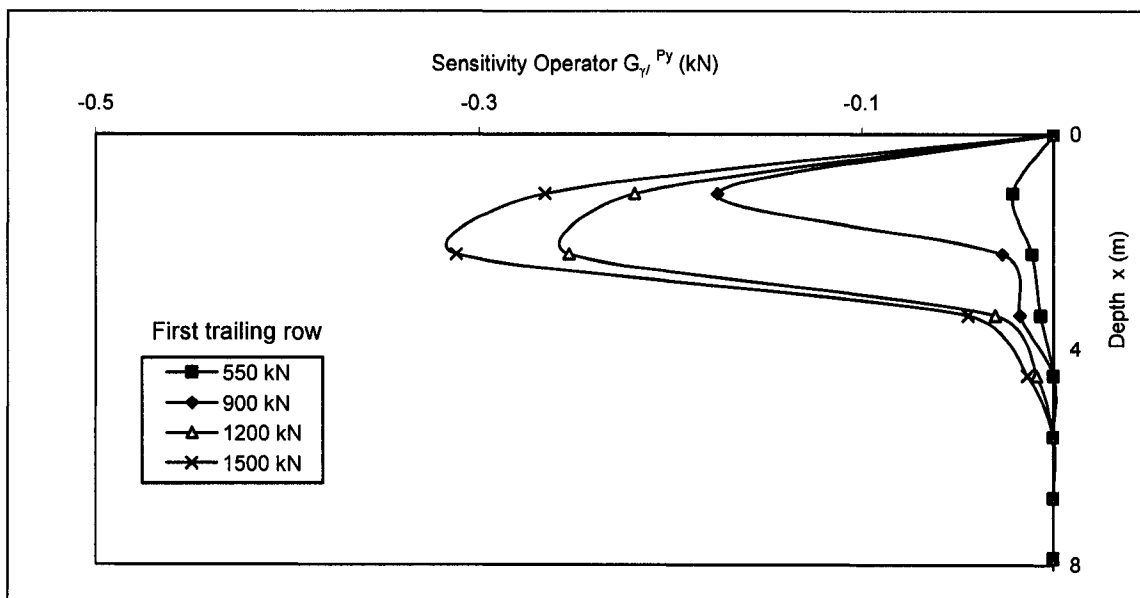


Figure 8-49 Distribution of sensitivity operators $G_{\gamma'}^{Py}$ affecting the change of δy_t due to the variation of design variable $\delta \gamma'$ for the pile of length, $10T=18\text{m}$, located at centre of first trailing row subjected to variable horizontal forces P_G applied to the group.

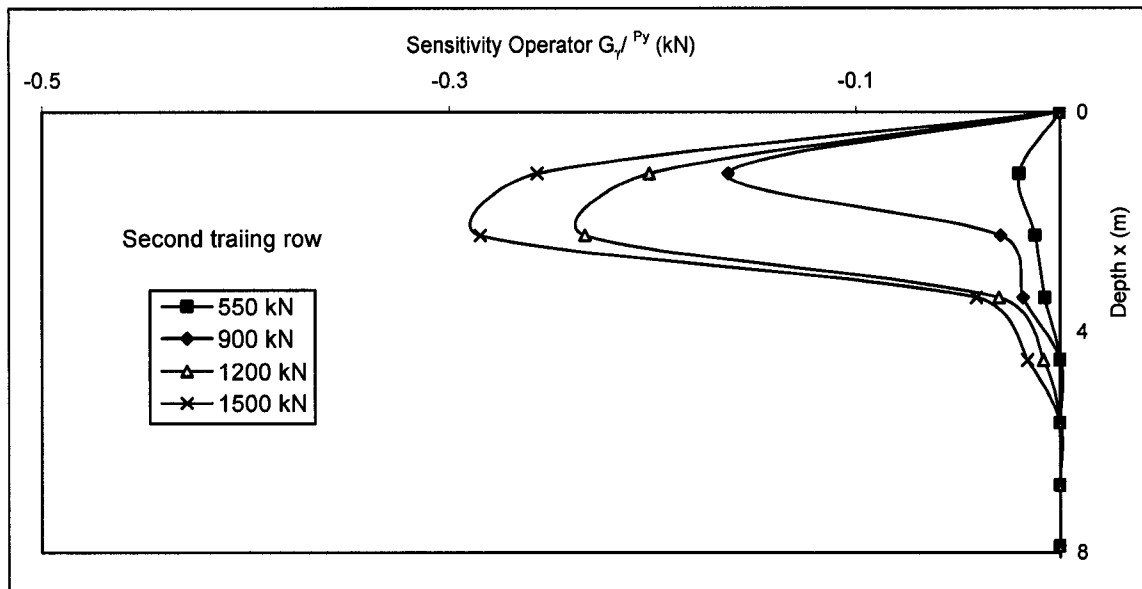


Figure 8-50 Distribution of sensitivity operators $G_{\gamma'}^{Py}$ affecting the change of δy_t due to the variation of design variable $\delta \gamma'$ for the pile of length, $10T=18\text{m}$, located at centre of second trailing subjected to variable horizontal forces P_G applied to the group.

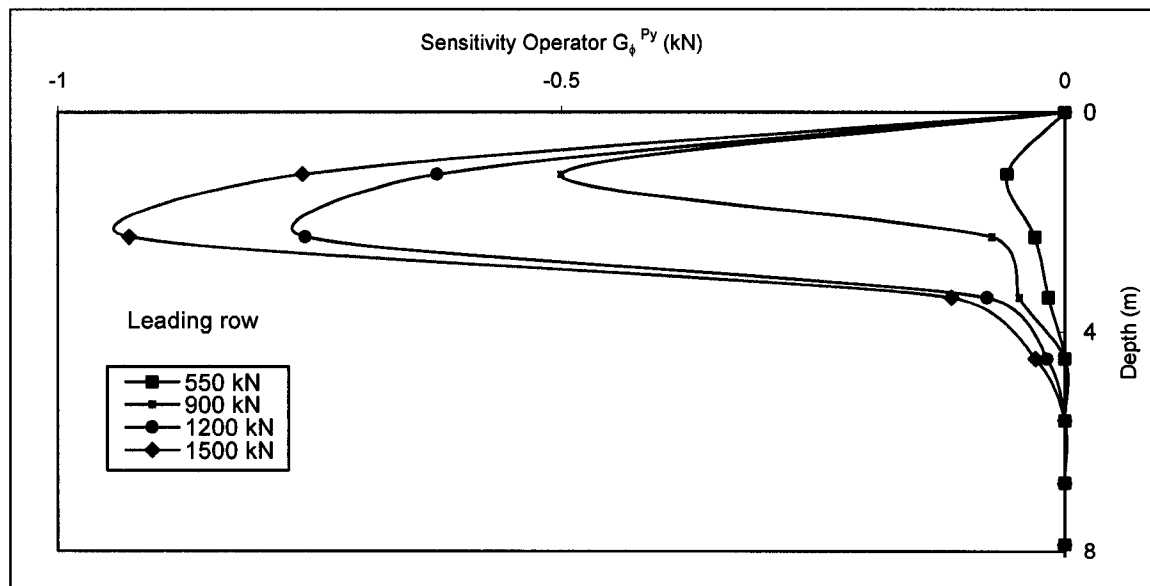


Figure 8-51 Distribution of sensitivity operators G_{ϕ}^{Py} affecting the change of δy_t due to the variation of design variable $\delta \phi$ for the pile of length, $10T=18\text{m}$, located at centre of leading row subjected to variable horizontal forces P_G applied to the group.

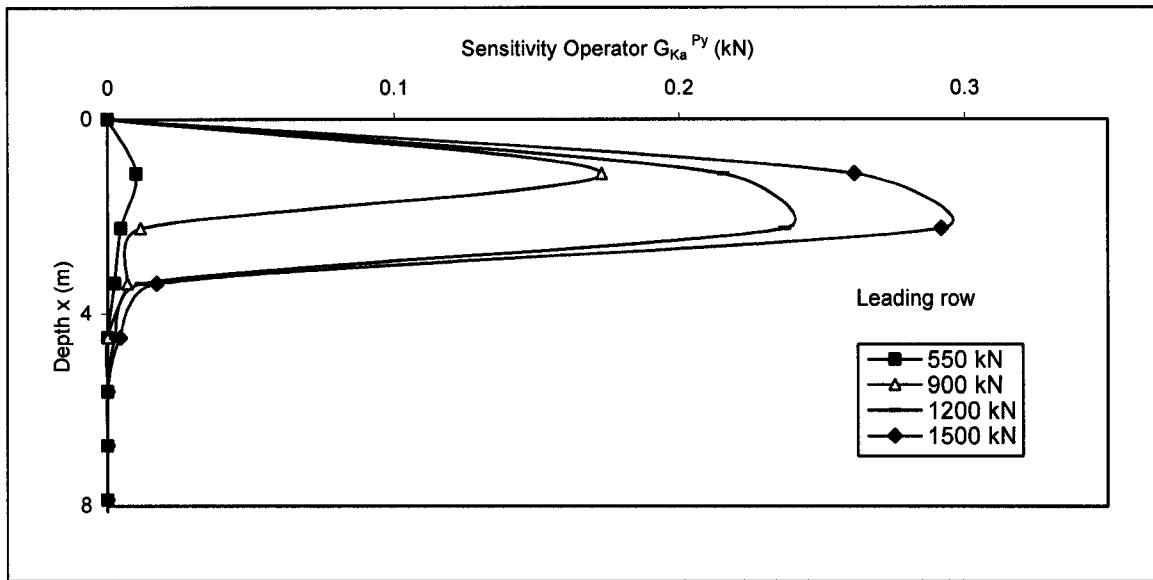


Figure 8-54 Distribution of sensitivity operators $G_{K_a}^{P_y}$ affecting the change of δy_i due to the variation of design variable δK_a for the pile of length, $10T=18\text{m}$, located at centre of leading row subjected to variable horizontal forces P_G applied to the group.

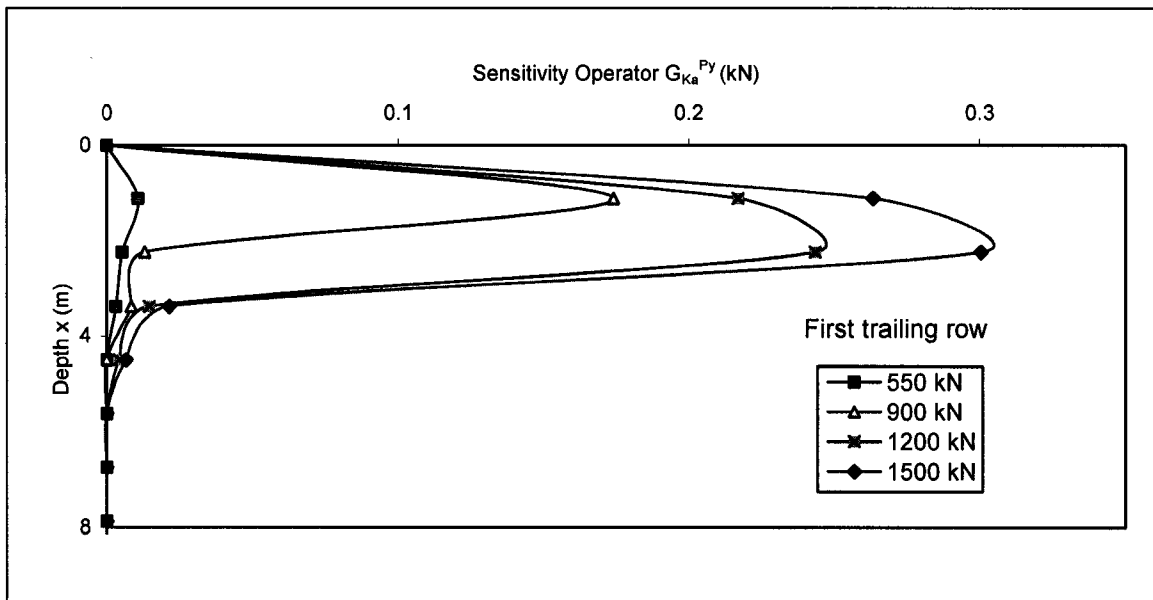


Figure 8-55 Distribution of sensitivity operators $G_{K_a}^{P_y}$ affecting the change of δy_i due to the variation of design variable δK_a for the pile of length, $10T=18\text{m}$, located at centre of first trailing row subjected to variable horizontal forces P_G applied to the group.

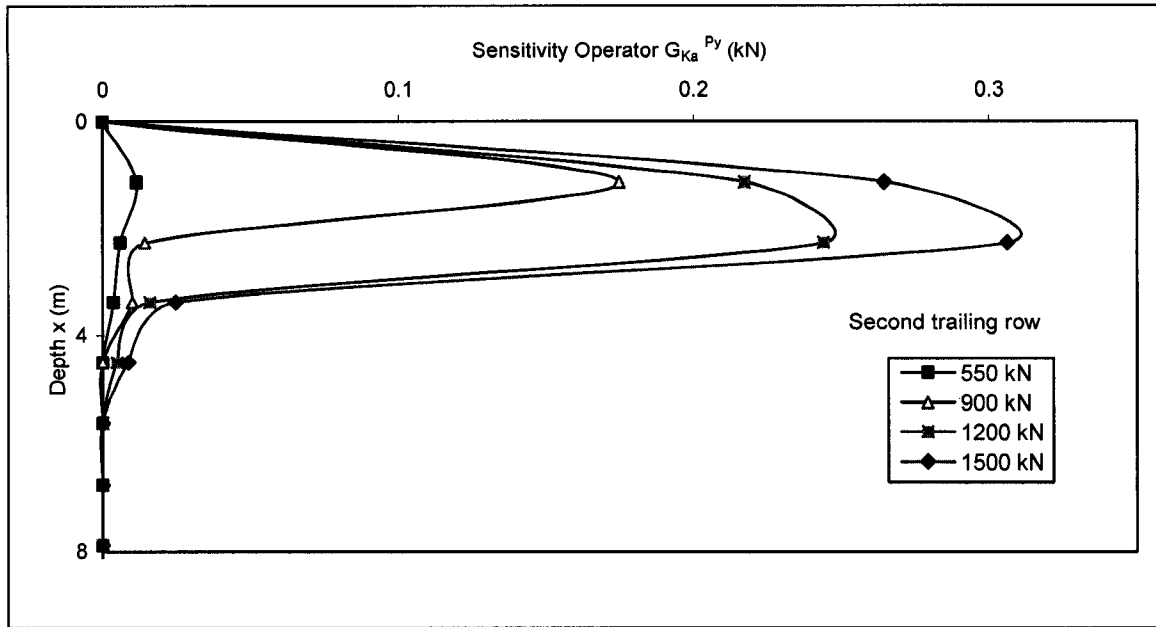


Figure 8-56 Distribution of sensitivity operators $G_{K_a}^{P_y}$ affecting the change of δy_i due to the variation of design variable δK_a for the pile of length, $10T=18\text{m}$, located at centre of second trailing subjected to variable horizontal forces P_G applied to the group.

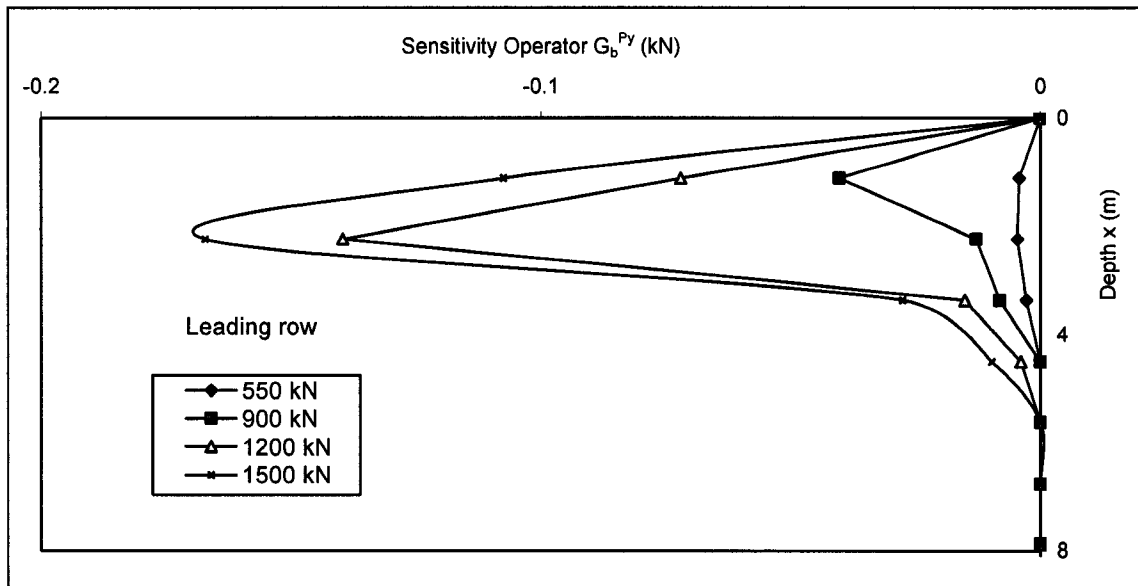


Figure 8-57 Distribution of sensitivity operators $G_b^{P_y}$ affecting the change of δy_i due to the variation of design variable δb for the pile of length, $10T=18\text{m}$, located at centre of leading row subjected to variable horizontal forces P_G applied to the group.

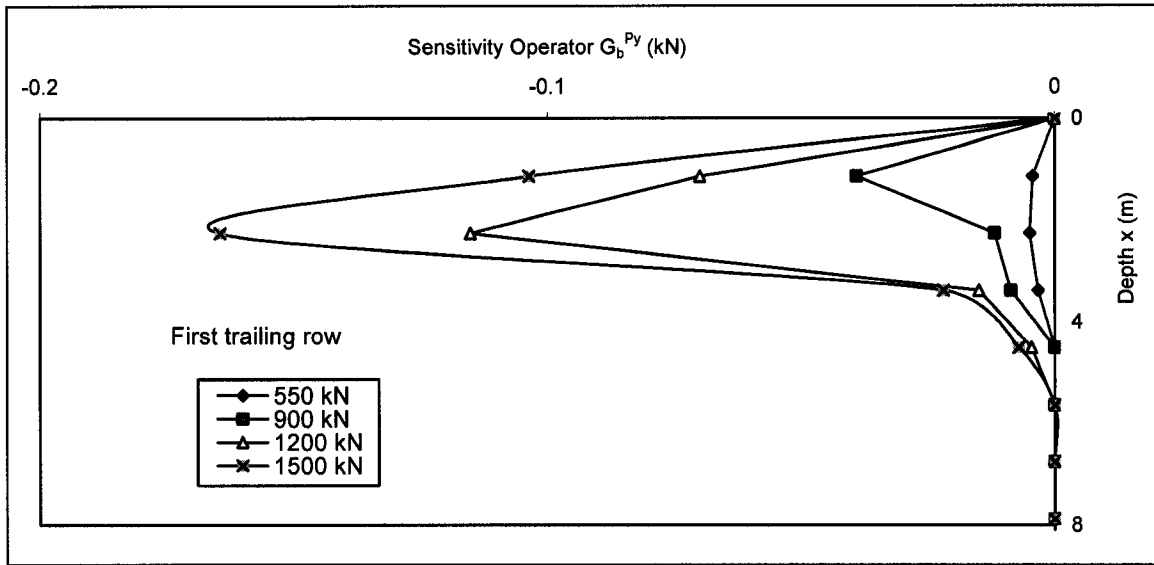


Figure 8-58 Distribution of sensitivity operators G_b^{Py} affecting the change of δy_i due to the variation of design variable δb for the pile of length, $10T=18m$, located at centre of first trailing row subjected to variable horizontal forces P_G applied to the group.

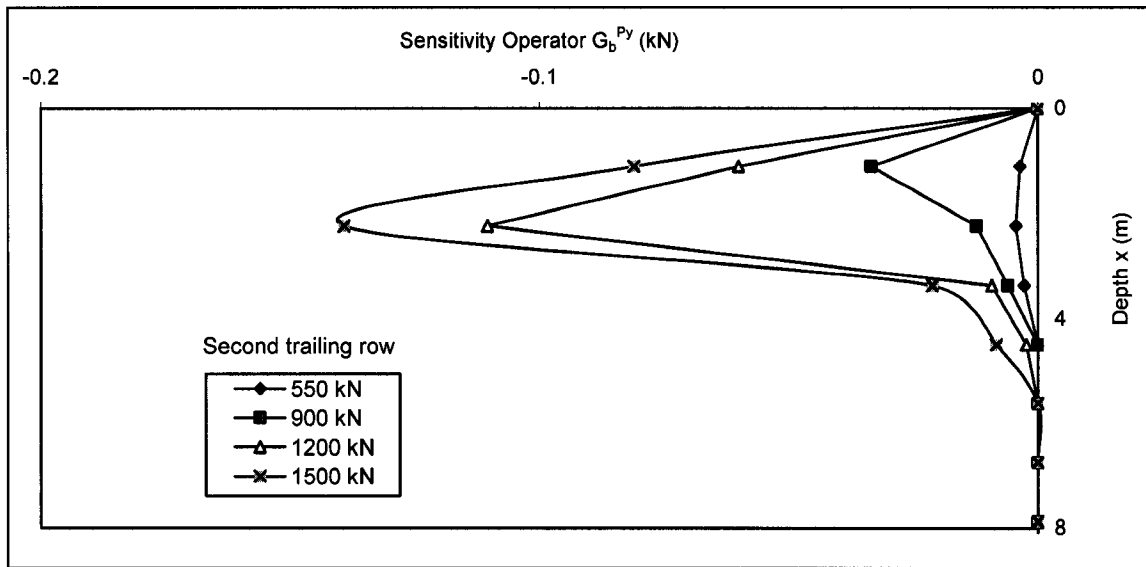


Figure 8-59 Distribution of sensitivity operators G_b^{Py} affecting the change of δy_i due to the variation of design variable δb for the pile of length, $10T=18m$, located at centre of second trailing row subjected to variable horizontal forces P_G applied to the group.

Figure 8-14 shows the distribution of horizontal force P_g applied to the member piles of leading row, first trailing row and second trailing row due to the application of horizontal force P_G applied to the pile cap of the group. The pile spacing is $3D$ in both directions. This figure compares the magnitude of P_g of member piles to single isolated pile. Equivalent P_g for single isolated pile has been obtained by FB Pier by setting member pile spacing equal to $6D$. For the same deflection single isolated pile carries more loads than the member piles of a group. Among the member piles of a group, pile of leading row carry greatest magnitude of horizontal force, followed by those of first trailing and then the second trailing row.

Distribution of sensitivity operators $G_{EI}, G_k, G_{\gamma'}, G_{\phi}, G_{K_a}$ and G_b of piles of leading row, first trailing row and second trailing row affecting the sensitivities of top lateral deflection y_t due to the changes of design variables $EI, k, \gamma', \phi, K_a$ and b . Maximum values of G_{EI} in Figures 8-42 to 8-44 occurs at the top of the pile where the bending moment is maximum that develops due to the fixicity of member pile to the group cap. Value of G_{EI} is maximum for piles of leading row, followed by those of first trailing row and then the second trailing row for same value of applies load P_G and depth. His is the usual trend for all the sensitivity operators except G_{K_a} . G_{K_a} of second trailing row has the maximum value and of leading the least.

In general distribution of sensitivity operators of member piles of a pile group follows the same pattern of the single isolated pile although the absolute values of operators for single isolated piles are greater.

CHAPTER IX

OBSERVATION AND DISCUSSION

9.1 Discussion on graphical representation of sensitivity operators

Evaluation and graphical representation of sensitivity operators $S_{(\cdot)}^{(\cdot)}$ in case of single piles and $G_{(\cdot)}^{(\cdot)}$ for group of piles affecting maximum generalized deformation due to the changes of design variables are vital part of this sensitivity investigation. Study of the sensitivity operators connected to the change in corresponding design variables along the length of the pile subjected to variable lateral load and bending moment reveals the following:

- 1) The graphical representation of sensitivity operator shows the pattern of change of generalized maximum deformation, $\delta\bar{g}$ due to the change in design variable which is connected to the operator. $\delta\bar{g}$ includes top lateral deflection δy_t and $\delta\theta$, rotation at the top of the pile. In the sensitivity analysis, a virtual unit horizontal load applies to the adjoint structure results in sensitivity of δy_t in the direction of the applied unit load and a virtual unit moment gives sensitivity of $\delta\theta$. For example, in the case of “Short free headed single pile of length $2T$ - Sensitivity of top lateral deformation δy_t ” under 10 kN force, $\delta(EI)$ and δk are capable of producing changes in y_t but other design variables do not.

-
- 2) The region along the length of the pile in which change in a design variable causes change in $\delta\bar{g}$. In figure 8-5 sensitivity operator S_k^{Py} is zero between top of the pile to a depth of 2.0m for loads 30 kN and above. What that means is change in design variable k does not create change in top lateral deflection under top lateral load of 30kN. But below a depth of 2.0m the same design variable is capable of changing y_t without any change in applied force.
- 3) If change in a design variable strengthen the pile-soil system, in other words if increase in value of a design variable decreases the deformation at the top of the pile. In Figure 8-8 the $S_{K_a}^{Py}$ curves show positive values, if not zero, along the upper part of the pile meaning that change in design variable in above mentioned portion of pile increases y_t for that pile length, applied force and boundary condition of the pile.
- 4) The distribution of sensitivity operator $S_{EI}^{(\cdot)}$ of maximum generalized deformation, $\delta\bar{g}$ due to the change in design variable EI follows the distribution of moment at the primary structure. Design parameter EI is a property of pile structure. Hence, the sensitivity operator $S_{EI}^{(\cdot)}$, due to the changes in EI changes with the flexural deformation of the pile structures not the soil phase. The other design variables, angle of internal friction of sand ϕ , submerged unit weight of soil γ , the coefficient of subgrade reaction k , the coefficient of active lateral earth pressure k_a of Rankine type and width of pile b are connected to soil property. So, the distribution sensitivity operators $S_{(\cdot)}^{(\cdot)}$ due to the changes of these design variables changes with soil phase.

-
- 5) The distribution of $G_{(.)}^{(.)}$ for the member piles of pile group is of same pattern as in the single isolated pile. Distribution of sensitivity operators $G_{(.)}^{Py}$ affecting the change of δy_i due to the variation of design variables of the member piles of length, 10T=18m of the pile group subjected to variable horizontal forces P_G applied to the group. Study of these graphical representation shows that piles of the leading are most sensitive to the changes of design variables for a particular applied load followed by the piles of first trailing row and the second trailing row.
- 6) In case of short piles sensitivity operators curves showing distribution of sensitivity due to the changes of design variables display nonzero values almost through out the length of the pile. This means that in short piles changes in design variables anywhere along the length of the pile are capable of affecting the performance of the pile-soil system. On the other hand in long piles sensitivity operators curves showing distribution of sensitivity due to the changes of design variables shows nonzero values along the top portion of the length of the pile and the bottom part of the curves either go along the axis of the undeformed pile or show very small values. This means that the changes of design variables along the top part of the pile are effective in affecting the performance of the pile soil system. In general a depth of 3 m from the ground surface is crucial where changes in design variables affect the performance of long pile.

9.2 Discussion on sensitivity factors

The sensitivity factors $A_{(\cdot)}^{(\cdot)}$ are the direct measure of change of change in maximum generalized deformation due to the changes in design variables of the pile-soil system. They are calculated by integrating the area of the sensitivity Factor curves. The value of sensitivity factors $A_{(\cdot)}^{(\cdot)}$ connected the changes of each design variables are calculated and assessed for every single pile and pile group investigated for discrete values of the variable loads. The value of sensitivity factors $A_{(\cdot)}^{(\cdot)}$ due to changes the changes of each design variable for each pile investigated are plotted against the discrete values of the applied load. From these graphs the pattern of changes of sensitivity factors $A_{(\cdot)}^{(\cdot)}$ due to the changes of design variables can be assessed for entire range of the possible loading and the value of $A_{(\cdot)}^{(\cdot)}$ due to the change of particular design variables can be estimated for any arbitrary value of applied load though interpolation or regression method.

Figure 8-12 shows the quantitative assessment of sensitivity factors, A_{EI}^{Py} , A_k^{Py} , $A_{\gamma'}^{Py}$, A_{ϕ}^{Py} , $A_{K_a}^{Py}$ and A_b^{Py} affecting the top lateral deformation y_t of free head pile of length $2T_p = 3.5$ m due to the changes of design variables EI , k , γ' , ϕ , K_a and b . Study of this figure reveals the following:

- Value of A_{EI}^{Py} increases in nonlinear fashion with increase in horizontal force applied to the pile. A relatively steeper slope of the pattern shows that the increase in value of this sensitivity factor is more pronounced at higher load.

-
- Values of A_k^{Py} , $A_{\gamma'}^{Py}$, A_{ϕ}^{Py} , $A_{K_a}^{Py}$ and A_b^{Py} increases with increase in applied horizontal force for lower values and decreases again after reaching a peak value for further increase in applied load.

Quantitative assessment of sensitivity factors $A_{EI}^{M\theta}$, $A_k^{M\theta}$, $A_{\gamma'}^{M\theta}$, $A_{\phi}^{M\theta}$, $A_{K_a}^{M\theta}$ and $A_b^{M\theta}$ affecting the top lateral deformation θ_t of free head pile of length $7T_m = 12.5$ m due to the changes of design variables EI , k , γ' , ϕ , K_a and b reveals the following:

- Value of A_{EI}^{Py} increases in nonlinear fashion with increase in horizontal force applied to the pile. A relatively steeper slope of the pattern shows that the increase in value of this sensitivity factor is more pronounced at higher load.
- Values of A_k^{Py} , $A_{\gamma'}^{Py}$, A_{ϕ}^{Py} and $A_{K_a}^{Py}$ increases initially with increase in applied horizontal force and decrease as load increase before increasing again at higher values of load in a sinusoidal manner.
- Values of A_b^{Py} has negative value for lower values of horizontal forces and increases to positive value at higher value of applies loads.

9.3 Discussion on relative sensitivity factors

Relative sensitivity factors $F_{(.)}$ are defined by the Equations 6-4 to 6-9. They are the measures of importance of a design variable in changing the generalized maximum

deformation of the pile compared to total contribution produced by all design variables in aggregate. For every discrete value of load applied to the piles investigated, relative sensitivity factors $F_{(.)}$ are evaluated and shown in graphically. Figure 8-11 shows quantitative assessment of relative sensitivity factors $F_{(.)}$ (in %) of sensitivity of top lateral displacement δy_t due to design variables for pile (free head) length of, 2.0Tm = 3.5 m subjected to variable horizontal forces, P . Study of this diagram reveals the following:

- $F_{EI} = A_{EI} / A_{tot}(\%)$ has a value of about 10% at lower value of applied loads and decreases to about 1% as the load increases
- $F_k = A_k / A_{tot}(\%)$ has a value of 90% when a horizontal force of 10 kN is applied to the pile and decreases to 21% at 15 kN, consequently becoming minimum at higher loads.
- $F_{\gamma'} = A_{\gamma'} / A_{tot}(\%)$ has a value of less than 1% at 10 kN, increases gradually to 25% at 20 kN and decreases again to attain average value of about 7% at higher loads.
- $F_{\phi} = A_{\phi} / A_{tot}(\%)$ has a value of less than 1% at 10kN and abruptly increases to about 65% for higher loads.
- $F_{K_a} = A_{K_a} / A_{tot}(\%)$ has a value of 1% at 10 kN and increases to an average value of 17% at higher loads.
- $F_b = A_b / A_{tot}(\%)$ has a value of less than 1% at 10 kN and increases to about 20% at higher loads

This trend of relative sensitivity factors $F_{(.)}$ for respective design variables is observed for piles with different length and boundary conditions. The average values of relative sensitivity factors $F_{(.)}$ estimated from investigated piles in this research are shown in Table 9-1a.

Table 9-1a Average value in percentage of relative sensitivity factors.

Relative sensitivity factors	Value in percentage
F_{EI}	6%
F_k	4%
$F_{\gamma'}$	8%
F_{ϕ}	60%
F_{K_a}	10%
F_b	12%

9.4 Discussion on soil phases

Development of soil phases along the length of the pile at different values of load applied to the pile has been determined for every pile investigated and represented in graphical form. Figure 8-10 shows quantitative assessment of location and size of soil phases developed with depth determined based on the distributions of sensitivity operators of δy_i for pile (free head) of length, $2.0T_m = 3.5$ m, subjected to variable horizontal forces, P . Linear elastic phase occurs along the pile member at every value of horizontal force

or bending moment. In this phase sensitivity operators $S_{EI}^{(\cdot)}$ and $S_k^{(\cdot)}$ have nonzero values. Hence, changes in design variables EI and k in a zone where the pile-soil system is in deformation state linear elastic phase are capable of producing changes in maximum generalized deformation of the pile. $S_{EI}^{(\cdot)}$, $S_{\gamma'}^{(\cdot)}$, $S_{\phi}^{(\cdot)}$, $S_{K_a}^{(\cdot)}$ and $S_b^{(\cdot)}$ have nonzero values in non-linear and bi-linear phase. In plastic flow phase none of the sensitivity operators has nonzero values.

9.5 Verification of results

Throughout this study computer hardware and software have been used. Although consistency of outputs has been carefully monitored and any inconsistency did not appear, necessity of verification cannot be ruled out. Following computer tools has been used in the research.

- COM624P has been used for analysis of single piles
- FB-pier has been used for group of piles
- MS Excel has been used for sensitivity analysis operations.

An 11.0 m long free head pile embedded in sand with 100 kN horizontal force applied at the pile head has been analyzed. The pile-soil system is shown in Figure 9-1

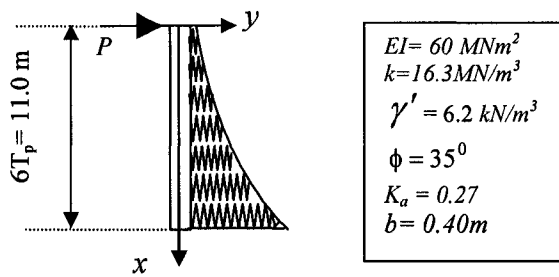


Figure 9-1 Free head pile with design variables.

The pile has been discretized into 50 elements. The result obtained from COM624P is shown in Table 9-1. Using equations of p - y model, shown in figure 3-8, soil resistance has been calculated and shown in Table 9-2. Comparison of two set of p -values are shown in Table 9-3.

When compared, the two sets of results, one from COM 624P and the other calculated by the use of p - y curves reveal the following.

- ❖ Average difference in value of soil resistance is .21 kN/m
- ❖ Maximum difference in value of soil resistance is 3.17 kN/m
- ❖ Average difference in percentage of soil resistance is 0.37%
- ❖ Maximum difference in percentage of soil resistance is 7.37%
- ❖ Forces of soil response on every element have been calculated using trapezoidal rule. The summation of forces on all the elements have been summed and found to be 96.96 kN which is very close in value and opposite in sense to the force of 100 kN applied to the top of the pile. This proves the equilibrium of horizontal forces through out the length of the pile.

-
- ❖ Considering the force of soil resistance to the pile deflection passes through the centroid of respective pile element, moment of all the element about top of the pile forces had been calculated. The sum of moments of all the forces is 0.0084 kN-m, which is very close to zero. This in addition to the above item proves the equilibrium of the pile-soil system.
 - ❖ The above observations prove that COM624P is being properly used and the software itself is free of flaws. The difference in calculated values from the ones from COM624P may be attributed to approximation and truncation used in manual calculations whereas the COM624P results may to be closer to the actual.

FB Pier and COM624P are two different softwares developed by two different groups of engineers. Using COM624P, single piles can be analyzed whereas by FB Pier group of piles as well as single piles can also be analyzed. A single pile has been modeled by FB Pier, and deflection obtained from this software has been compared with those from COM624P. Figure 9-2 shows the deflections obtained from both of the softwares. The values of deflections are very close which suggests the accuracy of both softwares.

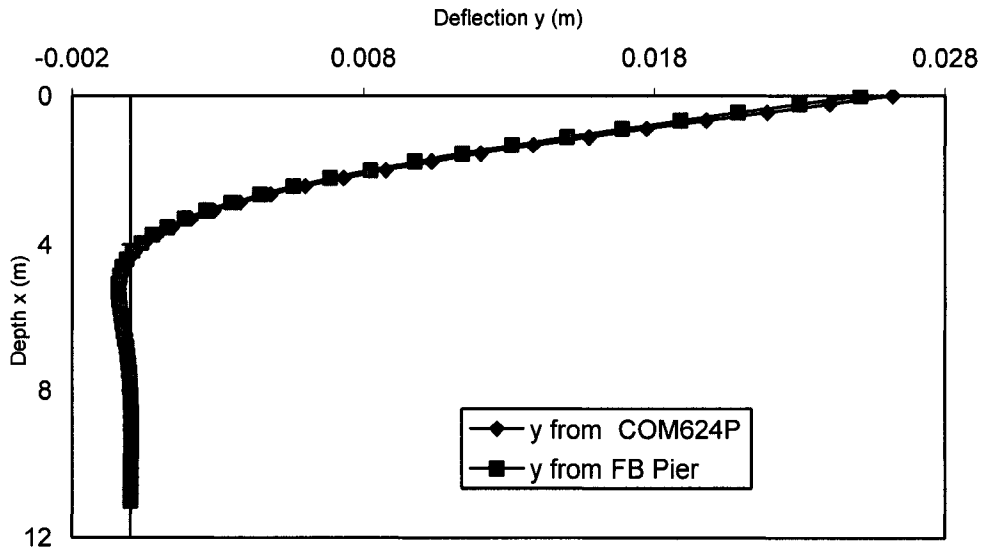


Figure 9-2 Comparison between deflections COM624P and FB Pier.

Equation 5-15 shows the sensitivity of maximum generalized deformation due to the changes of design variables. For ease of study it is shown below.

$$\begin{aligned} \bar{I} \cdot \delta \bar{g} = & \int_0^l y_a'' y'' \delta(EI) \frac{EI}{EI} dx - \int_0^l p_a \frac{\partial y}{\partial p} \frac{\partial p}{\partial k} k \delta k \frac{1}{k} dx - \int_0^l p_a \frac{\partial y}{\partial p} \frac{\partial p}{\partial \gamma} \gamma \delta \gamma \frac{1}{\gamma} dx \\ & - \int_0^l p_a \frac{\partial y}{\partial p} \frac{\partial p}{\partial \phi} \phi \delta \phi \frac{1}{\phi} dx - \int_0^l p_a \frac{\partial y}{\partial p} \frac{\partial p}{\partial K_a} K_a \delta K_a \frac{1}{K_a} dx - \int_0^l p_a \frac{\partial y}{\partial p} \frac{\partial p}{\partial b} b \delta b \frac{1}{b} dx \end{aligned} \quad 5-15$$

This equation relates the change of top lateral deformation to the changes of design variables. The relationship should be valid for change of any one variable or more than one at a time. As an attempt to verify this equation a free head long pile of length $5T = 9.0$ m has been investigated. First the pile-soil input data shown in Figure 9-3 has been used in FB Pier and the out put data obtained after execution is shown in first three columns of Table 9-4.

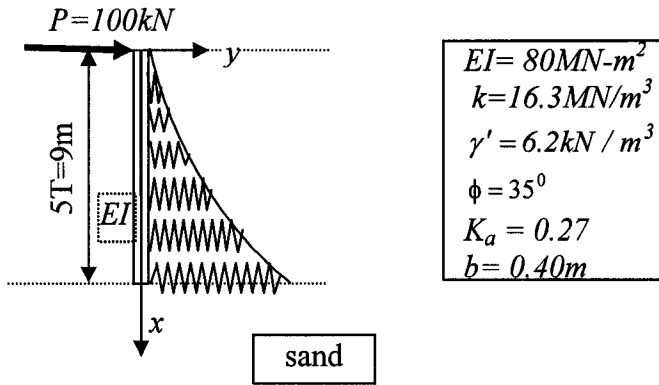


Figure 9-3 Soil and pile properties.

Keeping all other parameters of pile-soil system only EI of the pile has been changed to $60 MN-m^2$ from $80 MN-m^2$ also keeping the applied load unchanged at 100 kN. Input data for second execution is shown in Figure 9-3 and output in Table 9-5.

Taking data first execution as initial data we get:

$$y_o = 0.0277 \text{ m} \quad (\text{from Table 9-4})$$

$$y_I = 0.0305 \text{ m} \quad (\text{from Table 9-5})$$

$$\delta y = 0.0028 \text{ m}$$

$$\delta EI = 20,000 \text{ kN-m}$$

$$A_{EI}^{Py} = -0.0107582 \text{ kN-m}$$

Plugging these values to Equation 6-1,

$$\bar{I} \cdot \delta y_t = A_{EI} \delta(EI)_N - A_k \delta k_N - A_\gamma \delta \gamma_N - A_\phi \delta \phi_N - A_{K_a} \delta(K_a)_N - A_b \delta b_N$$

Table 9-1b Out-put data from COM624P

depth x (m)	deflection y (m)	Shear force (kN)	soil resistance p (kN/m)
0.00E+00	2.62E-02	1.00E+02	0.00E+00
2.20E-01	2.40E-02	9.93E+01	6.74E+00
4.40E-01	2.19E-02	9.69E+01	1.49E+01
6.60E-01	1.98E-02	9.27E+01	2.28E+01
8.80E-01	1.77E-02	8.69E+01	3.00E+01
1.10E+00	1.58E-02	7.96E+01	3.62E+01
1.32E+00	1.38E-02	7.11E+01	4.17E+01
1.54E+00	1.20E-02	6.15E+01	4.50E+01
1.76E+00	1.03E-02	5.12E+01	4.91E+01
1.98E+00	8.76E-03	3.99E+01	5.31E+01
2.20E+00	7.31E-03	2.78E+01	5.70E+01
2.42E+00	5.99E-03	1.49E+01	6.01E+01
2.64E+00	4.80E-03	1.53E+00	6.17E+01
2.86E+00	3.75E-03	-1.21E+01	6.17E+01
3.08E+00	2.84E-03	-2.54E+01	5.98E+01
3.30E+00	2.07E-03	-3.82E+01	5.61E+01
3.52E+00	1.42E-03	-4.99E+01	5.04E+01
3.74E+00	8.90E-04	-6.01E+01	4.25E+01
3.96E+00	4.71E-04	-6.81E+01	3.04E+01
4.18E+00	1.51E-04	-7.26E+01	1.03E+01
4.40E+00	-8.33E-05	-7.31E+01	-5.98E+00
4.62E+00	-2.45E-04	-7.04E+01	-1.84E+01
4.84E+00	-3.46E-04	-6.53E+01	-2.73E+01
5.06E+00	-4.00E-04	-5.87E+01	-3.30E+01
5.28E+00	-4.17E-04	-5.11E+01	-3.59E+01
5.50E+00	-4.07E-04	-4.32E+01	-3.65E+01
5.72E+00	-3.78E-04	-3.53E+01	-3.53E+01
5.94E+00	-3.38E-04	-2.78E+01	-3.27E+01
6.16E+00	-2.91E-04	-2.10E+01	-2.92E+01
6.38E+00	-2.43E-04	-1.50E+01	-2.53E+01
6.60E+00	-1.96E-04	-9.91E+00	-2.11E+01
6.82E+00	-1.52E-04	-5.73E+00	-1.69E+01
7.04E+00	-1.14E-04	-2.43E+00	-1.30E+01
7.26E+00	-8.06E-05	5.41E-02	-9.54E+00
7.48E+00	-5.32E-05	1.82E+00	-6.49E+00
7.70E+00	-3.14E-05	2.96E+00	-3.94E+00
7.92E+00	-1.46E-05	3.61E+00	-1.89E+00
8.14E+00	-2.32E-06	3.85E+00	-3.08E-01
8.36E+00	6.18E-06	3.79E+00	8.42E-01
8.58E+00	1.16E-05	3.52E+00	1.62E+00
8.80E+00	1.45E-05	3.11E+00	2.08E+00
9.02E+00	1.56E-05	2.63E+00	2.29E+00
9.24E+00	1.53E-05	2.12E+00	2.31E+00
9.46E+00	1.41E-05	1.63E+00	2.18E+00
9.68E+00	1.23E-05	1.18E+00	1.95E+00
9.90E+00	1.02E-05	7.83E-01	1.64E+00
1.01E+01	7.88E-06	4.59E-01	1.30E+00
1.03E+01	5.50E-06	2.14E-01	9.26E-01
1.06E+01	3.10E-06	5.34E-02	5.34E-01
1.08E+01	7.14E-07	0.00E+00	1.25E-01
1.10E+01	-1.67E-06	0.00E+00	-2.99E-01

Table 9-2 Soil resistance calculated applying equations of p - y model.

depth, x	p_s	y_k	A_s	B_s	deflection y (m)	Soil resistance p (kN/m)
0.00E+00	0	0.0008	2.9403	2.2592	2.62E-02	0
2.20E-01	2.757501	0.000877	2.460034	1.880565	2.40E-02	6.783544987
4.40E-01	7.297835	0.000945	2.043907	1.543017	2.19E-02	14.9160981
6.60E-01	13.621	0.000893	1.691921	1.248632	1.98E-02	23.04565353
8.80E-01	21.727	0.000744	1.404073	0.999487	1.77E-02	30.50630767
1.10E+00	31.61584	0.000534	1.180366	0.797658	1.58E-02	37.31825906
1.32E+00	43.2875	0.000312	1.020798	0.64522	1.38E-02	41.92471736
1.54E+00	56.74201	0.000143	0.92537	0.544251	1.20E-02	44.82600089
1.76E+00	71.97934	4.09E-05	0.92	0.5	1.03E-02	49.31563676
1.98E+00	88.99951	5.46E-05	0.92	0.5	8.76E-03	53.88955753
2.20E+00	107.8025	7.11E-05	0.92	0.5	7.31E-03	57.38034278
2.42E+00	128.3883	9.05E-05	0.92	0.5	5.99E-03	59.71243652
2.64E+00	150.757	0.000113	0.92	0.5	4.80E-03	60.4554909
2.86E+00	174.9085	0.00014	0.92	0.5	3.75E-03	59.45308859
3.08E+00	200.8428	0.00017	0.92	0.5	2.84E-03	56.65006096
3.30E+00	228.56	0.000204	0.92	0.5	2.07E-03	52.04194767
3.52E+00	258.06	0.000243	0.92	0.5	1.42E-03	45.62009831
3.74E+00	289.3428	0.000286	0.92	0.5	8.90E-04	37.38575603
3.96E+00	322.4085	0.000334	0.92	0.5	4.71E-04	27.17088503
4.18E+00	357.257	0.000387	0.92	0.5	1.51E-04	10.288234
4.40E+00	393.8884	0.000446	0.92	0.5	-8.33E-05	-5.9771448
4.62E+00	432.3025	0.000511	0.92	0.5	-2.45E-04	-18.4349088
4.84E+00	472.4995	0.000581	0.92	0.5	-3.46E-04	-27.3281888
5.06E+00	514.4794	0.000658	0.92	0.5	-4.00E-04	-32.9912
5.28E+00	558.242	0.000741	0.92	0.5	-4.17E-04	-35.8800816
5.50E+00	603.7875	0.000831	0.92	0.5	-4.07E-04	-36.46962
5.72E+00	651.1159	0.000928	0.92	0.5	-3.78E-04	-35.2525316
5.94E+00	700.227	0.001033	0.92	0.5	-3.38E-04	-32.6967894
6.16E+00	751.121	0.001145	0.92	0.5	-2.91E-04	-29.2388096
6.38E+00	803.7979	0.001265	0.92	0.5	-2.43E-04	-25.2497432
6.60E+00	858.2575	0.001393	0.92	0.5	-1.96E-04	-21.064164
6.82E+00	906.7531	0.00149	0.92	0.5	-1.52E-04	-16.9305818
7.04E+00	936.0032	0.00149	0.92	0.5	-1.14E-04	-13.0473024
7.26E+00	965.2533	0.00149	0.92	0.5	-8.06E-05	-9.53685942
7.48E+00	994.5034	0.00149	0.92	0.5	-5.32E-05	-6.49001452
7.70E+00	1023.754	0.00149	0.92	0.5	-3.14E-05	-3.9385038
7.92E+00	1053.004	0.00149	0.92	0.5	-1.46E-05	-1.88738352
8.14E+00	1082.254	0.00149	0.92	0.5	-2.32E-06	-0.308087604
8.36E+00	1111.504	0.00149	0.92	0.5	6.18E-06	0.8414549
8.58E+00	1140.754	0.00149	0.92	0.5	1.16E-05	1.61671224
8.80E+00	1170.004	0.00149	0.92	0.5	1.45E-05	2.07988
9.02E+00	1199.254	0.00149	0.92	0.5	1.56E-05	2.29066508
9.24E+00	1228.504	0.00149	0.92	0.5	1.53E-05	2.30586972
9.46E+00	1257.754	0.00149	0.92	0.5	1.41E-05	2.17727576
9.68E+00	1287.004	0.00149	0.92	0.5	1.23E-05	1.94547672
9.90E+00	1316.255	0.00149	0.92	0.5	1.02E-05	1.6443603
1.01E+01	1345.505	0.00149	0.92	0.5	7.88E-06	1.299523368
1.03E+01	1374.755	0.00149	0.92	0.5	5.50E-06	0.926475374
1.06E+01	1404.005	0.00149	0.92	0.5	3.10E-06	0.533941056
1.08E+01	1433.255	0.00149	0.92	0.5	7.14E-07	0.125459796
1.10E+01	1462.505	0.00149	0.92	0.5	-1.67E-06	-0.2990724

Table 9-3 Comparison values of Table 1 and Table 2.

depth x	p-value from COM	p-value from p-y eq	difference in p	% difference	F on each element	Moment @ top of pile
0.00E+00	0.00E+00	0	0	0.00%	0.74085	0.0814935
2.20E-01	6.74E+00	6.783545	-0.048545	-0.72%	2.37765	0.7846245
4.40E-01	1.49E+01	14.916098	-0.0360981	-0.24%	4.1481	2.281455
6.60E-01	2.28E+01	23.045654	-0.2156535	-0.94%	5.8091	4.473007
8.80E-01	3.00E+01	30.506308	-0.5263077	-1.76%	7.2798	7.207002
1.10E+00	3.62E+01	37.318259	-1.1182591	-3.09%	8.5646	10.363166
1.32E+00	4.17E+01	41.924717	-0.2647174	-0.64%	9.5348	13.634764
1.54E+00	4.50E+01	44.826001	0.1939991	0.43%	10.3576	17.09004
1.76E+00	4.91E+01	49.315637	-0.1756368	-0.36%	11.2475	21.032825
1.98E+00	5.31E+01	53.889558	-0.7795575	-1.47%	12.1165	25.323485
2.20E+00	5.70E+01	57.380343	-0.3403428	-0.60%	12.8876	29.770356
2.42E+00	6.01E+01	59.712437	0.4075635	0.68%	13.4035	33.910855
2.64E+00	6.17E+01	60.455491	1.2745091	2.06%	13.5751	37.331525
2.86E+00	6.17E+01	59.453089	2.2269114	3.61%	13.365	39.69405
3.08E+00	5.98E+01	56.650061	3.169939	5.30%	12.749	40.66931
3.30E+00	5.61E+01	54.041948	2.0380523	3.63%	11.7084	39.925644
3.52E+00	5.04E+01	49.620098	0.7399017	1.47%	10.2168	37.086984
3.74E+00	4.25E+01	39.385756	3.134244	7.37%	8.0223	30.885855
3.96E+00	3.04E+01	29.170885	1.239115	4.07%	4.4759	18.216913
4.18E+00	1.03E+01	10.288234	-0.008234	-0.08%	0.47311	2.0296419
4.40E+00	-5.98E+00	-5.9771448	-0.0018552	0.03%	-2.68609	-12.11427
4.62E+00	-1.84E+01	-18.434909	-0.0050912	0.03%	-5.0347	-23.81413
4.84E+00	-2.73E+01	-27.328189	-0.0018112	0.01%	-6.6363	-32.84969
5.06E+00	-3.30E+01	-32.9912	-0.0088	0.03%	-7.5768	-39.17206
5.28E+00	-3.59E+01	-35.880082	8.16E-05	0.00%	-7.9585	-42.89632
5.50E+00	-3.65E+01	-36.46962	-0.00038	0.00%	-7.8892	-44.25841
5.72E+00	-3.53E+01	-35.252532	0.0025316	-0.01%	-7.4734	-43.56992
5.94E+00	-3.27E+01	-32.696789	0.0067894	-0.02%	-6.8112	-41.20776
6.16E+00	-2.92E+01	-29.23881	0.0088096	-0.03%	-5.9928	-37.57486
6.38E+00	-2.53E+01	-25.249743	-0.0002568	0.00%	-5.0941	-33.06071
6.60E+00	-2.11E+01	-21.064164	0.004164	-0.02%	-4.1789	-28.04042
6.82E+00	-1.69E+01	-16.930582	0.0005818	0.00%	-3.2967	-22.84613
7.04E+00	-1.30E+01	-13.047302	0.0073024	-0.06%	-2.48347	-17.75681
7.26E+00	-9.54E+00	-9.5368594	-0.0001406	0.00%	-1.76286	-12.99228
7.48E+00	-6.49E+00	-6.4900145	0.0010145	-0.02%	-1.14708	-8.706337
7.70E+00	-3.94E+00	-3.9385038	-0.0004962	0.01%	-0.64086	-5.005117
7.92E+00	-1.89E+00	-1.8873835	0.0003835	-0.02%	-0.24145	-1.938844
8.14E+00	-3.08E-01	-0.3080876	8.76E-05	-0.03%	0.058685	0.4841513
8.36E+00	8.42E-01	0.8414549	4.51E-05	0.01%	0.270435	2.2905845
8.58E+00	1.62E+00	1.6167122	0.0002878	0.02%	0.40667	3.5339623
8.80E+00	2.08E+00	2.07988	0.00012	0.01%	0.48081	4.2840171
9.02E+00	2.29E+00	2.2906651	0.0003349	0.01%	0.50567	4.6167671
9.24E+00	2.31E+00	2.3058697	0.0001303	0.01%	0.49313	4.6107655
9.46E+00	2.18E+00	2.1772758	-0.0002758	-0.01%	0.45342	4.3392294
9.68E+00	1.95E+00	1.9454767	-0.0004767	-0.02%	0.39479	3.8649941
9.90E+00	1.64E+00	1.6443603	-0.0003603	-0.02%	0.32384	3.2416384
1.01E+01	1.30E+00	1.2995234	0.0004766	0.04%	0.244904	2.5053679
1.03E+01	9.26E-01	0.9264754	-7.537E-05	-0.01%	0.160633	1.6786149
1.06E+01	5.34E-01	0.5339411	-4.106E-05	-0.01%	0.072523	0.7738204
1.08E+01	1.25E-01	0.1254598	-5.98E-05	-0.05%	-0.01911	-0.208075
1.10E+01	-2.99E-01	-0.2990724	-2.76E-05	0.01%	-0.0329	0.0036191
		average =	0.2141937	0.37%	99.9623	0.0084047
		Max =	3.169939	7.37%	Sum	Sum

Table 9-4 Out-put from FB Pier for free head pile of length 9.0 m.

P=100 kN-m and EI=80,000 kN-m ²						
x (m)	defl. y (m)	m (kN-m)	y _a (m)	y'' (m ⁻¹)	y _a '' (m ⁻¹)	A (kN-m)
0.00E+00	0.00E+00	0.00E+00	0.00047	0	0	0
0.00E+00	2.77E-02	0.00E+00	0.00046	0.000125	-6.25E-07	-6.25E-06
1.80E-01	2.68E-02	1.00E+01	0.00044	0.0002625	-0.0000025	-0.00005
3.60E-01	2.58E-02	2.00E+01	0.00043	0.0003875	-3.75E-06	-0.0001125
5.40E-01	2.49E-02	3.00E+01	0.00041	0.000525	-0.000005	-0.0002
7.20E-01	2.40E-02	4.00E+01	0.0004	0.00065	-6.25E-06	-0.0003063
9.00E-01	2.30E-02	4.90E+01	0.00038	0.000775	-0.0000075	-0.0004425
1.08E+00	2.21E-02	5.90E+01	0.00037	0.0009	-8.75E-06	-0.000595
1.26E+00	2.12E-02	6.80E+01	0.00036	0.0010125	-0.00001	-0.00077
1.44E+00	2.03E-02	7.70E+01	0.00034	0.001125	-1.125E-05	-0.0009675
1.62E+00	1.94E-02	8.60E+01	0.00032	0.0012375	-0.0000125	-0.001175
1.80E+00	1.85E-02	9.40E+01	0.00032	0.001375	-0.0000175	-0.00175
1.98E+00	1.77E-02	1.00E+02	0.0003	0.0015	-0.000025	-0.00275
2.16E+00	1.68E-02	1.10E+02	0.00029	0.0015	-0.0000125	-0.0015
2.34E+00	1.60E-02	1.20E+02	0.00028	0.001625	-0.0000125	-0.0015
2.52E+00	1.51E-02	1.20E+02	0.00026	0.00175	-0.000025	-0.00325
2.70E+00	1.43E-02	1.30E+02	0.00025	0.00175	-0.0000125	-0.00175
2.88E+00	1.35E-02	1.40E+02	0.00024	0.001875	-0.000025	-0.0035
3.06E+00	1.28E-02	1.40E+02	0.00022	0.001875	-0.0000125	-0.00175
3.24E+00	1.20E-02	1.40E+02	0.00021	0.002	-0.000025	-0.00375
3.42E+00	1.13E-02	1.50E+02	0.000193	0.002	-0.000025	-0.00375
3.60E+00	1.05E-02	1.50E+02	0.000187	0.002	-0.0000125	-0.001875
3.78E+00	9.82E-03	1.50E+02	0.00017	0.002125	-0.000025	-0.004
3.96E+00	9.13E-03	1.60E+02	0.000163	0.002125	-0.000025	-0.004
4.14E+00	8.47E-03	1.60E+02	0.000151	0.002125	-0.000025	-0.004
4.32E+00	7.82E-03	1.60E+02	0.00014	0.002125	-0.000025	-0.004
4.50E+00	7.19E-03	1.60E+02	0.000129	0.002125	-0.000025	-0.004
4.68E+00	6.58E-03	1.60E+02	0.000118	0.002125	-0.000025	-0.004
4.86E+00	6.00E-03	1.60E+02	0.000108	0.002	-0.000025	-0.00375
5.04E+00	5.43E-03	1.50E+02	0.000098	0.002	-0.000025	-0.00375
5.22E+00	4.88E-03	1.50E+02	0.000089	0.002	-0.000025	-0.00375
5.40E+00	4.35E-03	1.50E+02	0.000078	0.001875	-0.000025	-0.0035
5.58E+00	3.83E-03	1.40E+02	0.000069	0.00175	-0.0000125	-0.00175
5.76E+00	3.34E-03	1.40E+02	0.00006	0.00175	-0.000025	-0.00325
5.94E+00	2.86E-03	1.30E+02	0.000051	0.001625	-0.000025	-0.003
6.12E+00	2.40E-03	1.20E+02	0.000042	0.0015	-0.0000125	-0.001375
6.30E+00	1.95E-03	1.10E+02	0.000033	0.001375	-1.375E-05	-0.0015125
6.48E+00	1.52E-03	1.10E+02	0.000025	0.00125	-0.0000125	-0.0012
6.66E+00	1.10E-03	9.60E+01	0.0000167	0.00115	-1.375E-05	-0.0011825
6.84E+00	6.92E-04	8.60E+01	0.0000085	0.0010125	-1.125E-05	-0.000855
7.02E+00	2.95E-04	7.60E+01	4.3E-07	0.000875	-0.00001	-0.00066
7.20E+00	-9.23E-05	6.60E+01	-0.0000075	0.00075	-0.00001	-0.00056
7.38E+00	-4.71E-04	5.60E+01	-0.0000154	0.0006125	-0.0000075	-0.000345
7.56E+00	-8.43E-04	4.60E+01	-0.000023	0.0004875	-6.25E-06	-0.0002313
7.74E+00	-1.21E-03	3.70E+01	-0.000031	0.000375	-0.000005	-0.00014
7.92E+00	-1.57E-03	2.80E+01	-0.000039	0.0002625	-0.0000025	-0.00005
8.10E+00	-1.93E-03	2.00E+01	-0.000046	0.000175	-0.0000025	-0.0000325
8.28E+00	-2.28E-03	1.30E+01	-0.000054	0.0001038	-1.25E-06	-9.75E-06
8.46E+00	-2.64E-03	7.80E+00	-0.000062	0.0000475	-0.0000005	-0.0000018
8.64E+00	-2.99E-03	3.60E+00	-0.000069	0.0000125	-1.5E-07	-1.425E-07
8.82E+00	-3.34E-03	9.50E-01	0.0003298	0	0	0
					sum=	-0.007799

Table 9-5 Out-put from COM 624P for free head pile of length 9.0 m

P=100 kN-m ; EI=60,000 kN-m ²						
x (m)	defl. y (m)	m (kN-m)	y _a (m)	y'' (m ⁻¹)	y _a '' (m ⁻¹)	A (kN-m)
0.00E+00	3.05E-02	0.00E+00	0.00052	0	0	0
1.80E-01	2.94E-02	1.00E+01	0.0005	0.00016667	-8.333E-07	-8.333E-06
3.60E-01	2.83E-02	2.00E+01	0.00048	0.00035	-3.333E-06	-6.667E-05
5.40E-01	2.72E-02	3.00E+01	0.00047	0.00051667	-0.000005	-0.00015
7.20E-01	2.62E-02	4.00E+01	0.00045	0.0007	-6.667E-06	-0.0002667
9.00E-01	2.51E-02	4.90E+01	0.00043	0.00086667	-8.333E-06	-0.0004083
1.08E+00	2.40E-02	5.90E+01	0.00042	0.00103333	-0.00001	-0.00059
1.26E+00	2.30E-02	6.80E+01	0.00041	0.0012	-1.167E-05	-0.0007933
1.44E+00	2.19E-02	7.70E+01	0.00038	0.00135	-1.333E-05	-0.0010267
1.62E+00	2.09E-02	8.60E+01	0.00037	0.0015	-0.000015	-0.00129
1.80E+00	1.99E-02	9.40E+01	0.00035	0.00165	-1.667E-05	-0.0015667
1.98E+00	1.89E-02	1.00E+02	0.00034	0.00183333	-2.333E-05	-0.0023333
2.16E+00	1.79E-02	1.10E+02	0.00032	0.002	-3.333E-05	-0.0036667
2.34E+00	1.70E-02	1.20E+02	0.0003	0.002	-1.667E-05	-0.002
2.52E+00	1.60E-02	1.20E+02	0.00029	0.00216667	-1.667E-05	-0.002
2.70E+00	1.51E-02	1.30E+02	0.00027	0.00233333	-3.333E-05	-0.0043333
2.88E+00	1.42E-02	1.40E+02	0.00027	0.00233333	-1.667E-05	-0.0023333
3.06E+00	1.33E-02	1.40E+02	0.00025	0.0025	-3.333E-05	-0.0046667
3.24E+00	1.25E-02	1.40E+02	0.00024	0.0025	-1.667E-05	-0.0023333
3.42E+00	1.16E-02	1.50E+02	0.00022	0.00266667	-3.333E-05	-0.005
3.60E+00	1.08E-02	1.50E+02	0.000207	0.00266667	-3.333E-05	-0.005
3.78E+00	1.00E-02	1.50E+02	0.000189	0.00266667	-3.333E-05	-0.005
3.96E+00	9.29E-03	1.60E+02	0.000178	0.00283333	-3.333E-05	-0.0053333
4.14E+00	8.56E-03	1.60E+02	0.000168	0.00283333	-3.333E-05	-0.0053333
4.32E+00	7.86E-03	1.60E+02	0.000155	0.00283333	-3.333E-05	-0.0053333
4.50E+00	7.18E-03	1.60E+02	0.000144	0.00283333	-3.333E-05	-0.0053333
4.68E+00	6.53E-03	1.60E+02	0.000132	0.00283333	-3.333E-05	-0.0053333
4.86E+00	5.91E-03	1.50E+02	0.000121	0.00266667	-3.333E-05	-0.005
5.04E+00	5.31E-03	1.50E+02	0.00011	0.00266667	-3.333E-05	-0.005
5.22E+00	4.73E-03	1.50E+02	0.000099	0.00266667	-3.333E-05	-0.005
5.40E+00	4.18E-03	1.40E+02	0.000088	0.0025	-3.333E-05	-0.0046667
5.58E+00	3.66E-03	1.40E+02	0.000079	0.0025	-3.333E-05	-0.0046667
5.76E+00	3.16E-03	1.30E+02	0.000068	0.00233333	-3.333E-05	-0.0043333
5.94E+00	2.68E-03	1.30E+02	0.00006	0.00216667	-1.667E-05	-0.0021667
6.12E+00	2.22E-03	1.20E+02	0.00005	0.00216667	-3.333E-05	-0.004
6.30E+00	1.78E-03	1.10E+02	0.000041	0.002	-3.333E-05	-0.0036667
6.48E+00	1.36E-03	1.00E+02	0.000033	0.00183333	-2.333E-05	-0.0023333
6.66E+00	9.56E-04	9.40E+01	0.0000238	0.00166667	-0.00002	-0.00188
6.84E+00	5.68E-04	8.40E+01	0.0000156	0.0015	-1.833E-05	-0.00154
7.02E+00	1.95E-04	7.40E+01	0.0000075	0.00131667	-1.667E-05	-0.0012333
7.20E+00	-1.66E-04	6.40E+01	-5E-07	0.00113333	-1.333E-05	-0.0008533
7.38E+00	-5.17E-04	5.40E+01	-0.0000082	0.00096667	-1.167E-05	-0.00063
7.56E+00	-8.58E-04	4.40E+01	-0.0000159	0.0008	-0.00001	-0.00044
7.74E+00	-1.19E-03	3.50E+01	-0.000023	0.00063333	-8.333E-06	-0.0002917
7.92E+00	-1.52E-03	2.70E+01	-0.000031	0.00048333	-6.667E-06	-0.00018
8.10E+00	-1.84E-03	1.90E+01	-0.000038	0.00035	-0.000005	-0.000095
8.28E+00	-2.16E-03	1.30E+01	-0.000046	0.00023333	-3.333E-06	-4.333E-05
8.46E+00	-2.48E-03	7.50E+00	-0.000053	0.00013333	-1.667E-06	-0.0000125
8.64E+00	-2.80E-03	3.50E+00	-0.00006	6.1667E-05	-8.333E-07	-2.917E-06
8.82E+00	-3.12E-03	9.10E-01	-0.000068	1.6167E-05	-0.0000002	-1.82E-07
9.00E+00	-3.43E-03	0.00E+00	-0.000075	0	0	0
					sum=	-0.0107582

LHS= 0.0028 m, obtained from COM 624 as out put.

$$\text{RHS} = -0.0107582 \frac{-20}{80} - A_k(0) - A_\gamma(0) - A_\phi(0) - A_{K_a}(0) - A_b(0) = 0.0027$$

% error = (0.0028-0.0027)/0.0028= 3.5% which may be attributed to approximation introduced by the application of trapezoidal method for integration in addition other approximations employed in the investigation. Percentage of error has been calculated for changes in other design variables and shown in Table 9-6.

Table 9-6 An example of percent of error of sensitivity factor $A_{(.)}^{Py}$ for the sensitivity analysis of a free head long pile of length $L = 5T_p = 9.0$ m subjected to variable lateral force P .

Normalized changes in design variables		Sensitivity factors	Error in % at loads applied to the pile				
			50 kN	100 kN	150 kN	200 kN	250 kN
δEI_N	25%	A_{EI}^{Py} (%)	2.7	3.5	3.6	3.8	4.5
δk_N	10%	A_k^{Py} (%)	1.8	2.2	2.2	2.4	3.1
$\delta \gamma'_N$	6.25%	$A_{\gamma'}^{Py}$ (%)	2.0	2.1	2.1	2.7	2.9
$\delta \phi_N$	11%	A_ϕ^{Py} (%)	5.5	5.7	6.2	6.3	7.9
$\delta K_{a N}$	9%	$A_{K_a}^{Py}$ (%)	3.4	3.8	3.9	3.9	4.3
δb_N	5%	A_b^{Py} (%)	-2.7	-1.2	2.3	5.8	6.9

CHAPTER X

CONCLUSION AND FUTURE RESEARCH WORK

10.1 Closing notes

Design and analysis of laterally loaded pile is lengthy, complicated and time consuming process because of involvement of numerous design variables and their complex relationship which often leads to erroneous results. Results of sensitivity analysis on laterally loaded pile can be used as a useful tool for substantially minimizing calculation time and chances of error. Results of this study may useful in following aspects.

- Design optimization
- Serviceability limit state design
- Rehabilitation
- Fast Execution and save time
- Improvement
- Identification of most active design variable

Engineers these days use general purpose computer softwares for design purposes. Often the user of such software packages does not have any access to the source program, and it is unlikely that the user engineers have thorough knowledge of the details of the structural analysis algorithm used in the software package. Therefore, it is vital for research engineers to develop methods that are suitable for use with such software packages. In many real life design situations engineer who is assigned with the design of structure cannot afford to analyze the system more than a handful of times. This is in the

first case true because of the high computational cost involved in the analysis of many real life complex problems. In addition to that design engineers are tied within limited time and other resources frame, as a result study of enough alternatives to reach the best solution remains remote. This environment motivates a focus on optimization techniques that call for minimum interference with the structural analysis package and requires only a small number of structural analysis runs. This study of sensitivity analysis of laterally loaded piles is intended to serve that purpose.

10.2 Conclusion

This research in investigating sensitivity analysis of laterally loaded single piles and pile group embedded in sand located below water table. Sensitivities connected to maximum lateral deflection and angle of flexural rotation had been calculated where the applied load is either horizontal force or bending moment. The mechanical parameters the pile-soil system includes:

- Flexural stiffness of pile EI ,
- Coefficient of subgrade reaction k ,
- Submerged unit weight of sand γ' ,
- Angle of internal friction ϕ ,
- Coefficient of active lateral earth pressure of Rankine type K_a ,
- Width b of the pile at which the soil reaction is developed.

They are taken as design variables. Flexural stiffness of pile EI is the pile property and the rest of the design variables are connected to soil response. Sensitivities connected to each design variables have been investigated. Study of the results of this investigation lead to following conclusion:

- The design variables $EI, k, \gamma', \phi,$ and b strengthen the pile-soil system whereas K_a weakens the system. Thus, the sensitivity operators $S_{EI}, S_k, S_{\gamma'}, S_{\phi}$ and S_b connected to sensitivity of maximum generalized deformation due to the changes of design variables $EI, k, \gamma', \phi,$ and b respectively have negative values. Their integrations, the sensitivity factors $A_{EI}, A_k, A_{\gamma'}, A_{\phi}$ and A_b have negative values accordingly. Increase in value of these design variables will decrease deformation of the system and hence regarded as favourable in improvement of performance of the infrastructure. On the other hand, the sensitivity operator S_{K_a} connected to sensitivity of maximum generalized deformation due to the changes of design variables K_a has positive value. Its integrations, the sensitivity factor A_{K_a} has positive value accordingly. Increase in value of design variable K_a will increase deformation of the system and hence regarded as unfavourable in improvement of performance of the infrastructure.
- Changes in design variable ϕ are capable of producing highest changes in maximum generalized deformation of the pile-soil system. Relative sensitivity factor F_{ϕ} is measure for that. The average value of F_{ϕ} estimated from results of

this research is 60%. Values of F_b , F_{K_a} , $F_{\gamma'}$, F_{EI} and F_k are 12%, 10%, 8%, 6% and 4% respectively.

- The sensitivity operators have nonzero values along almost entire lengths of the short piles. So, changes in design variables at any zone along the length of the short piles are capable of changing maximum generalized deformation of the pile-soil system. In case of long piles changes in design variables along top part of the length of the pile is capable of producing changes in maximum generalized deformation.
- Sensitivity operators due to the changes of design variables of pile-soil-pile system of group of piles follow the same pattern of the single isolated piles. Piles of leading row possess highest value of sensitivity factor followed by first trailing row and then the second trailing row for any value of load applied P_G to the group and spacing of the member piles. This distribution of sensitivity factors among the member piles in different rows becomes more pronounced as the spacing decreases from 6D to 2D, where D is the diameter of the piles of the group.

10.3 Engineering applications

Analysis of laterally loaded pile-soil system is a length and time consuming operation due to the involvement of many strength parameters and complex relationship governing the interaction of the system. The results of sensitivity investigation can be used as a useful in the following:

-
- Design optimization: Through the study of graphical representation of sensitivity operator $S_{(.)}^{(.)}$, sensitivity factors $A_{(.)}^{(.)}$ and sensitivity $F_{(.)}^{(.)}$ most suitable values of design parameters can be identified than will lead to proportioning of the most economical pile-soil system. This can be done by traditional procedures through lengthy calculations and tedious efforts but use of results of sensitivity analysis will allow avoiding trials.
 - Serviceability state design: Techniques are available to predict the changes especially degradation of strength parameters due to the construction defects, aging and environmental effects at the end of the period for which the structure is design for. With the use of the results of sensitivity analysis the state of deformation of the system can be estimated. Previsions can be made at the design stage to ensure intended serviceability of the structure throughout design life time.
 - Improvement of existing system: To improve the sustainability of structural system repair, improvement, rehabilitation and replacement of exiting system are often become necessary. Using the results of sensitivity investigations the most feasible and economical method can be selected.

10.4 Recommendation for future research

In order to improve the process of design and analysis of laterally loaded pile following future research on sensitivity of laterally piles are recommended.

- Sensitivity analysis can be performed in all types of soil

-
- In field soil is usually not available as pure sand or clay or in any other type, rather is often a mixer. Sensitivity analysis should be performed in mixed soil.
 - Layered soil should also be investigated.
 - Comparing and compiling results from researchers a complete data bank can be established for use of engineers.
 - An electronic data bank would be more user-friendly and easy to use.
 - A soft ware can be developed for sensitivity analysis of laterally loaded pile-soil system of various type and combination.

REFERENCES

1. Baguelin, F., Jezequel, J. F., Shields D. H. (1978) *The Pressuremeter and Foundation Engineering*-Transtech Publications, Aedrmannsdorf (Switzerland).
2. Baquelin, F., Frank, R. and Said Y.H. (1977). Theoretical Study of Lateral Reaction Mechanism of Piles. *Geotechnique* 27(3): 405-434.
3. Brown, D. A. and Reese, L. C. (1985). Behaviour of Large Scale Pile Group Subjected to Cyclic Loading. *Reports to the Minerals Management Services, US Department of Interior, Reston, VA; Department of Research, FHWA, Washington DC and US Army Engineers Waterways Experiment Station, Vicksburg, Mississippi.*
4. Budkowska, B. B. 1997. Sensitivity Analysis of Short Piles Subjected to Bending Embedded in Homogeneous Soil. Part I. Theoretical Formulation. *Computer and Geotechnics* 21(2): 87-101.
5. Budkowska, B. B. and Priyanto, D. G. (2002)a. "Investigation of Pile Group in Soft Clay Subjected to Horizontal Loading - Sensitivity Analysis". *Proceedings of International Symposium on Numerical Model in Geomechanics, NUMOG VIII*, 10-12 April 2002, Rome, Italy.
6. Budkowska, B. B. and Priyanto, D. G. (2002)b. "Comperative Analysis of Lateral Deformation of Short Pile and Long Piles Embedded in Nonlinear Soft Clay – Sensitivity Analysis.". *Proceedings of International Symposium on Lowland Technology, Saga University*, 18-20, September 2002, Saga, Japan.
7. Budkowska, B. B. and Suwarno, D. (2002)a. Distributed Parameter Sensitivity Analysis of Nonlinear Behavior of Laterally Loaded Piles. *Proceedings of*

International Symposium on Numerical Model in Geomechanics, NUMOG VIII,
10-12, April 2002, Rome, Italy.

8. Budkowska, B. B. and Suwarno, D. (2002)b. Assessment of Horizontal Loading of Pile Group Penetrating Stiff Clay Below the Water Table – Sensitivity Analysis. *Proceedings of International Symposium on Lowland Technology, Saga University*, 18-20, September 2002, Saga, Japan.
9. Budkowska, B. B., Szymczak, C. (1995). On first Variation of Extremum Values of Displacements and Internal Forces of Laterally Loaded Piles. *Computer and Structures* 57(2): 303-307.
10. Conte, J. P., Vijalapura, P. K. and Meghella, M. (2003). Consistent Finite-Element Response Sensitivity Analysis - *Journal of Engineering Mechanics* 129(12):1380-1393.
11. Cox, W. R, Reese, L. C. and Grubbs, B. R. (1974). Field Testing of Laterally Loaded Piles in Sand. *Proceedings of Offshore Technical Conference, Paper No. 2079*, Huston, Texas.
12. Dems, K. and Mroz, Z. (1983). Variational Approach by Means of Adjoint System to Structural Optimization and Sensitivity Analysis - I. *International Journal of Solids and Structures* 19: 677-692.
13. Evans, L. T. and Duncan, J. M. (1982). Simplified Analysis of Laterally Loaded Piles. *Report No. UCB/GT 82-04, Berkeley: Department of Civil Engineering University of California, USA.*
14. Haftka, R. T., Gurdal, Z. and Kamat, M. P. (1990) Elements of Structural Optimization, Second revised edition, *Kluwer Academic Publishers.*

-
15. Kleiber, M., Antunez, H., Hien, T. D. and Kowalczyk, P. (1997). Parameter Sensitivity in Nonlinear Mechanics, Theory and Finite Element Computation. *Chichester: J. Willy & Sons.*
 16. Matlock, H. (1970). Correlations for Design of Laterally Loaded Piles in Soft Clay, *Proceedings of Second Annual Offshore Technology Conference, Huston, Texas, 577-594.*
 17. Menard, L. (1962). Component D'une Foundation Profonde Soumise a Des Effort de Renversement, *Sols-Soils 3: 9-23.*
 18. Mokwa, R. L. and Duncan, J. M. (2001). Laterally Loaded Pile Group Effect and p - y Multipliers. *Foundation and Ground Improvements, Proceedings of a Specialty Conference. Blackburg, Virginia: 728-842.*
 19. O'Neil, M. W. and Gazioglu, S. M. (1984). Evaluation of p - y Relationship in Sand. *Proceedings, Analysis and Design of Pile Foundation, ASCE Technical Council on Codes and Standards, ASCE National Convention, San Francisco, California, J. Meyers Edition: 192-213.*
 20. O'Neil, M. W. and Huang, A. B. (2003). Comparative Behavior of Laterally Loaded Groups of Bored and Driven Piles in Cohesionless Soil. *International Journal of Offshore and Polar Engineering, 13(3): 161-167.*
 21. Poulos, H. G. (1971). Behavior of Laterally Loaded Pile. *Journal of Soil Mechanics, Foundation Division, American Society of Civil Engineers, 97(5): 711-731.*

-
22. Reese, L. C., Cox, W. R. and Koop, F. D. (1975). Field Testing and Analysis of Laterally Loaded Piles in Stiff Clay. *Proceedings of Seventh Offshore Technology Conference, Huston, Texas.*
 23. Rollins, K.M., Olsen, R. J. And Garrett, B. J. (2002). Dynamic Lateral Response of a Full Scale Pile Group. *Proceedings of Deep Foundation Institute Annual Conference: 221-230.*
 24. Sanders, B. F. and Katopodes, N. D. (2000). Adjoint Sensitivity Analysis for Shallow-Water Wave Control. *Journal of Engineering Mechanics*, 126(6): 909-919.
 25. Terzaghi, K., (1955) Evaluation of Coefficients of Subgrade Reaction *Geotechnique 5(4): 297-326.*
 26. Wang, S. T. and Reese, L. C. (1993). COM624P- Laterally Loaded Pile Analysis Program for Microcomputer, Version 2.0. *Report No. FHWA –SA-91-084: Washington, D. C.*
 27. Washizu, K. (1976). *Variational Method in Elasticity and Plasticity, Oxford: Pergamon Press.*
 28. Welch, R. C. and Reese, L. C. (1972). Lateral Loaded Behavior of Drilled Shafts. *Research Report No. 3-5-65-99, Conducted for Texas Highway Department and US Department of Transportation, Federal Highway Administration, Bureau of Public Roads, Centre for Highway Research, The University of Texas at Austin.*
 29. Winkler, E. (1867). *Die lehre von elastizitat und festigkeit. Prague.*

APPENDIX A

Explicit form of sensitivity operators

Sensitivity operators are applicable to appropriate segment of p - y curve demonstrating a defined soil phase due to deflection y above or below depth x_r .

Sensitivity operator, S_{EI} connected to variation in design variable EI :

For $x \leq x_r$ and $0 \leq y \leq y_k$, meaning linear elastic phase above x_r , sensitivity operator affecting generalized maximum deflections due to the changes of the design variables EI , is named $(S_{EI})_L^T$ [where superscript T indicates top of x_r and subscript L stands for linear elastic phase].

From Equation 5-16:

$$(S_{EI})_L^T = \frac{M M_a}{EI} \quad \text{A-1}$$

Design variable, EI affects the sensitivity operator in all soil phases through out the length of the pile. $(S_k)_L^T$ in Equation A-1 is also valid for depths above and below x_r for all soil deformation phases.

Sensitivity operator, S_k connected to variation in design variable k :

For $x \leq x_r$ and $0 \leq y \leq y_k$, meaning linear elastic phase above x_r , sensitivity operator affecting generalized maximum deflections due to the changes of the design variables k , is named $(S_k)_L^T$ [where superscript T indicates top of x_r and subscript L stands for linear elastic phase].

From Equation 3-15:

$$p = (kx)y \quad 3-15$$

$$p_a = (kx)y_a \quad A-2$$

$$p_{,y} = kx \quad A-3$$

From Equation 5-17,

$$S_k = \begin{bmatrix} p_a & \frac{p_{,k}}{p_{,y}} k \end{bmatrix} \quad 5-17$$

$$(S_k)_L^T = y \ y_a \ x \ k \quad A-4$$

Design variable, k affects the sensitivity operator in this phase that is linear phase only.

$(S_k)_L^T$ in Equation A-4 is also valid for depths below x_r , that is for $x \geq x_r$ and $0 \leq y \leq y_k$.

Sensitivity operator, $S_{\gamma'}$ connected to variation of design variable γ' :

For $x \leq x_r$ and $y_k \leq y \leq y_m$

From Equation 3-14:

$$p = B_s p_{st} (60y/b)^{0.8(A_s/B_s-1)} \quad 3-14$$

$$p_a = B_s p_{st} (60y_a/b)^{0.8(A_s/B_s-1)} \quad 3-15$$

$$p_{st} = \gamma' x \left[\frac{K_0 x \tan\phi \tan\beta}{\tan(\beta - \phi) \tan\alpha} + \frac{\tan\beta}{\tan(\beta - \phi)} (b + x \tan\beta \tan\alpha) + K_0 x \tan\beta (\tan\phi \sin\beta - \tan\alpha) - K_a b \right] \quad 3-18$$

$$\frac{p_a}{p_{,y}} = \frac{y}{0.8 \left(\frac{A_s}{B_s} - 1 \right)} \left(\frac{y}{y_a} \right)^{-0.8 \left(\frac{A_s}{B_s} - 1 \right)} \quad A-5$$

$$p_{,\gamma'} = \frac{p_{st} B_s}{\gamma'} \left(\frac{60}{b} y \right)^{0.8 \left(\frac{A_s}{B_s} - 1 \right)} \quad A-6$$

$$(S_{\gamma'})_{NL}^T = \frac{p_a}{p_{,y}} p_{,y} \quad A-7$$

where:

subscript NL indicates non-linear elastic phase,

$\frac{p_a}{p_{,y}}$ and $p_{,\gamma'}$ are given by Equations A-5 and A-6, respectively.

For $x \leq x_r$ and $y_m \leq y \leq y_u$

From Equation 3-16:

$$p = p_{st} \left[B_s + \left(y - \frac{b}{60} \right) \frac{A_s - B_s}{0.02086 b} \right] \quad 3-16$$

$$p_a = p_{st} \left[B_s + \left(y_a - \frac{b}{60} \right) \frac{A_s - B_s}{0.02086 b} \right] \quad A-8$$

$$\frac{p_a}{p_{,y}} = \frac{B_s b}{48(A_s - B_s)} + \left(y_a - \frac{b}{60} \right) \quad A-9$$

$$p_{,\gamma'} = \frac{p_s}{\gamma} \left[B_s + \frac{48}{b} \left(y - \frac{b}{60} \right) (A_s - B_s) \right] \quad A-10$$

$$\left(S_{\gamma'} \right)_{BL}^T = \frac{p_a}{p_{,y}} p_{,\gamma'} \quad A-11$$

where:

subscript *BL* indicates bi-linear elastic phase,

$\frac{p_a}{p_{,y}}$ and $p_{,\gamma'}$ are given by Equations A-9 and A-10, respectively.

For $x \geq x_r$ and $y_k \leq y \leq y_m$

From Equation 3-14:

$$p = B_s p_{sd} (60y/b)^{0.8(A_s/B_s-1)} \quad 3-14$$

$$p_a = B_s p_{sd} (60y_a/b)^{0.8(A_s/B_s-1)} \quad A-12$$

$$p_{sd} = K_a b \gamma' (\tan^8 \beta - 1) + K_0 \beta \gamma' x \tan \phi \tan \beta \quad 3-19$$

$$(S_{\gamma'})_{NL}^B = \frac{p_a}{p_{,y}} p_{,y} \quad A-13$$

where:

subscript *NL* indicates non-linear elastic phase,

$\frac{p_a}{p_{,y}}$ and $p_{,\gamma'}$ are given by Equations A-5 and A-6, respectively.

For $x \geq x_r$ and $y_m \leq y \leq y_u$

From Equation 3-16:

$$p = p_{sd} \left[B_s + \left(y - \frac{b}{60} \right) \frac{A_s - B_s}{0.02086 b} \right] \quad 3-16$$

$$p_a = p_{sd} \left[B_s + \left(y_a - \frac{b}{60} \right) \frac{A_s - B_s}{0.02086 b} \right] \quad A-14$$

$$(S_{\gamma'})_{BL}^B = \frac{p_a}{p_{,y}} p_{,\gamma'} \quad A-15$$

where:

subscript *BL* indicates bi-linear elastic phase,

$\frac{p_a}{p_{,y}}$ and $p_{,\gamma'}$ are given by Equations A-9 and A-10, respectively.

Design variable, γ' affects the sensitivity operator in non-linear and bilinear phase above and below x_r .

Sensitivity operator, S_{K_a} connected to the variation in design variable K_a :

For $x \leq x_r$ and $y_k \leq y \leq y_m$

From Equation 3-14:

$$p = B_s p_{st} (60y/b)^{0.8(A_s/B_s-1)} \quad 3-14$$

$$p_a = B_s p_{st} (60y_a/b)^{0.8(A_s/B_s-1)} \quad A-16$$

$$p_{st} = \gamma' x \left[\frac{K_0 x \tan \phi \tan \beta}{\tan(\beta - \phi) \tan \alpha} + \frac{\tan \beta}{\tan(\beta - \phi)} (b + x \tan \beta \tan \alpha) + K_0 x \tan \beta (\tan \phi \sin \beta - \tan \alpha) - K_a b \right] \quad 3-18$$

$$p_{,K_a} = -B_s \gamma' x \left[\frac{K_0 x \tan \phi \sin \beta}{2 \cos \alpha (K_a)^{3/2}} + \frac{\tan \beta}{2(K_a)^{3/2}} (b + x \tan \beta \tan \alpha) + b \right] \left(\frac{60}{b} y \right)^{0.8 \left(\frac{A_s}{B_s} - 1 \right)} \quad A-17$$

$$(S_{K_a})_{NL}^T = \frac{p_a}{p_{,y}} p_{,K_a} \quad A-18$$

where:

subscript NL indicates non-linear elastic phase,

$\frac{p_a}{p_{,y}}$ and $p_{,K_a}$ are given by Equations A-5 and A-17, respectively.

For $x \leq x_r$ and $y_m \leq y \leq y_u$

$$p_{,K_a} = -\gamma'x \left[\frac{K_o x \tan \phi \sin \beta}{(K_a)^{3/2} \cos \alpha} + \frac{\tan \beta}{(K_a)^{3/2}} (b + x \tan \beta \tan \alpha) + b \right] \left[B_s + \left(y - \frac{b}{60} \right) \left(\frac{48}{b} \right) (A_s - B_s) \right]$$

A-19

$$(S_{K_a})_{BL}^F = \frac{p_a}{p_{,y}} p_{,K_a}$$

A-20

where:

subscript *BL* indicates bi-linear elastic phase,

$\frac{p_a}{p_{,y}}$ and $p_{,K_a}$ are given by Equations A-9 and A-19, respectively.

For $x \geq x_r$ and $y_k \leq y \leq y_m$

From Equation 3- 14:

$$p = B_s p_{sd} (60y/b)^{0.8(A_s/B_s-1)}$$

3-14

$$p_a = B_s p_{sd} (60y_a/b)^{0.8(A_s/B_s-1)}$$

A-21

$$p_{sd} = K_a b \gamma' (\tan^8 \beta - 1) + K_o \beta \gamma' x \tan \phi \tan \beta$$

3-19

$$p_{,K_a} = -B_s \gamma' b x (\tan^8 \beta - 1) \left(\frac{60}{b} y \right)^{0.8 \left(\frac{A_s}{B_s} - 1 \right)}$$

A-22

$$(S_{K_a})_{NL}^B = \frac{p_a}{p_{,y}} p_{,K_a}$$

A-23

where:

subscript *NL* indicates non-linear elastic phase,

$\frac{P_a}{p_{,y}}$ and $p_{,K_a}$ are given by Equations A-5 and A-22, respectively.

For $x \leq x_r$ and $y_m \leq y \leq y_u$

From Equation 3-16:

$$p = p_{sd} \left[B_s + \left(y - \frac{b}{60} \right) \frac{A_s - B_s}{0.02086 b} \right] \quad 3-16$$

$$p_a = p_{sd} \left[B_s + \left(y_a - \frac{b}{60} \right) \frac{A_s - B_s}{0.02086 b} \right] \quad A-24$$

$$p_{,K_a} = -b\gamma'x \left(\tan^8 \beta - 1 \right) \left[B_s + \left(y - \frac{b}{60} \right) \left(\frac{48}{b} \right) (A_s - B_s) \right] \quad A-25$$

$$\left(S_{K_a} \right)_{BL}^B = \frac{P_a}{p_{,y}} p_{,K_a} \quad A-26$$

where:

subscript *BL* indicates bi-linear elastic phase,

$\frac{P_a}{p_{,y}}$ and $p_{,K_a}$ are given by Equations A-9 and A-25, respectively.

Design variable, K_a affects the sensitivity operator in non linear and bilinear phase above and below x_r .

Sensitivity operator, S_ϕ connected to variation in design variable, ϕ :

For $x \leq x_r$ and $y_k \leq y \leq y_m$

From Equation 3-14:

$$p = B_s p_{st} (60y/b)^{0.8(A_s/B_s-1)} \quad 3-14$$

$$p_a = B_s p_{st} (60y_a/b)^{0.8(A_s/B_s-1)} \quad A-27$$

$$p_{st} = \gamma'x \left[\frac{K_0 x \tan\phi \tan\beta}{\tan(\beta - \phi)\tan\alpha} + \frac{\tan\beta}{\tan(\beta - \phi)} (b + x \tan\beta \tan\alpha) + K_0 x \tan\beta (\tan\phi \sin\beta - \tan\alpha) - K_a b \right] \quad 3-18$$

$$p_{,\phi} = B_s \gamma'x \left\{ \left[\frac{\phi_1^T}{2K_a \cos\alpha} \right] + \left[\frac{\phi_2^T}{2K_a} \right] + \left[\frac{\phi_3^T}{2K_a} \right] + \left[\frac{\phi_4^T}{2} \right] + \left[\phi_5^T \right] \right\} \left(\frac{60}{b} y \right)^{0.8 \left(\frac{A_s}{B_s} - 1 \right)} \quad A-28$$

where:

$$\phi_1^T = K_0 x \left[\cos\alpha \tan\phi \cos\beta + 2\sqrt{K_a} \sin\beta \sec^2\phi \cos\alpha + \tan\phi \sin\beta \sec^2\left(45^\circ - \frac{\phi}{2}\right) \cos\alpha + \sqrt{K_a} \tan\phi \sin\beta \sin\alpha \right]$$

$$\phi_2^T = b \left[\sqrt{K_a} \sec^2\beta + \tan\beta \sec^2\left(45^\circ - \frac{\phi}{2}\right) \right]$$

$$\phi_3^T = x \left[\sqrt{K_a} \tan^2\beta \sec^2\alpha + 2\sqrt{K_a} \tan\alpha \tan\beta \sec^2\beta + \tan^2\beta \tan\alpha \sec^2\left(45^\circ - \frac{\phi}{2}\right) \right]$$

$$\phi_4^T = xK_o \left[\tan \beta \left(\tan \phi \cos \beta + 2 \sin \beta \sec^2 \phi + \tan \phi \sec \beta \sec^2 \alpha + \tan \alpha \right) \right]$$

$$\phi_5^T = b\sqrt{K_a} \sec^2 \left(45^\circ - \frac{\phi}{2} \right)$$

$$(S_\phi)_{NL}^T = \frac{p_a}{p,y} p,\phi \quad \text{A-29}$$

where:

subscript *NL* indicates non-linear elastic phase,

$\frac{p_a}{p,y}$ and p,ϕ are given by Equations A-6 and A-28, respectively.

For $x \leq x_r$ and $y_m \leq y \leq y_u$

$$p,\phi = \gamma x \left\{ \left[\frac{\phi_1^T}{2K_a \cos \alpha} \right] + \left[\frac{\phi_2^T}{2K_a} \right] + \left[\frac{\phi_3^T}{2K_a} \right] + \left[\frac{\phi_4^T}{2} \right] + \left[\phi_5^T \right] \right\} \left\{ B_s + \frac{48}{b} (A_s - B_s) \left(y - \frac{b}{60} \right) \right\}$$

A-30

where:

$$\phi_1^T = K_o x \left[\begin{aligned} & \cos \alpha \tan \phi \cos \beta + 2\sqrt{K_a} \sin \beta \sec^2 \phi \cos \alpha + \tan \phi \sin \beta \sec^2 \left(45^\circ - \frac{\phi}{2} \right) \cos \alpha \\ & + \sqrt{K_a} \tan \phi \sin \beta \sin \alpha \end{aligned} \right]$$

$$\phi_2^T = b \left[\sqrt{K_a} \sec^2 \beta + \tan \beta \sec^2 \left(45^\circ - \frac{\phi}{2} \right) \right]$$

$$\phi_3^T = x \left[\sqrt{K_a} \tan^2 \beta \sec^2 \alpha + 2\sqrt{K_a} \tan \alpha \tan \beta \sec^2 \beta + \tan^2 \beta \tan \alpha \sec^2 \left(45^\circ - \frac{\phi}{2} \right) \right]$$

$$\phi_4^T = xK_o \left[\tan \beta \left(\tan \phi \cos \beta + 2 \sin \beta \sec^2 \phi + \tan \phi \sec \beta \sec^2 \alpha + \tan \alpha \right) \right]$$

$$\phi_5^T = b\sqrt{K_a} \sec^2 \left(45^\circ - \frac{\phi}{2} \right)$$

$$(S_\phi)_{BL}^T = \frac{P_a}{P_{,y}} p_{,\phi} \quad \text{A-31}$$

where:

subscript *BL* indicates bi-linear elastic phase,

$\frac{P_a}{P_{,y}}$ and $p_{,\phi}$ are given by Equations A-6 and A-30, respectively.

For $x \geq x_r$ and $y_k \leq y \leq y_m$

From Equation 3- 14:

$$p = B_s p_{sd} (60y/b)^{0.8(A_s/B_s-1)} \quad \text{3-14}$$

$$P_a = B_s p_{sd} (60y_a/b)^{0.8(A_s/B_s-1)} \quad \text{A-32}$$

$$P_{sd} = K_a b \gamma' (\tan^8 \beta - 1) + K_o \beta \gamma' x \tan \phi \tan \beta \quad \text{3-19}$$

$$p_{,\phi} = B_s \gamma b x \phi_l^B \left(\tan^8 \beta - 1 \right) \left(\frac{60}{b} y \right)^{0.8 \left(\frac{A_s}{B_s} - 1 \right)} \quad \text{A-33}$$

where:

$$\begin{aligned} \phi_l^B = & 4K_a \tan^7 \beta \sec^2 \beta - \sqrt{K_a} \tan^8 \sec^2 \left(45^\circ - 1 \right) + \sqrt{K_a} \sec^2 \left(45^\circ - \frac{\phi}{2} \right) \\ & + K_o \left[\tan^4 \beta \sec^2 \phi + 2 \tan \phi \tan \beta \sec^2 \beta \right] \end{aligned}$$

$$\left(S_\phi \right)_{NL}^B = \frac{p_a}{p_{,y}} p_{,\phi} \quad \text{A-34}$$

where:

subscript *NL* indicates non-linear elastic phase,

$\frac{p_a}{p_{,y}}$ and $p_{,\phi}$ are given by Equations A-5 and A-33, respectively.

For $x \geq x_r$ and $y_m \leq y \leq y_u$

From Equation 3-16

$$p = p_{sd} \left[B_s + \left(y - \frac{b}{60} \right) \frac{A_s - B_s}{0.02086 b} \right] \quad \text{3-16}$$

$$p_a = p_{sd} \left[B_s + \left(y_a - \frac{b}{60} \right) \frac{A_s - B_s}{0.02086 b} \right] \quad \text{A-35}$$

$$p_{,\phi} = B_s b \gamma x \phi_l^B \left\{ B_s + \frac{48}{b} (A_s - B_s) \left(y - \frac{b}{60} \right) \right\} \quad \text{A-36}$$

where:

$$\phi_1^B = 4K_a \tan^7 \beta \sec^2 \beta - \sqrt{K_a} \tan^8 \sec^2 (45^\circ - 1) + \sqrt{K_a} \sec^2 \left(45^\circ - \frac{\phi}{2}\right) + K_o \left[\tan^4 \beta \sec^2 \phi + 2 \tan \phi \tan \beta \sec 2\beta \right]$$

$$(S_\phi)_{BL}^B = \frac{p_a}{p_{,y}} p_{,\phi} \quad \text{A-37}$$

where:

subscript *BL* indicates bi-linear elastic phase,

$\frac{p_a}{p_{,y}}$ and $p_{,\phi}$ are given by Equations A-9 and A-36, respectively.

Design variable, ϕ affects the sensitivity operator in non-linear and bilinear phase above and below x_r .

Sensitivity operator, S_b connected to variation in design variable b :

For $x \leq x_r$ and $y_k \leq y \leq y_m$

From Equation 3-14:

$$p = B_s p_{st} (60y/b)^{0.8(A_s/B_s-1)} \quad \text{3-14}$$

$$p_a = B_s p_{st} (60y_a/b)^{0.8(A_s/B_s-1)} \quad \text{A-38}$$

$$p_{st} = \gamma' x \left[\frac{K_0 x \tan \phi \tan \beta}{\tan(\beta - \phi) \tan \alpha} + \frac{\tan \beta}{\tan(\beta - \phi)} (b + x \tan \beta \tan \alpha) + K_0 x \tan \beta (\tan \phi \sin \beta - \tan \alpha) - K_a b \right] \quad 3-18$$

$$p_{,b} = \left[B_s \gamma x \left(\frac{\tan \beta}{\sqrt{K_a}} - K_a \right) - \frac{0.8 p_{st}}{b} (A_s - B_s) \right] \left(\frac{60}{b} y \right)^{0.8 \left(\frac{A_s}{B_s} - 1 \right)} \quad A-39$$

$$(S_b)_{NL}^T = \frac{P_a}{p_{,y}} p_{,b} \quad A-40$$

where:

subscript *NL* indicates non-linear elastic phase,

$\frac{P_a}{p_{,y}}$ and $p_{,b}$ are given by Equations A-5 and A-39, respectively.

For $x \leq x_r$ and $y_m \leq y \leq y_u$

$$p_{,b} = \gamma' x \left[\frac{\tan \beta}{\sqrt{K_a}} - K_a \right] \left[B_s + \left(y - \frac{b}{60} \right) \left(\frac{48}{b} \right) (A_s - B_s) \right] - \frac{48}{b^2} (A_s - B_s) p_s y \quad A-41$$

$$(S_b)_{BL}^T = \frac{P_a}{p_{,y}} p_{,y} \quad A-42$$

where:

subscript *BL* indicates bi-linear elastic phase,

$\frac{P_a}{p_{,y}}$ and $p_{,b}$ are given by Equations A-9 and A-41, respectively.

For $x \geq x_r$ and $y_k \leq y \leq y_m$

From Equation 3-14:

$$p = B_s p_{sd} (60y/b)^{0.8(A_s/B_s-1)} \quad 3-14$$

$$p_a = B_s p_{sd} (60y_a/b)^{0.8(A_s/B_s-1)} \quad A-43$$

$$p_{sd} = k_a b \gamma' (\tan^8 \beta - 1) + K_0 \beta \gamma' x \tan \phi \tan \beta \quad 3-19$$

$$p_b = (1.8B_s - 0.8A_s) \frac{p_s}{b} \left(\frac{60}{b} y \right)^{0.8 \left(\frac{A_s}{B_s} - 1 \right)} \quad A-44$$

$$(P_b)_{NL}^B = \frac{p_a}{p_{,y}} p_{,b} \quad A-45$$

where:

subscript *NL* indicates non-linear elastic phase,

$\frac{p_a}{p_{,y}}$ and $p_{,b}$ are given by Equations A-5 and A-44, respectively.

For $x \geq x_r$ and $y_m \leq y \leq y_u$

From Equation 3-16:

$$p = p_{sd} \left[B_s + \left(y - \frac{b}{60} \right) \frac{A_s - B_s}{0.02086 b} \right] \quad 3-16$$

$$p_a = p_{sd} \left[B_s + \left(y_a - \frac{b}{60} \right) \frac{A_s - B_s}{0.02086 b} \right] \quad A-46$$

$$p_{,b} = \frac{p_s}{b} (1.8 B_s - 0.8 A_s) \quad A-47$$

$$(S_b)_{BL}^B = \frac{p_a}{p_{,y}} p_{,b} \quad A-48$$

where:

subscript *BL* indicates bi-linear elastic phase,

$\frac{p_a}{p_{,y}}$ and $p_{,y}$ are given by Equations A-6 and A-25, respectively.

Design variable, *b* affects the sensitivity operator in non-linear and bilinear phase above and below x_r .

The sensitivity operators play an important role in the whole process of sensitivity investigation. Each operator is connected with the corresponding single design variable. Graphical representation of individual sensitivity operator displays the following features:

-
- 1) Spatial location along the length of pile where change in particular design variable contributes to the generalized maximum deformation in turn the performance of the pile soil system.
 - 2) Location where change in design variable generates maximum contribution to top deformation.
 - 3) Identification of area, if any, where changes in particular design variable contributes in favour of the increase of top deformation.
 - 4) Relative contribution of change of all design parameters and identification of design variable with highest contribution.
 - 5) When integrated over the length of the pile each operator shows net contribution of the change the corresponding design variable.
 - 6) Comparing the integrated value of all design operators, relative contribution of change of each design variable can be assessed.
 - 7) Contribution of change of the design variable at different value of applied horizontal force or bending moment.

VITA AUCTORIS

NAME: Zain Al Abedin

PLACE OF BIRTH: Chittagong, Bangladesh

YEAR OF BIRTH: 2962

EDUCATION: Bangladesh University of Engineering and Technology,
Bangladesh. 1980-1984 B. Sc.

University of Windsor, Windsor, Ontario
2002-2004 M. A. Sc.